Desalination and Water Treatment
www.deswater.com

doi: 10.5004/dwt.2023.29579

297 (2023) 26–74
June

Synthesis and application of layered double hydroxides as a superior adsorbent for the removal of hazardous contaminants from aqueous solutions: a comprehensive review

Fatin A. Alnasrawi[a,*], Ahmed A. Mohammed[b], Tariq J. Al-Musawi[c]

[a]*Department of Civil Engineering, University of Karbala, Iraq, email: fatinen35@gmail.com*
[b]*Department of Environmental Engineering, University of Baghdad, Iraq, email: ahmed.abedm@yahoo.com*
[c]*Building and Construction Techniques Engineering Department, Al-Mustaqbal University College, 51001 Hillah, Babylon, Iraq, email: tariq.jwad@mustaqbal-college.edu.iq*

Received 26 December 2022; Accepted 19 April 2023

ABSTRACT

This review presents the recent progress in the application of layered double hydroxides (LDHs) as adsorptive agents for the removal of different pollutants. Co-precipitation, hydrothermal, and sol–gel are the dominant methods used for the synthesis of LDHs. The characterization parameters of the material are reviewed in detail, as it is found that they have unique morphological and structural parameters, making them effective adsorbents across a wide range of environmental conditions. However, these adsorbents are subjected to different modification processes to enhance their adsorptive performance. From the literature, the maximum adsorption capacity of LDHs for heavy metals and organic pollutants was found to be 800 mg/g for Cr(VI) and 9,127 mg/g for Congo red dye. From the kinetic investigations, studies showed that the adsorption process using LDHs mostly follows a pseudo-second-order model. In addition, the Langmuir model is the best model to describe the isothermal data. The variation in the adsorption capacity of LDHs concerning environmental conditions is summarized, and the best conditions are evaluated. From the information presented in this review, it can be said that LDHs have a promising future as alternative materials to many currently used adsorbents. However, the process of improving their surfaces and structural properties to suit the environmental conditions and to facilitate the process of separating them from solutions remains a subject in need of study. In addition, a few studies have examined the ability of LDHs to remove radioactive elements.

Keywords: Adsorption; Layered double hydroxides; Characterization; Synthesis method; Heavy metals; Organic pollutants

1. Introduction

Overall, in recent decades, the increasing levels of pollution in the aquatic environment have become a matter of concern for many countries [1–3]. Drinking water resources are polluted by many elements, whereby heavy metals, dyes, and emerging contaminants (ECs) are among the most dangerous as they directly affect human health. Industrial activities top the list of the releasers of these pollutants into water sources as they pump wastewater, after inefficient treatment, into the environment [2,4–8]. Heavy metals are highly toxic elements that are also non-biodegradable. They bio-accumulate in living things and hence can cause serious damage to human health and the quality of the environment [1,7]. Following the standards of the World Health Organization, the allowable limit of many heavy metals, such as copper (Cu), cadmium (Cd), chromium (Cr), lead (Pb), arsenic (As), mercury (Hg), nickel (Ni), and zinc (Zn), is less than

* Corresponding author.

1944-3994/1944-3986 © 2023 Desalination Publications. All rights reserved.

0.1 mg/L [9]. On the other hand, dyes are carcinogenic and highly toxic agents, and thus, they pose a huge threat to global public health and life safety, even at low concentrations. In addition, the dyes present in water bodies can restrict the photosynthesis process because of the ability of the dye molecules to absorb reflected sunlight, thereby damaging aquatic life. Numerous anthropogenic organic compounds are included in ECs, such as pharmaceuticals, pesticides, personal care products, and synthetic hormones, with many being associated with having harmful effects on both the environment and human health due to their high toxicity, persistence, and degradation-resistant properties [10–12]. Therefore, the removal of toxic heavy metals, dyes, and ECs from water solutions has been a primary concern of many researchers and environmental scientists.

On this front, many studies have demonstrated that adsorption, membrane separation, advanced oxidation, photocatalytic degradation, and reverse osmosis are successful processes in terms of the removal of numerous inorganic and organic pollutants from water solutions [13–16]. The adsorption process has been intensively studied for decades because of its ability to overcome all the drawbacks of conventional treatment techniques due to its simplicity, affordability, the possibility to reuse the adsorbents, and no sludge production [13,17]. In the adsorption process, the capacity of the used adsorbents is the key factor in the fast and efficient adsorption of target pollutants. Adsorbents fall into three main classes: organic absorbents, inorganic absorbents, and biological absorbents. Organic absorbents are mainly managed by unpaired electrons and the heavy metal ions in oxygen, sulfur, nitrogen, and other atoms of the included functional groups. Inorganic absorbents layered double hydroxides (LDHs, activated carbon, zeolite, graphene, mesoporous silica, etc.) have large specific surface areas and controllable pore structures. The advantages of bio-absorbents are their high adsorption capacity and renewable nature [18]. Due to its great adsorptive properties, such as a large specific surface area, high porosity, and hydrophobicity, activated carbon is the most efficient adsorbent for different inorganic and organic pollutants [19]. However, the high cost of activated carbon is a stumbling block that stands in the way of its widespread use. Accordingly, many alternative materials have been proposed, which are characterized by their affordable price and high practical performance. In this regard, many studies have provided excellent adsorbents, both in theory and in practice; one of the most superior ones is layered double hydroxide (LDH).

LDH materials are gathering a lot of interest for many applications. Their use as adsorbents in water treatment has garnered great attention due to their large surface area, highly tunable interior, architecture [8,20], exchangeable anionic features [8], and non-toxicity [21]. Therefore, LDHs provide the possibility of a high adsorption capacity [2]. In recent years, LDHs have been used as sorbent materials for a wide range of hazardous and toxic contaminants in aqueous environments. Previous studies have shown LDHs to be effective adsorbents for the removal of heavy metals [22–26], organic pollutants such as dyes [15,27,28], and ECs [29–31]. The versatility in the LDH structures and composition makes them promising adsorbents for removing a variety of toxic contaminants from water solutions [8,32,33]. Nanostructured LDHs can be utilized to remove contaminants from wastewater, mainly by adsorption and an ion-exchange mechanism [8].

LDH, also known as hydrotalcite-like compounds, belong to a versatile class of bi-dimensional (2D) anionic lamellar nanostructured materials. A hydrotalcite is composed of individual layers of a brucite-like structure [$Mg(OH)_2$] [34]. A positively charged layer is formed by a stack of brucite-like layers [$Mg(OH)_2$] with a positive residual charge due to partial Mg^{2+} substitution by Al^{3+} cations [34,35]. Layers in brucite are electrically neutral, with a magnesium cation situated at the center of an octahedron, with six hydroxyl groups located in the vertices [36]. The chemical composition of LDH is generally represented as shown in Eq. (1).

$$\text{LDH chemical formula} = \left[M^{++}_{1-x} \cdot M^{+++}_{x} (OH)_2\right]^{+x} \left[\left(A^{-n}\right)_{x/2} \cdot mH_2O\right]^{-x} \quad (1)$$

where M^{++} and M^{+++} represent the di- and trivalent layer cations, respectively, in octahedral positions within the hydroxide layers; A^{-n} is an anion, and the charge densities of the LDH layers are NO_3^-, Cl^-, CO_3^{2-} [36,37]; m is the number of water molecules occupying the interlamellar layer sites, where no anions are present [36]. Additionally, the pure hydrotalcite phase can be obtained when x lies between 0.2 and 0.33, where x is a ratio of $M^{+++}/(M^{++} + M^{+++})$ [36,38,39], resulting in the M^{++}/M^{+++}ratios of 2:1 to 4:1 being reasonably stable. Thus, different LDH compounds can be obtained by varying the cations, their ratio, and the interlamellar anions [40]. The structural characterization of LDH is shown in Fig. 1.

In the LDHs, the di- and trivalent cations are linked by OH units coordinated at the octahedral position, forming sheets that are then stacked on top of each other to give a layered structure, analogous to that of the mineral brucite [42]. Approximately half to one-quarter of the divalent cations are substituted by trivalent metal cations, resulting in metal hydroxide layers of positively charged, mixed $[M^{++}_{1-x}M^{+++}_{x}(OH)_2]^{x+}$, which then stabilize with negatively charged interlayers containing anions and water molecules $[(A^{-n})_{x/2} \cdot mH_2O]^{-x}$ [43–45]. The lack of cross-linking between the

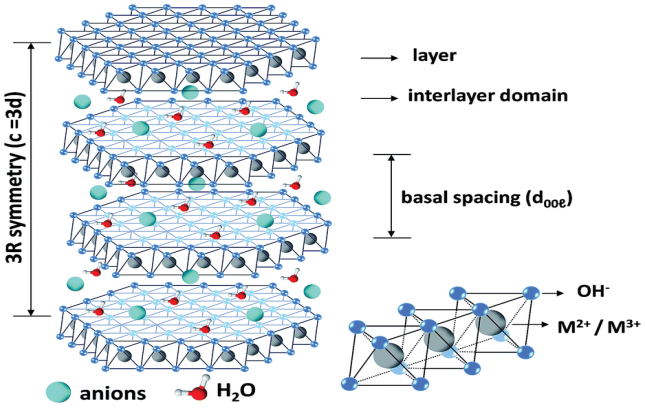

Fig. 1. Schematic of the layered double hydroxides structure [41] (Copyright 2023 Royal Society of Chemistry, Open Access).

cation layers is a significant property of LDHs, allowing the interlayer spacing to shrink or expand to accommodate a broad range of interlayer anions [40,42,46].

There are many sets of di- and trivalent cations for the synthesis of LDHs. Commonly used divalent M^{++} cations are Mg^{++}, Zn^{++}, Mn^{++}, Ni^{++}, Co^{++}, and Fe^{++}, whereas the trivalent M^{+++} cations include Al^{+++}, Cr^{+++}, Fe^{+++}, and Mn^{+++} [36,38,47]. Table 1 lists the combination styles of di- and trivalent cations in LDH used for the adsorption of various toxic contaminants [18].

The LDHs represent one of the most technologically promising nanostructured materials in recent years, due to their relative ease of preparation and broad use as adsorbents [44], high surface area, low cost, highly tunable interior architecture [8,20], non-toxicity [8,21] and exchangeable anionic features [8]; these properties result in excellent adsorption properties as well as high mechanical and chemical stability [47].

Another advantage of using LDHs as adsorbents is the simple technique of modification and intercalation, which enhances their removal efficiency. The temperature is raised to 400°C–600°C during calcination, resulting in a calcined clay with a larger surface area, greater thermal and chemical stability, and a greater number of active sites. Calcination substantially enhances the adsorption capability of these hydrotalcite-like materials [48,49]. The nanocomposites generated by the hybridization of LDHs, with other nanomaterials, demonstrate a considerable increase in surface characteristics and adsorption ability [48].

LDH materials provide a new line of investigation into the outstanding adsorption tendency of different toxic contaminants onto the LDHs from water bodies [8].

This literature review focuses on presenting the studies that investigated the characteristics of LDHs and their adsorption capacity in removing different materials from aqueous solutions. In addition, the variation in the LDH adsorption capacity as a function of different operating parameters, such as contact time, pH, adsorbent dosage, initial contaminant concentration, temperature, and coexisting and competitive anions, is discussed in detail.

Table 1
Combination of di- and trivalent cations in the layered double hydroxides structure

	Ca^{++}	Mg^{++}	Fe^{++}	Zn^{++}	Ni^{++}	Cu^{++}	Mn^{++}	Co^{++}
Al^{+++}	√	√	√	√	√	√	√	√
Fe^{+++}	√	√		√	√			√
Cr^{+++}	√			√	√			

2. Unique adsorptive characteristics of LDHs

2.1. Crystal structure and morphological properties

Adsorbent characteristics are important in determining the adsorption capacity of materials, as well as the mechanisms used to remove contaminants from aqueous media [50,51]. Fig. 2a shows the structural properties of LDH, indicating a normally well-crystallized form. Fig. 2b presents the X-ray diffraction (XRD) pattern of LDH, displaying two

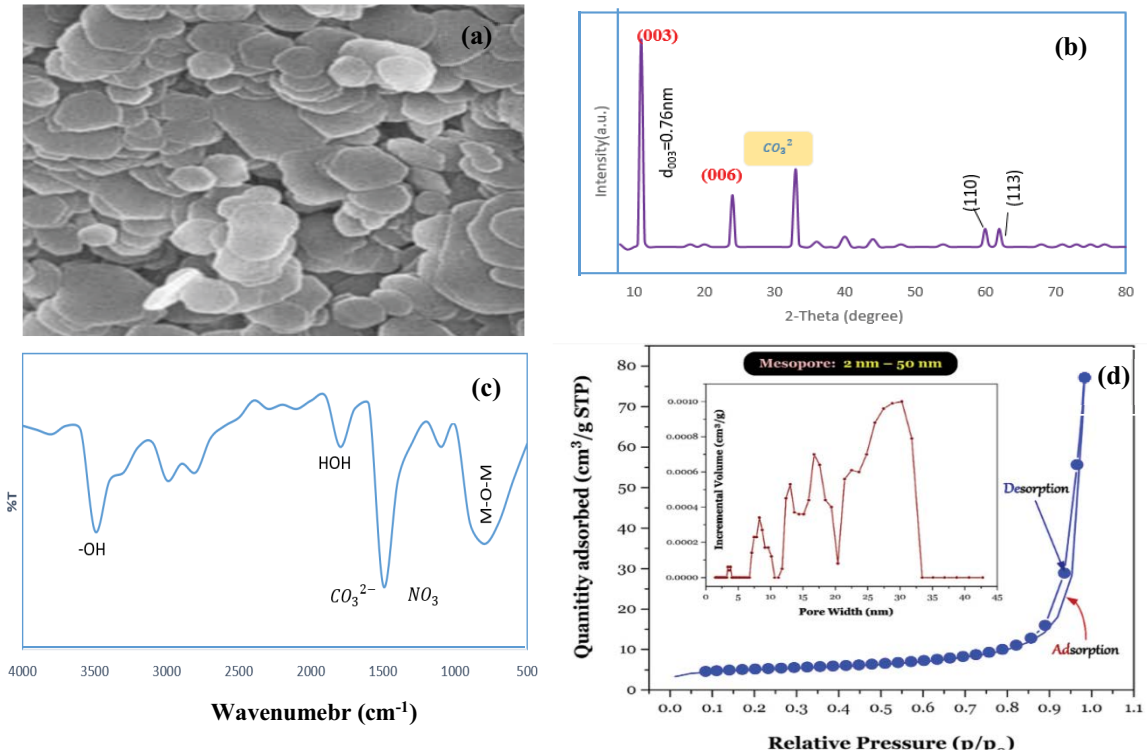

Fig. 2. (a) Field-emission scanning electron microscopy of MgAl-LDHs, (b) X-ray diffraction of MgAl-LDHs, (c) Fourier-transform infrared spectroscopy of MgAl-LDHs [52], (d) N_2 sorption/desorption isotherms of MgAl-LDH [55] (Copyright 2023 Elsevier).

characteristic peaks at 2θ = 23.2° and 11.6°, which correspond to the interlayer spacing and LDH basal spacing, respectively. The interlayer spacing (d_{006}) and basal spacing (d_{003}) are generally determined by Bragg's law [52].

2.2. Functional groups

Fig. 2c presents the main functional groups in the hydrotalcite-like material. The LDH materials show poor functionality, with some defined apices. First, the overlap of several forms of O–H bonding vibrations is attributed to an extremely broad apex, around 3,500 cm^{-1}, such as the interlayer water molecules, the hydroxyl group in the brucite-like layers, and even physically adsorbed water [50]. Second, a well-defined apex at nearly 1,650 cm^{-1} most likely corresponds to the N=O and/or C=O functional groups, built from the internal anion [(CO_3^{2-}) and/or (NO_3^-)]. The N=O and/or C=O stretching vibrations of the interlayer anion are also observed to be close to 1,380 cm^{-1}. Through an anion-exchange mechanism, those exchangeable anions in the interlayer matrix can help in the removal of the toxic oxy-anion from the aqueous solution. Finally, the lattice modes of (O–M–O) vibration are characterized by an observed apex at roughly 680 cm^{-1} [52].

2.3. Zeta potential

The LDH's material is comprised of brucite ($Mg(OH)_2$)-like layers, with positively charged sheets that result from the plentiful protonated hydroxyl groups $–OH_2^+$ on the external surface of this material. This indicates that LDH has a positive zeta potential in a wide range of pH solutions. Protonation and deprotonation of the surface functional groups characterize LDHs, like other adsorbents. As the LDH's zeta potential usually indicates a highly charged positive value, the pH of such a material's isoelectric point (pH_{IEP}) is frequently greater than 9. This includes, for instance, MgAl/LDHs (synthesized by the sol/gel method); MgAl/LDHs (alkoxide-free sol/gel method); and MgAl/LDHs (hydrothermal precipitation method) [51,53]. A high IEP value of MgAl/LDH is most likely due to the dissociation of mainly $Mg(OH)_2$ and some $Al(OH)_2^+$ sites [54].

2.4. Anion-exchange capacity

Layered double hydroxide materials typically present an excellent anion-exchange capacity (AEC) value because they have more exchangeable anions in their matrix. As a result, they can function as inorganic anion-exchangers with a high affinity for diverse anionic pollutants in the solution. The values of the AEC of the MgAl/LDH sample increase in the following manner: 300 m_{eq}/100 g for the alkoxide sol/gel. <400 m_{eq}/100 g for the hydrothermal precipitation, and <450 m_{eq}/100 g for the alkoxide-free sol/gel [53]. Similarly, a high value of ACE of MgAl-hydrous oxides (420–550 m_{eq}/100 g) was verified [54].

2.5. Textural properties

Fig. 2d depicts the nitrogen (N_2) sorption–desorption isotherm of LDH. The isotherm is classified as IV-type category by IUPAC, with a noticeable H_3-type hysteresis loop at a high relative pressure [(P/P_0) > 0.8]. The study revealed that LDH has mesopores with slit-shaped pores, which are formed by layering the nanosheet building blocks [53,55]. Generally, LDH adsorbents are classified as porous materials, meaning that LDHs often exhibit a high Brunauer–Emmett–Teller (BET) specific surface area (S_{BET}) and total pore volume [53,55]. In addition, the M^{2+}/M^{3+} molar ratio of the metal salts used in the LDH synthesis, calcination process, and preparation method all affect the LDH texture. The S_{BET} and V_{total} values of LDH were hereby found to be lower with increasing molar ratios of metal salts used, as reported by Bravo-suárez et al. [43]. This result is consistent with those of some authors [56,57], but not with those of Clark et al. [58].

In regards to the calcination process, the S_{BET} of LDH is typically improved during calcination under atmospheric air [59]. For instance, the S_{BET} and V_{total} values of SO_4-Mg/Al-LDH (95 m^2/g and 0.28 cm^3/g) were found to significantly increase after calcination at 350°C (142 m^2/g and 0.42 cm^3/g), as reported by Ramírez-Llamas et al. [60].

3. Synthesis of LDHs and their composites and modification of LDHs

LDHs are green nanomaterials because they are eco-friendly, non-toxic, do not exhaust natural resources, and the solvent used in their synthesis is water [61]. Although LDH is considered a rare mineral in nature, it can be synthesized in the lab using chemicals that are much less expensive [62]. Selection of the preparation method greatly depends on the cations in the hydroxide layer, the intercalated metal anions [36], the concentration of the interacting metal ions [62], and the desired physio-chemical properties, such as crystallinity, phase purity, morphology, porosity, and optical and electronic characteristics of the final material [36]. The ability to control the preparation process is mostly governed by parameters such as system pH, stirring speed, reaction time, titration rate, temperature [63], and the atmospheric pressure [62]. Preparation of the LDH can be accomplished by using various methods, which are categorized into two types: direct and indirect methods [8]. The most conventional direct methods utilized for the preparation of LDH are co-precipitation, hydrothermal, sol–gel, and *in-situ* growth film. The most common indirect methods for LDH synthesis are anion-exchange, delamination followed by restacking, and memory effect reconstruction [36]. First, the most conventional methods used for pristine LDH synthesis are discussed, followed by the most prevalent techniques for the preparation of LDH composites. The third subsection contains a variety of LDH composites that have been synthesized via specific methods. Table S1 displays the outcomes. These results are also presented in the text, where the table is divided into three subdivisions (heavy metal, dyes, and ECs). The first column of this division contains the LDH/composite, and the contaminant name(s) are listed in the second column. Also included in this table are the methods of synthesis and experimental details, such as the chemicals used, the steps and/or conditions of the experiment, the pH of the reaction mixtures, and the conditions of calcination.

3.1. Direct methods

3.1.1. Co-precipitation method

Co-precipitation, also called the salt-based method, is the most conventional preparative method for LDH preparation and is mainly used due to its simplicity, the flexibility of conditions (constant or variable pH), and large-scale production capability, and because it can be conducted in a single reactor [19,47]. It is further subdivided into the precipitation of low super-saturation and the precipitation of high super-saturation [46,64]. Ideally, the pH adjustment approach should differ between the two methods [40,46,65].

Depending on the precipitation conditions, a well-crystallized hydrotalcite or amorphous material can be obtained. These conditions are as follows: The M^{2+}/M^{3+} molar ratios, pH of the reaction media, base solution concentration, base solution nature, aging temperature, aging time, and total cation concentration [40].

"LDH co-precipitation" refers to the simultaneous precipitation of $M(OH)_2$ and $M(OH)_3$, where metal salts are used as precursors [40,46,64], and it is based on the mixing of metal salt solutions in a proper proportion in a reactor containing deionized water [19,46]. Metal salts are mostly composed of nitrates, sulfates, chlorides, and other soluble salts [66]. An alkaline solution is also added and vigorously mixed to elevate the pH value, resulting in the co-precipitation of an LDH having two metallic salts [19]. The alkaline solutions include NaOH, KOH, NH_3, Na_2CO_3, K_2CO_3, urea, and other alkaline solutions [66]. To obtain a well-crystallized and reproducible LDH structure, the produced mixture has to age for a long period in the synthesis solution. The pH is maintained at a slightly above-the-required value for both metal salts to precipitate simultaneously [19,46,67]. On the other hand, higher pH levels may lead to the inclusion of some hydroxide as a counter ion on the LDH surface, or even within the interlayer. By filtration, the precipitates are separated, and then washed well using deionized water; the LDH is then dried overnight in an oven [67].

The most disadvantageous phenomenon that occurs during the preparation of LDH is carbonate, CO_3^{2-}, intercalation between the layers. This occurs as a result of the absorption of CO_2 from the atmosphere, which dissolves in the solution, especially at basic pH conditions. The carbonate CO_3^{2-} ion is among the most firmly held anions within the lattice of LDH, and to prevent its inclusion, the reactions should take place in an atmosphere free of CO_2 or under inert gaseous conditions, such as N_2. A carbonate CO_3^{2-} ion is strongly bound in the interlayer. Thus, it is difficult to replace them with adsorbate ions during ion-exchange. This means the LDH adsorption efficiency will be better only when the interlayer ion is weakly bonded [19,67].

The interlamellar anions can be selectively intercalated depending on the experimental conditions. Such key conditions are the pH of the reaction medium, the reactor temperature, the concentration of the alkaline solution, the concentration of the metallic salt solutions, the aging of the precipitate, and the low rate of the reactant [68]. When this LDH is calcined, it first loses the interlayer water, up to 200°C, then decomposes and dehydroxylates all the carbonate into CO_2 at around 450°C–500°C. Finally, metal oxides with a high specific area and a narrow pore-size distribution are produced [69]. In some situations of LDH calcination, the dehydroxylation or water loss causes a collapse of the LDH structure, and quasi-amorphous mixed oxides are produced [19,70,71].

Despite the advantages that co-precipitation presents, such as the capability to intercalate various anionic species, high yield, crystallinity, as well as LDHs of the utmost purity, it faces several challenges, such as changes in the operational conditions of the process from the beginning to the end that produce differences in crystallinity. Furthermore, super-saturation is usually low, except in the alkali introduction point region, and this does not assist the fashioning of uniform nanometer-sized particles [46]. Another co-precipitation shortfall is that the particles agglomerate, forming aggregates with an extremely large-sized distribution. This is attributed to the strong interactions among the edge surface platelets, called "sand rose morphology" (Fig. 3), caused by the high-base super-saturation conditions imposed by the co-precipitation conditions [72].

The co-precipitation mechanism is based on the condensation of the hexa-aquo complexes in the solution, which results in the formation of brucite-like layers with a uniform distribution of both the solvated interlamellar anion and the metallic cation. Precipitation at low super-saturation and precipitation at high super-saturation are the two techniques of co-precipitation [64].

- Precipitation at high super-saturation includes adding mixed metal cations, in the proper ratio, to an alkaline solution containing choice interlayer anions. The addition of metal salts causes a pH change, leading to the formation of $M(OH)_3$ and $M(OH)_2$ impurities and undesired metal ratios. Precipitation at a high super-saturation condition leads to the formation of fewer crystalline materials [46,64].
- Precipitation at low super-saturation is the most commonly used co-precipitation method. It proceeds by adding a solution of metal ions slowly, in the desired ratios, to a vessel containing a solvated solution of anions. The pH at which the metal salts precipitate is monitored and adjusted by the simultaneous addition of basic

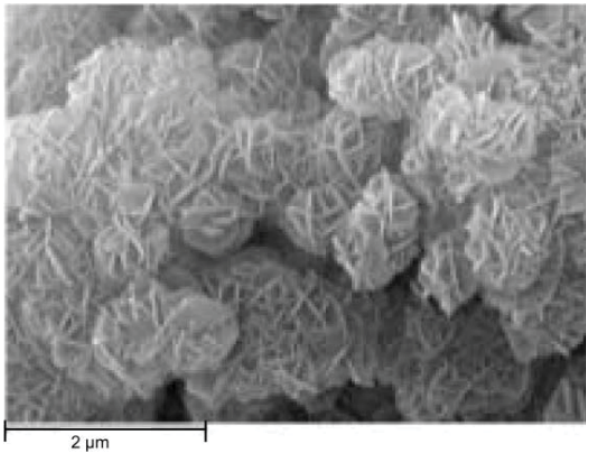

Fig. 3. Scanning electron microscopy image of MgAl co-precipitation agglomeration [72] (Copyright 2023 Elsevier).

solutions. In comparison to the material formed by precipitation under high super-saturation conditions, the material formed under low super-saturation conditions has a high crystallinity [46,64].

3.1.2. In-situ hydrothermal method

The hydrothermal treatment is also known as "urea hydrolysis" [73] because it uses urea instead of NaOH as a precipitation agent. Urea is a very weak Bronsted base, with a pK_b of 13.8, and a hydrolysis rate that may be readily controlled by adjusting the reaction temperature, which produces a slow rate of urea hydrolysis and leads to the low super-saturation of LDHs during precipitation. It is highly soluble in water and its controlled urea hydrolysis produces ammonium cyanate or its ionic form, while prolonged urea hydrolysis can yield CO_3^{2-} in a basic environment or CO_2 in an acidic medium. During the reaction, a temperature greater than 60°C causes it to proceed into a slow decomposition of urea in ammonium hydroxide (NH_4OH), resulting in a homogeneous precipitate that undergoes the following reactions [Eqs. (2)–(4)] [74]:

$$NH_2 - CO - H_2N \rightarrow NH_{4+} + NCO^- \quad (2)$$

$$NCO^- + 2H_2O \rightarrow NH_{4+} + CO_3^{2-} \quad (3)$$

$$NCO^- + H^+ + 2H_2O \rightarrow NH_{4+} + HCO_3^- \quad (4)$$

Traditionally, urea and precursor salts (chlorides, nitrates, hydroxides, or sulfates) are mixed in certain ratios and placed in a Teflon-lined stainless-steel autoclave. This mixture is then heated to an appropriate temperature for a set period of time. Filtration is used to get the precipitated product, followed by thorough washing and overnight drying. The particle size and morphology can be controlled, and there are no competing anions in this method [19].

Lei et al. [75] prepared a triple-metal, MgNiAl-LDH, utilizing $MgSO_4$, $Al(NO_3)_3$, $NiSO_4$, and urea, in a molar ratio of (1:1:1:6). After stirring for 1 h, the solution was put in a 100 mL stainless steel autoclave with a Teflon lining and kept at 160°C for 6 h, before being cooled to room temperature. Centrifugation was used to separate the produce. Deionized water and ethanol were used to wash it five times, and then it was dried for 12 h at 80°C.

3.1.3. Sol–gel method

The term "sol–gel" is derived from a reaction's physical characteristics. Metallic-alkoxides are commonly employed in this process as metallic precursors, but sometimes acetylacetonates or acetates are used, and many inorganic salts can also be employed as metallic precursors. The alkoxides are dissolved in an organic solvent (e.g., ethanol, acetone) and then refluxed. Water is slowly added to this refluxed solution. Thus, initially, hydrolysis forms a sol, then a metallic precursor partially condenses, leading to the production of a colloidal gel as a result of internal cross-linking. The solid LDH properties are based on the rates of hydrolysis and condensation of the metallic precursors, which can be tuned by adjusting the reaction parameters, such as pH, the type of solvent used, the nature and concentration of the metallic precursor, and the temperature at synthesis. The resulting LDH features are a well-customized pore size, a large surface area, and high purity, and the material exhibits relatively good control of the stoichiometry [19,67,76,77]. MgAl-LDH, the most common of the LDHs synthesized by this method, has been formed with Mg/Al ratios of nearly 6, compared to the more common ratios of 2 and 3 for materials obtained through other methods of preparation [67].

Ahmed et al. [68] synthesized MgFe-LDH using the sol–gel method, dissolving a specific ratio of $Mg(NO_3)_2$ and $Fe(NO_3)_3$ in distilled water with continuous stirring for 1 h. Just above the critical concentration of the micelle, a bromide of cetyltrimethylammonium was added, and additional stirring was performed. The brown precipitate that formed was the result of adding NaOH drop by drop with stirring for an additional 2 h. The gel particles were filtered, and then washed and dried at 100°C for 24 h.

3.2. Indirect methods

3.2.1. Anion-exchange synthesis

The anion-exchange approach involves adding a concentrated solution of anions of interest to a pre-formed LDH structure. The resulting solution is kept at 50°C–70°C for several hours with constant stirring. The efficiency of the exchange varies based on the capability of the exchanged anions to stabilize the lamellae and/or their proportion relative to the LDH precursor anions [76].

Anion-exchange is a very effective method, commonly employed when co-precipitation is not applicable, for example, when the metal ions are unstable at a higher pH value or a potential for interaction exists between the metal anions and the guest ions [46,62]. In such cases, the anion in the interlayer area can be directly or indirectly substituted with the desired anion [46]. A direct ion-exchange includes the incorporation of carboxylic acid into LDH-A by direct contact with a suitably concentrated aqueous or non-aqueous solution of the desired acid salt, where A = chloride (Cl^-) or nitrate (NO_3^-) is used as an interlayer anion [46,78] and indirect methods are needed to expel the divalent anions (e.g., CO_3^{2-}) as they are held strongly [46]. These two methods are illustrated in Eqs. (5) and (6) [62,64].

$$LDH \cdot A^{m-} + xB^{n-} \rightarrow LDH \cdot \left(B^{n-}\right)_{x/n} + A^{m-} \quad (5)$$

$$LDH \cdot A^{m-} + xB^{n-} + mH^+ \rightarrow LDH \cdot \left(B^{n-}\right)_{x/n} + A^{m-} + H_mA \quad (6)$$

Some factors that must be considered when performing anion-exchange are:

- The pH value: a low pH value is favorable for basic anion de-intercalation and re-intercalation by less basic ones. However, if the pH falls below 4.0, the LDH matrix may dissolve.
- The incoming anion affinity: exchangeability is favored when the incoming anions have greater charges than the anions that are leaving, as well as when they have a smaller ionic radius. The order decreases for

divalent anions as follows: $CO_3^{2-} > HPO_4^{2-} > SO_4^{2-}$; and for monovalent ions it is: $OH^- > F^- > Cl^- > Br^- > NO_3^- > I^-$.

- The exchange medium: The inorganic solvent favors the inorganic anion, even as the organic solvent favors the organic anion.
- Chemical composition of the layer: The charge density of an anion is influenced by the chemical composition of the layer, which affects how the anion interacts with the matrix [46,62,64].

3.2.2. Calcination-reconstruction "memory effect"

One unique property of anionic clays is that after thermal decomposition they have the ability to retrieve the layered structure [46]. The LDH is heated to around 400°C–600°C in an inert atmosphere, which leads to the loss of interlayer water and carbonate, as a result of which mixed metal oxides are formed known as calcined layered double hydroxides, represented by (LDO) and/or (CLDH) [19].

For example, LDHs are intercalated with carbonate anions by urea hydrolysis. Similarly, the lack of a fully inert atmosphere during co-precipitation synthesis results in unwanted anions, particularly carbonates, which are strongly held by their matrix. To remove these unwanted anions, powdered LDH is calcined and then reconstructed with any anion that is needed. This is referred to as "the memory effect" [64,79]. Thermal- and chemical-stable calcined clays with a higher surface area and more active sites are the result of calcination. It is recommended that heating be done at a constant rate of 1°C/min to retain crystallinity. This prevents the rapid release of CO_2 and water, thus protecting the LDH's original structure [19]. Calcination of LDH forms the spinel phase, $M^{2+}M_2^{3+}O_4$, as the major product [46]. Reconstruction of the layered structures is done by using a solution of the required anion under a fully inert environment to avert competitive intercalation by the carbonate ions. The calcination temperature has a direct impact on the reconstruction process; for example, to achieve complete reconstruction, it takes 1 d for a sample calcined at around 400°C–450°C and 3 d for a sample calcined at 750°C, while at 1,000°C, only a fractional reconstruction is recognized [80]. The typical layered structure can be recovered, as shown in Fig. 4.

With these tunable features, it is possible to intercalate numerous anions with varying molecular sizes and active sites [64]. Starukh et al. [81] used a co-precipitation method to prepare ZnAl-CO_3-LDH and heated it to 450°C for 2 h. Regeneration was done by making a sodium dodecyl sulfate (SDS) solution in CO_2-free deionized water and then mixing it with calcined LDH. The suspension was stirred at room temperature for 24 h to build ZnAl-LDHs.

3.2.3. Ageing process

Ageing is the hydrothermal or thermal treatment of LDHs that is typically performed after the nucleation process. Ageing improves the crystallinity of the prepared materials, especially for those prepared using conventional methods. In the thermal treatment, the sample is heated to 70°C–120°C for a long period, 1 h or 1 d, under atmospheric pressure [46,64]. A bath of oil is sufficient. On the other hand, hydrothermal treatment involves heating the samples in enclosed reactor containers, in the presence of water vapor, provided the temperature of decomposition is not overridden. There are two possible experiments available. The first is in a stainless-steel reactor at an autogenous pressure and high temperature, which is referred to as autoclaving, while the second involves using a silver or gold tube at 1,500 bar and a high temperature. There are two possible experiments available. As reported by Roy et al. [79], Ni/Al-CO_3/LDH and Ni/Cr-X/LDH (with X: Cl^-, CO_3^{2-}, SO_4^{2-}) were synthesized and thermally treated at 10°C and 18°C for 10 d and 18 h, respectively, at a pressure of 1,500 bar. The hydrothermally treated samples showed improved crystallization at 180°C for 72 h, as seen in Fig. 5 [61].

To obtain an axiomatic comparison, one can refer to Table 2, which is a summary of the pros and cons of various methods of preparing LDH. If all the synthesis methods used are compared, co-precipitation can be considered the most favorable because it produces products with good crystallinity and relatively high corrosion resistance.

3.3. Methods of LDH-composite synthesis

An LDH has the capability of intercalating neutral molecules or exchanging organic or inorganic ions with their authentic interlayer anions, where LDHs behave as a host material for the formation of an organic-inorganic host–guest composite, which will incorporate or increase the desired chemical and physical properties. The flexibility and versatility of LDHs and the availability of a large number of "guests" permits the preparation of a wide variety of innovative materials [19,46]. This section will discuss the commonly utilized techniques for preparing LDH composites.

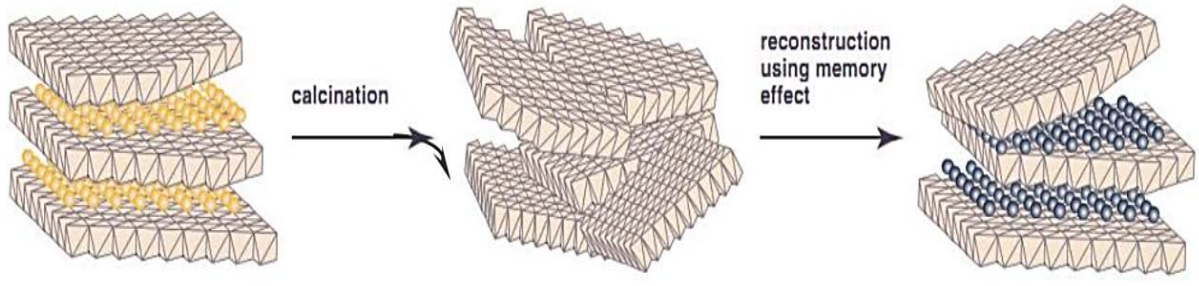

Fig. 4. Schematic illustration of recovering the layered structure of layered double hydroxides via the reconstruction process [80] (Copyright 2023 Elsevier).

3.3.1. Co-perception method

This is a process that is more frequently used, not only for the preparation of pristine LDH but also for the preparation of their composites. Metal salts are chosen such that their anions have less affinity for LDH, or else the anions that will be incorporated with the hydroxide layer will face more competition. Chloride and nitrate salts are the most commonly used anionic precursors. Furthermore, to accurately control charge density, the pH is kept at a constant value, where M^{2+} and M^{3+} can both precipitate at the same time [19].

3.3.2. Anion-exchange method

The anion-exchange method is another approach that is commonly used in the preparation of LDH composites. First, the LDHs are synthesized using one of the most common methods. The LDH precursors are then mixed in a solution of excess anions and stirred to be intercalated. To avert carbonate (CO_3^{2-}) intercalation, the whole process is performed in a completely inert environment of N_2 or Ar. The electrostatic forces between the exchanging anions and positively charged LDH layers enforce the exchange of the host and guest anions [19,46]. This process is operated at higher temperatures and a pH value ≥ 4.0 to avoid the possibility of a hydroxyl layer breaking.

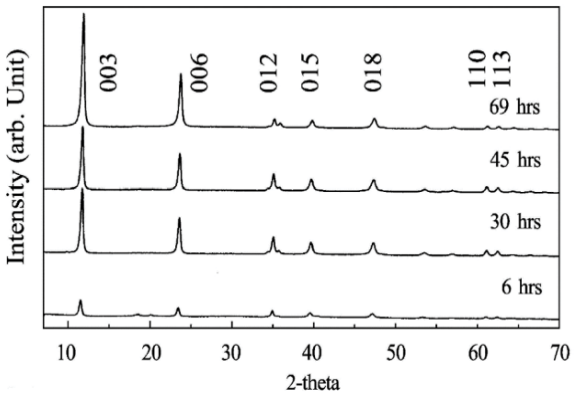

Fig. 5. X-ray diffraction image of urea-synthesized hydrotalcite demonstrating enhanced crystallinity with time [61] (Copyright 2023 Elsevier).

3.4. Some specific synthetic LDH composites

Due to their highly tunable interior architecture and high surface area, LDHs are considered efficient adsorbents for contaminants in the liquid phase. Researchers are still investigating synergistic approaches between LDH and other materials in order to develop new composites with improved characteristics. The aim of the process could be to increase the pore dimensions and surface area, expand interlayer spacing, intercalate functional groups to increase the adsorption rate, or merely overcome the limitations faced, such as column clogging due to a small crystal size or costly regeneration process. Efforts have been made by synthesizing composites with a wide range of materials, like magnetic materials, biochar, carbon, surfactants, nanostructures, and so on. This section summarizes the procedures adopted by various groups to prepare a wide variety of novel composites with diverse properties, utilizing several innovative materials.

3.4.1. Template-assisted synthesis

LDHs prepared by classical hydrothermal or co-precipitation methods can be joined with surfactants or templates to obtain a flower-like morphology by using hard or soft templates. Soft-templating agents are organic molecules that can interact strongly with the inorganic species

Table 2
Comparison of different preparation methods

Method	Advantages	Disadvantages
Co-precipitation	- Simple process - Controllable chemical compositions - One-step synthesis	- Needs further crystallization - Weak adhesion and time-consuming
Hydrothermal synthesis	- Good crystallinity - Controllable size - Simple reactant	- Low output - High temperature - Long reaction time
Sol–gel	- Good uniformity - Insert large anionic groups	- Low output and high cost - Complex composition
Anion-exchange	- Avoids the formation of insoluble compounds	- Two-step synthesis - Neutral species cannot be intercalated
Calcination-reconstruction	- Higher purity anion - Takes full advantage of structure - Original reactant can be LDH intercalated with any anions	- Activity of metal oxides determines the reconstruction - Needs am LDH precursor prepared by other methods - Time-consuming
Ageing process	- Low pollution and high reactivity	- Impure crystal phase

that develop over them. Sodium dodecyl sulfate (SDS) is commonly utilized for soft-templating and acts as an agent that directs the structure as well. The SDS dose is a decisive factor in obtaining a specific morphology. For example, 0.005 mol/L of SDS concentration results in a rose flower structure, whereas a higher 0.02 mol/L concentration leads to spherical geometry, and so on. However, when the SDS concentration is equivalent to the critical micelle concentration (CMC), the petal size diminishes, and their number increases, eventually leading to their fusion. The process includes dissolving M^{3+}, M^{2+}, and urea in water and vigorously dispersing them for 60 min. The mixture is centrifuged after being heated to around 200°C in a 100 mL Teflon-lined stainless-steel autoclave for 6 h. The resulting product is washed four times with distilled water before being dried for 6 h at around 80°C [15,82–84]. The synthesis of ultrathin dodecyl sulfate intercalates the MgAl-LDH nanosheets. $Al(NO_3)_3 \cdot 9H_2O$, $Mg(NO_3)_2 \cdot 6H_2O$, hexamethylenetetramine (HMT), and SDS are combined in distilled water until a viscous, white liquid forms. After that, the blend is heated to 140°C for 24 h to improve crystallization.

3.4.2. Carbon-assisted method

Many research groups have employed carbon in various forms to produce LDH-based carbon composites. Li et al. [23] prepared ZnAl-CLDH@C by calcining ZnAl-LDH nanosheets and coating them with ultrathin amorphous carbon. ZnAl-LDH nanosheets synthesized by co-precipitation are modified with oleic acid (OA) ligands. The resulting ZnAl-LDH@OA is then calcined at 450°C under an N_2 atmosphere. The *in-situ* carbonization of OA ligands leads to ultrathin carbon shells and produces ZnAl-CLDH@C nanosheets that are characterized by a large specific surface area and superior ability to disperse. Amin et al. [85] investigated the feasibility of preparing the LDH of NiZnFe and its composites with hollow-layered carbon nanotubes (LDH-CNTs) as well as with biochar derived from date-palm leaves (LDH-DPb). The resulting LDH and its composites' adsorbents possess good adsorption properties. Almoisheer et al. [82] reported adopting the urea hydrolysis method to produce a CuAl-LDH/SWCNTs nanocomposite by complexing CuAl-LDH with single-walled carbon nanotubes (SWCNTs). Lyu et al. [86] hybridized MgAl-LDH with a carbon sphere (CS) by using the emulsion cross-linking method. Meanwhile, Zhang et al. [87] synthesized CSs-LDHs composites via a hydrothermal method, their surface properties were modified via calcination at temperatures between 300°C and 800°C.

3.4.3. Synthesis of negatively charged LDHs

LDH has difficulty absorbing cationic dye and inorganic cations due to ion repulsion from positively charged sheets. Therefore, Bin et al. [88] attempted to produce complex NiFe-LDH nanoflakes with montmorillonite (MMT). MMT consists of an Al^{3+} octahedral, adjoining two sheets of Si^{4+} tetrahedral. When Mg^{2+} or Zn^{2+} is substituted for Al^{3+}, a perpetual negative charge develops on the surface of the MMT and the interlayer. MMT/NiFe-LDHs are synthesized by the hydrothermal method at different molar ratios of LDH and MMT (2:1, 3:1, and 4:1), where the nickel, iron(III) nitrate hexahydrate, and urea are added to the MMT solution. In Fig. 6, four scanning electron microscopy (SEM) images

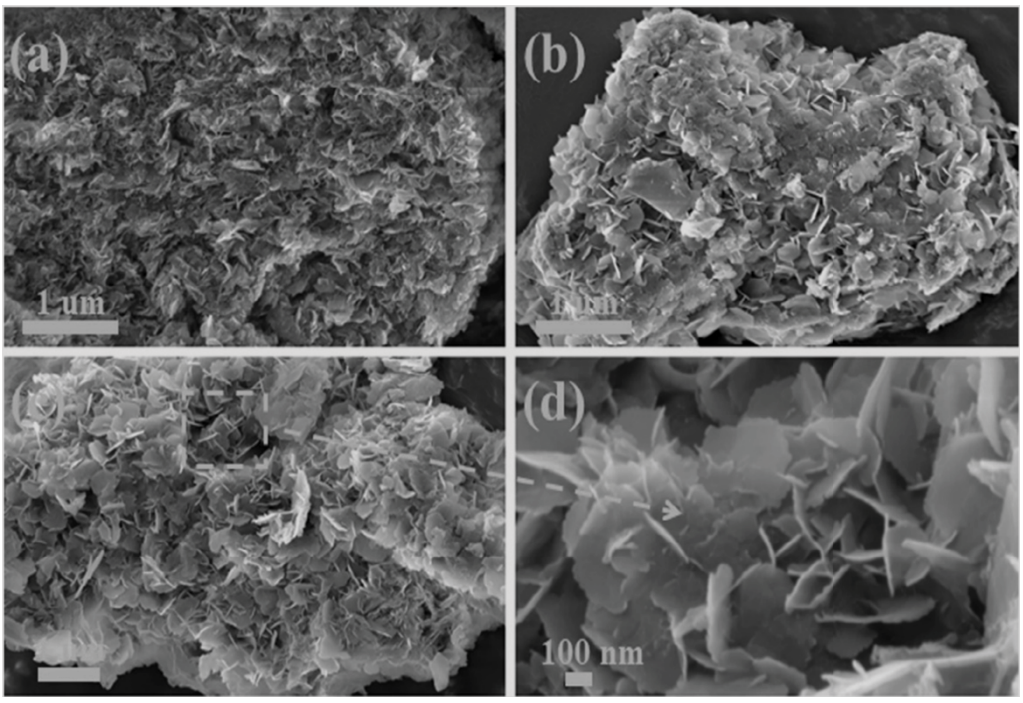

Fig. 6. Scanning electron microscopy images of MMT/Ni2Fe1-LDH, MMT/Ni3Fe1-LDH, and MMT/Ni4Fe1-LDH, and a close-up of MMT/Ni4Fe1-LDH [88] (Copyright 2023 Elsevier).

show the different shapes of the surfaces of three MMT@ NiFe LDHs.

3.4.4. Preparation of mesoporous-LDH

Zhang et al. [89] proposed a new hydrothermal method for the synthesis of mesoporous Cu/Ni/Al-LDH. The Cu, Ni, and Al salts were dissolved in 50 mL of 0.1M HCl solution, and then the mixture was heated to 80°C for 1 h using a reflux condenser, agitation, and ultrasonication. NaOH was added drop by drop to maintain a constant pH of 10. The precipitate was washed with deionizing water and then dried for 24 h at 90°C.

3.5. LDH modification

The adsorption capacity of pristine LDHs and their applications are limited due to the lack of structural components and functional groups. To address this problem, functionalized LDH was synthesized by incorporating functional groups or structural components. Due to the presence of a positive charge, the $[Mg(OH)_6]$ octahedron, and hydroxyl groups on the surface, LDH could interact chemically and electrostatically with the structural components or functional groups in this process. There are three types of functionalized LDH preparation methods: For small inorganic or organic molecules, the intercalation process is utilized, whereas, for larger organic molecules, the surface modification process is utilized. Also, LDHs are loaded onto substrates that are capable of providing attachment sites [18].

3.5.1. Intercalation

To increase the adsorption capacity of LDHs for hazardous contaminants, LDHs are intercalated with molecules that can cause complexation with the hazardous contaminant ions. Intercalated LDH with sulfide has a high capacity for absorbing ions, and its selective adsorption has received a lot of attention. In addition, LDHs are mainly intercalated to organic molecules that can significantly enhance the adsorption capacity, especially for heavy metal ions. For example, the maximum uptake of LDH intercalated with sodium dodecylbenzenesulfonate (SDBS) and citrate for Cu^{2+} increased by 72.7 mg/g compared to the uptake of intrinsic LDH [90]. The organic functional groups like $–NH_2$ and –COOH have many coordination atoms that can donate electron pairs; therefore, the heavy metal ions and organic compounds can undergo complex reactions to form complexes. LDHs are mainly bound with organic molecules by chemical bonding and electrostatic contact. Usually, when LDHs are intercalated with molecules, the crystal parameters of the LDHs are obviously changed. XRD is utilized to define the powder crystal structure. Unit cell parameters (usually d_{003}) can also be used to analyze the intercalated arrangement of the molecules between layers. Table 3 shows LDH intercalated with molecules, the basal spacing, and how molecules are arranged between layers. This table shows that basal spacing is related to the type and arrangement of the molecules between the layers [18].

3.5.2. Surface modification

Some molecules find it difficult to enter the interlayer due to the charge density, hydrodynamic radius, and other factors, so the method of surface modification is chosen for the preparation of LDH-based composites. Surface modification can enhance the adsorption capacity of LDH-based composites for contaminants and remove the limitations of other adsorption materials in the contaminant adsorption process. The combination of bio-adsorbent materials and LDH with high stability yields adsorbents with superior adsorption capacity [18]. Olivera et al. studied how to prepare LDH-based composites using proteins and MgAl-LDH. The proteins were extracted from Bilva Oil meal. The produced composites (LDH-BP) eliminate Pb^{2+} ions, and the authors found that 625 mg/g was the highest rate of Pb^{2+} removal [99]. The methods predominantly used to modify the surface of LDHs are direct cross-linking, indirect cross-linking, and *in-situ* film growth. The hydroxyl groups on the surface of LDHs play an importance role in surface modification. Moreover, the surface modification method combines the advantages of LDHs and other adsorption materials [18].

4.1. Adsorption mechanisms

The adsorption mechanisms of the various hazardous contaminants by LDH-based composites are mostly

Table 3
Layered double hydroxides basal spacing and molecule arrangement

Origin anions	d_{003}	Intercalated molecule	d'_{003}	Arrange	References
NO_3^-	8.9.	MoS_4	10.7		[91]
NO_3^-	7.51	L-cysteine	8	Horizontal monolayer	[83]
Cl^-	7.8	Humate hybrid	7.9		[92]
Cl^-	7.82	DTPA	14.21	Inclined monolayer	[93]
CO_3^{2-}	7.62	$[EDTA]^{4-}$	8.04	Inclined monolayer	[94]
CO_3^{2-}	7.6	Tartrate	12.2		[95]
NO_3^-	8.34	$[SnS_4]^{4-}$	9.3		[96]
CO_3^{2-}	8.8	$[EDTA]^{4-}$	13.9	Vertical monolayer	[97]
NO_3^-	7.69	Histidine	13.58		[15]
CO_3^{2-}	7.66	D_2EHPA	26.27	Inclination bilayer	[98]

dependent on the kind of adsorbent (hybridizing material) and adsorbate. Generally, the basic mechanisms involved in the adsorption process for controlling pollutants in aqueous environments by LDH-based adsorbates are physical adsorption, anion-metal complexes, ion-exchange, hydroxide precipitation, chemical bonding, electrostatic interaction, and π–π interactions [29,100–106].

Adsorption of heavy metal ions onto anionic/LDH surfaces is related to the formation of anion-metal complexes and the precipitation of hydroxide by chemical bonding with the hydroxyl groups of LDH [22,107,108]. Huang et al. [109] concluded that lead and copper could be removed onto Mg_2Al-LS-LDH through the mechanism of anion-exchange, as shown in Fig. 7, while Ma et al. [108] investigated the adsorption of metal-ions (M) on a polysulfide-LDH composite (SX-LDH). Following the formation of the (M-S) complex, (SX-LDH) is converted to pristine LDH, according to Eqs. (7) and (8).

$$\mathrm{LDH_{sx}} + M\left(\mathrm{NO_3}\right) \rightarrow \mathrm{LDH}\left(\mathrm{NO_3}\right)_2 + \mathrm{MS}_x \quad \text{for high metal concentration} \tag{7}$$

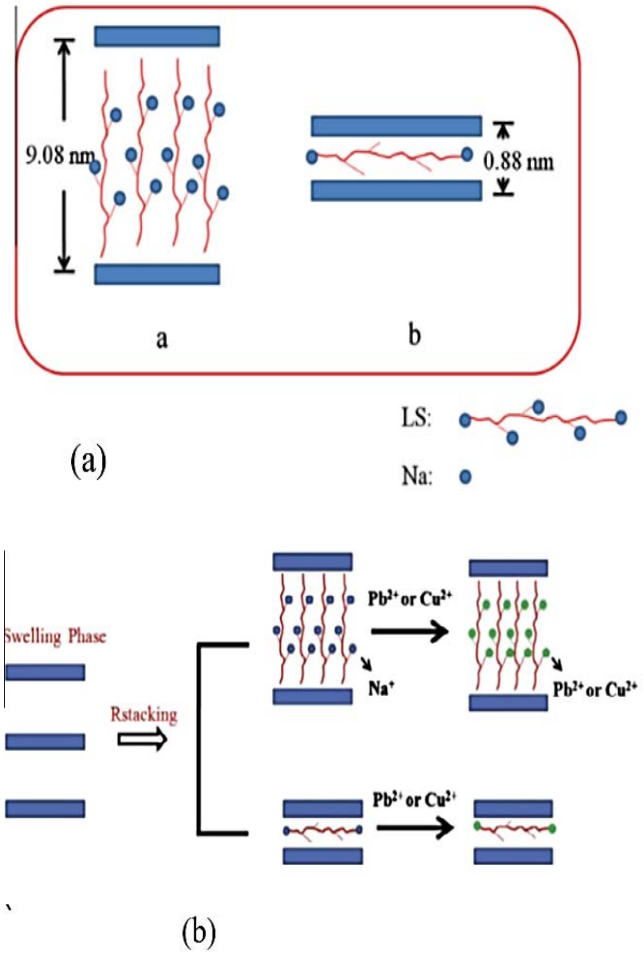

Fig. 7. Sketches of (a) LS in an Mg/Al-LDH interlayer and (b) Pb^{2+} and Cu^{2+} attachment with LS-LDH [109] (Copyright 2023 Elsevier).

$$\mathrm{LDH}\left(\mathrm{NO_3^-}\right)_m\left(\left[M^{2+}\left(\mathrm{Sx^{2-}}\right)_2\right]^{2-}\right)_n \quad \text{for very low metal concentration} \tag{8}$$

The LDH-based humate (H-LDH) was synthesized by González et al. [92] for the adsorption of Cu^{2+}, Cd^{2+}, and Pb^{++}, which involved the mechanism of precipitating hydroxide. Humate contains a large number of functional groups that have oxygen. They exist as anions over a wide pH range and then combine with the cation metal ions. The mechanism was confirmed by analyzing the final pH of the adsorption process. After a few minutes of starting the adsorption process, the pH of the solution suddenly increased. This was because metal-hydroxides formed on the surface of H/LDH.

The adsorption mechanism of the LDH-containing carbon nanostructure (CNS)/LDH is controlled by the interlayer anion-exchange, that is, CO_3^{2-}, NO_3^{2-}, Cl^{2-}, by the metal ions, through chemical bonding with the hydroxyl groups or other oxygen groups on the surfaces of the carbon materials, and by physical adsorption on the exterior surfaces of the carbon materials [38,100,110,111]. Yuan et al. [100] discovered that the adsorption of chrome on graphene-LDH(G-LDH) comprises two phases: During the first phase, the adsorption is inextricably tied to the memory effect of LDH, owing to its high adsorption rate. The second process involves the physical adsorption of G/LDH onto its exterior surface, which occurs at a sluggish pace. The adsorption mechanism of Cr(VI) ions onto G/LDH is depicted in Fig. 8.

For the LDH-based magnetic composites, this included the addition of iron oxide (Fe_3O_4) nanoparticles on the LDHs [104,112–115]. The water contaminant adsorption mechanism on magnetic-LDH composites included precipitation, ion-exchange, chelation, and surface modification. Due to its magnetic nature, introducing Fe_3O_4 into the LDH layers enhanced the adsorption capacity and simplified LDH separation after the adsorption process. Table S2 shows that the LDH-containing iron nanoparticles exhibited a large adsorption capacity of 9,127.08 mg/g for Congo red (CR) [116], 931.24 mg/g for Acid Red 66 (AR66) [117], and 800 mg/g for Cr(VI) [56]. The incorporation of carbon-based materials along with Fe_3O_4 on the layers of LDH evolved into a novel adsorbent with superb pollutant adsorption [104,118]. Zhang et al. [104] indicated that the

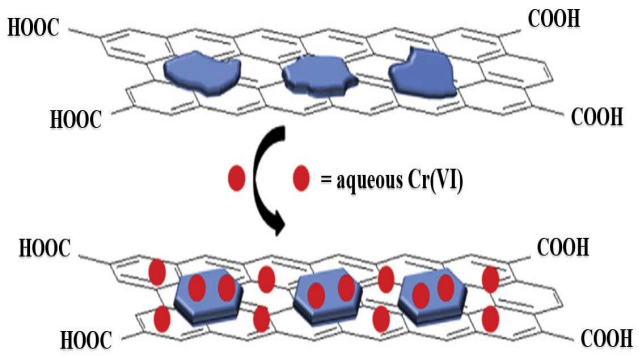

Fig. 8. Sketch presenting Cr(VI) adsorption onto G-Mg/Al-CLDH [100] (Copyright 2023 Elsevier).

precipitation of a carbon coating on Fe_3O_4-LDH caused an increase in the adsorption capacity of U^{6+} by Fe_3O_4@C-LDH. Although the precipitation reduced the surface area, the adsorption capacity of U^{6+} by the Fe_3O_4@C-LDHs increased due to the increased number of oxygen functional groups (OFGs). Similarly, carbon-based nanomaterials were used to increase the adsorption rate for other pollutants [119]. Other types of LDH-containing hybrid-like surfactants, such as titania, polymer, and so on, have also shown better water contaminant adsorption [120,121].

The two most common mechanisms reported for anionic and cationic dye adsorption by LDH-based composites are interlayer anion-exchange with anionic pollutants and external electrostatic interaction between cationic or anionic dyes and the negatively or positively charged surface of LDHs [8,32]. In many cases, it can be demonstrated that materials with high adsorption capacities possess both an anion-exchange and an electrostatic interaction mechanism [32]. Furthermore, the presence of hydroxyl groups on the LDH surface may result in H-bonding with the dye molecules [122–124]. The existence of OFGs on the surfaces of carbon materials acts as active sites for the removal of the dye. Fig. 9 depicts the uptake of methyl blue by the MgAl-LDH-carbon dots. They observe that the adsorption depends on pH and is preferable in an acid medium [110]. This reveals that the sorption is caused by the electrostatic interaction of the positive charge surface between the LDH-carbon dot and anionic dyes.

Furthermore, the inclusion of carbon dots into the LDHs improved the amount of methylene blue (MB) adsorbed due to the formation of H-bonding between the carbon dots and the MB [110]. Yang et al. [17] also observed that H-bonding, chemical bonding, and electrostatic interaction between the dye molecules and surface functional groups of CNT (C–OH and COO–) are the predominant adsorption mechanisms for CR removal onto the MgAl-LDH-CNT composite. Other studies have reported similar dye adsorption behavior on other LDHs [2,122,125–127]. Table S2 shows more mechanisms for the sorption of hazardous contaminants onto LDH-based adsorbates.

The mechanism of adsorbing ECs utilizing LDH-based composites as adsorbents involves chemical bonding, van

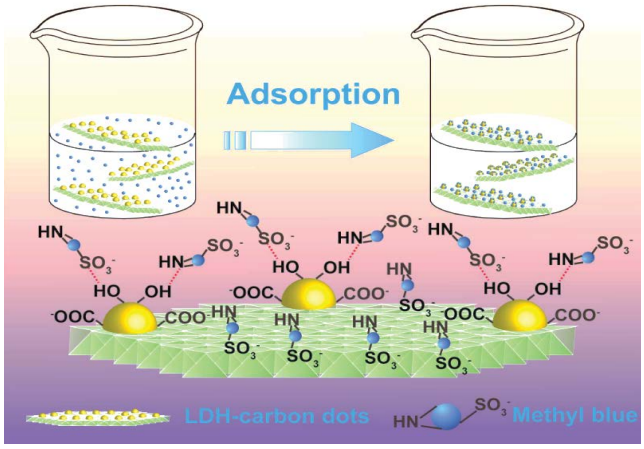

Fig. 9. Proposed schematic of MB adsorption onto LDH-carbon dots [110] (Copyright 2023 Elsevier).

der Waals forces, electrostatic interaction, and π–π interaction, as seen in Fig. 10a. Owing to the surplus of positively charged in the LDH structure, the removal of anionic antibiotic compounds is credited to an electrostatic attraction [128,129] and the higher anion-exchange of the LDH-based composites, as shown in Fig. 10b [130].

Moreover, antibiotic compounds contain nitrogen and oxygen atoms that polarize the molecules and promote interaction between the surface hydroxyl groups of the LDHs via van der Waals forces or H-bonding [130]. The adsorption mechanism for the removal of neutral antibiotic compounds includes non-electrostatic interactions, for example, H-bonds, π–π interactions, and surface complexation [131,132]. Table S2 shows more mechanisms of the sorption of toxic contaminants.

LDH-based carbon composites, like activated carbon, can also favor the removal of antibiotics with aromatic rings in their structures. Tan et al. [128] discovered that the alkoxy and hydroxyl groups of CLDH-biochar (BC) form H-bonds with the amino and hydroxyl functional groups of the tetracycline (TC) molecules. Moreover, the π–π interaction between the CLDH-BC and benzene rings of TC may be included in the antibiotic molecules.

4.2. Environmental factors affecting contaminant adsorption on LDH

To eliminate toxic contaminants from aqueous solutions via the adsorption process, the sorption of contaminants is determined by various variables, including pH solution, adsorbent dose, initial contaminant concentration, contact time of adsorbate–adsorbent, and so on. This provides an optimal condition for any adsorbate–adsorbent system [8].

4.2.1. Effect of pH

The initial pH-solution plays a crucial role in determining the adsorption efficiency of LDH adsorption in water-treatment applications. The pH significantly influences the chemistry of the adsorbent, the surface charge of the LDH-based composites [8], and the conditioning of the adsorption mechanism. The point zero charge (pH_{PZC}) is a crucial adsorbent property because it indicates that the pH at the surface of the LDH is electrically neutral [129]. When the LDH pH falls below pH_{PZC}, the surface is protonated, and the LDH surface becomes positively charged, facilitating electrostatic interaction with a contaminant that is negatively charged; in contrast, at a pH greater than pH_{PZC}, the LDH acquires a negative charge on its hydrated surface upon deprotonation [19]. As the pH solution rises, so does the OH^- ion concentration on the surface of the LDH-based composites [8]. For the LDH-based composites, most of the reported pH_{PZC} values are in the range of 7–8 [31,129].

Some researchers report that LDH-based composites dissolve at very low pH values owing to their acidic hydrolysis nature, which indirectly reduces their ability of adsorption [133,134], while at high pH values, greater than 7, they may cause divalent metal ions (Cu^{2+} and Pb^{2+}) to hydrolyze, which leads to a low adsorption capacity [92,95]. The Cr(VI) removal efficiency on calcined graphene (G)/MgAl/CLDH as a function of pH is shown in Fig. 9. The maximum efficiency

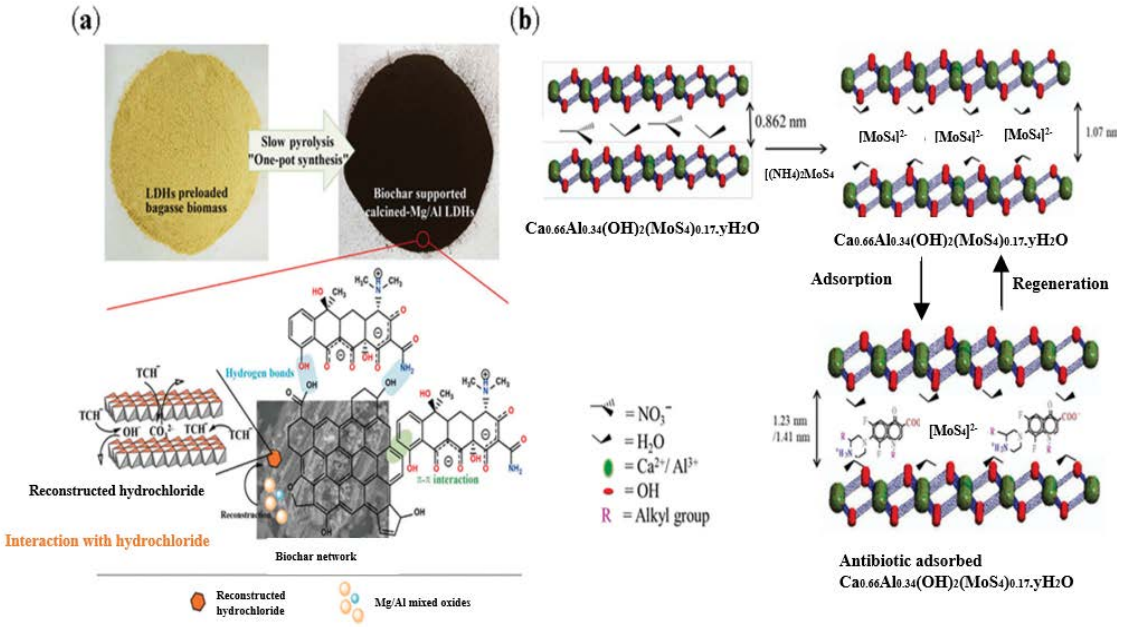

Fig. 10. Adsorption mechanism using LDH-based adsorbents [128,130] (Copyright 2023 Springer Nature).

occurs at a pH of 2, but as the solution-pH is raised, the removal efficiency drops. This behavior may be ascribed to the memory effect of the calcined LDH and the net surface charge of graphene (Fig. 11a) [100]. For higher pH values, the electrostatic repulsion between the G/LDH surface and chromium increases owing to the existence of oxygen functional groups on graphene (G), which makes it negatively charged. Calcined LDH releases OH^- ions at higher pH due to the memory effect. Thus, an increase in OH^- ions competes with the uptake of chromium anions [135].

Mallakpour et al. [136] investigated the impact of pH on methyl orange (MO) elimination (anionic dye) on poly(vinyl chloride)(PVC)-MgAl/LDH-MnO_2, and the finding showed that the removal efficiency decreased from 96% to 48% when the pH increased from 2 to 4. Two attractions interpreted this pattern: The first one was the electrostatic attraction between the MO molecule and the positively charged LDH-based adsorbate, and the second was the formation of H-bonds between the MO molecule and the hydroxyl group on the LDH surface.

A reverse tendency is seen for cationic dye adsorptions, where the highest adsorption of malachite green (MG) and crystal violet (CV) (cationic dyes) on C/ZnAl/CLDH is increased from 85.67% to 97.87% at a pH that is increased from 6 to 9, respectively. Sorption at high pH is attributable to the fact that the pH_{PZC} of LDHs is 5.8, and under this level of pH, cationic dyes cannot be adsorbed. Meanwhile, a low pH facilitates the protonation of MG and CV, which raises an electrostatic repulsion between the LDH surface and the dye molecule [13].

Li et al. [137] assessed the performance of minocycline (MC) elimination on (γ-AlO(OH)/MgAl/LDH/C) at diverse pH levels. The findings revealed that changes in pH have no considerable influence on MC adsorption, as MC with numerous ionizable functional groups exists as a cation, anion, and zwitterion at different pH values due to the direct impact of the pH solution on the contaminant structure. The higher uptake of MC on the LDH may be due to the π–π interactions and H-bonding.

4.2.2. Effect of sorbent dosage

The dose of the sorbent is an additional component that has a direct influence on the removal of hazardous pollutants from a liquid phase. According to the literature, increasing the adsorbent dose tends to increase the active sites on its surface, allowing more contaminants to be adsorbed, but exceeding an optimum amount attains a plateau owing to the saturation of active sites [8,19,129]. The effect of the adsorbent dosage on the removal efficiency of lead on MnO_2-MgAl-LDH is shown in Fig. 11b [138]. The removal percent of lead on modified MnO_2-MgAl-LDHs is raised from 20% when the adsorbent dosage is 0.01 g to almost 100% when the adsorbent dosage is 0.05 g. Although the lead adsorption capacity on MnO_2-MgAl-LDH increases up to 0.03 g of absorbent, it then begins to decline when the adsorptive dose is further increased. In a specific adsorbent dose range, the adsorbent dispersion in the watery medium is uniform and nearly all of the active sites are exposed, allowing the lead ions to reach a greater number of active sites. Even so, as the adsorbent dose increases, an increase in the number of adsorption active sites with more energy may cause a decrease in the number of adsorption active sites with less energy, which results in a decrease in the adsorption capacity. The elimination of Acid orange 7 (AO7) and methylene blue dyes on 3D/MgAl/LDH was studied by Pan et al. [139], who found that the removal efficiency of the dye AO7 rises from 82% when 3D/MgAl/LDH is dosed at 0.25 g/L to 99% when the adsorbate dose is 1 g/L, which then stabilizes with a further increase in the dose of LDHs.

A common starting dose of LDH for adsorbing an antibiotic compound is 1 g/L, and increasing the dose of

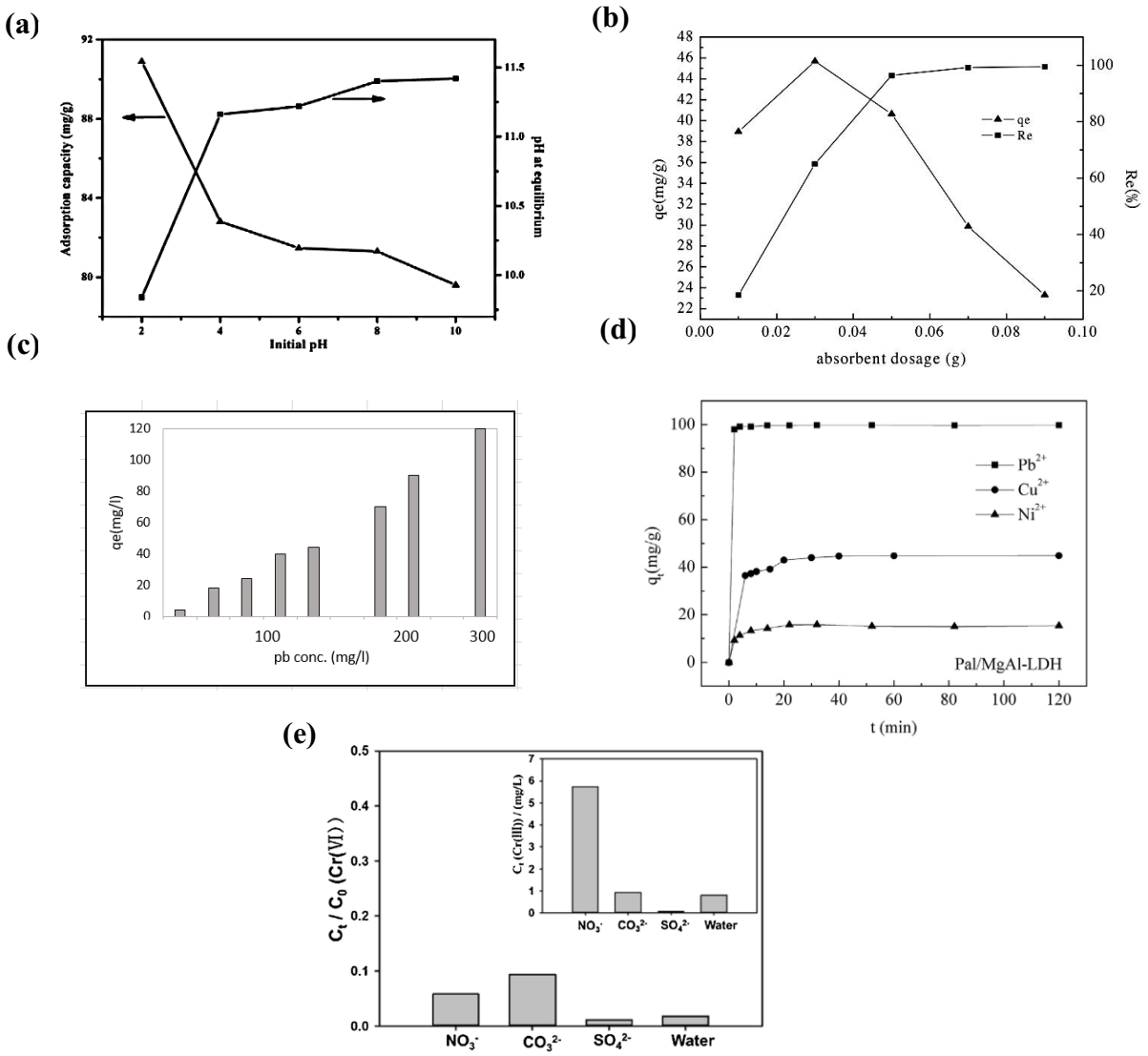

Fig. 11. (a) Effect of pH solution on Cr(VI) adsorption [100], (b) effect of dosage on Pb^{2+} the adsorption [138], (c) initial Pb^{2+} concentration effect on the adsorption process [95], (d) contact time effect on the removal of Ni^{2+}, Pb^{2+}, and Cu^{2+} [120], and (e) effect of the common anion on the sorption of Cr(VI) [34] (Copyright 2023 Elsevier).

the adsorbent leads to higher antibiotic retention [29]. Meanwhile, by increasing the absorbent dose, the adsorption capacity decreases. Usually, is the fact that the likelihood of agglomeration and collision of the adsorbent particles also rises with an increase in the quantity of the adsorbent, leading to a decrease in the adsorption–specific surface area [14,140].

4.2.3. Effect of the initial contaminant concentration

The initial concentration of the pollutant is the driving force for the sorption process; therefore, an increase in that concentration causes the initial adsorption rate to rise. However, the adsorption rate decreases as soon as the adsorbate molecules take over all the active sites of the adsorbent [19]. The higher uptake at elevated concentrations may be related to the creation of driving forces that encourage more collisions between the adsorbate molecules and the adsorbent active sites (i.e., overcoming the mass transfer resistance). It means that at higher initial solute concentrations, the driving force is higher than at lower initial concentrations. Thus, the adsorbed amount of the adsorbate per unit mass of adsorbent will be higher at higher initial contaminant concentrations [129]. When the initial concentration of contaminants is high, more contaminants will be taken up by the unit mass of adsorbents.

Other studies attributed the higher uptake to monolayer adsorption at a low initial concentration, which then transitioned to multilayer adsorption at a higher initial concentration. Shen et al. [95] studied the influence of changing the initial concentration of Pb^{2+} from 10–300 mg/L on the adsorptive removal by MgAl-CO_3-LDH. As shown in Fig. 11c, the adsorption capacity for Pb^{2+} was higher when there was a higher initial Pb^{2+} concentration.

Zhang et al. tested the influence of the initial concentrations of MO and Rhodamine B (RhB) dyes on the amount adsorbed by 3D-MgAl-LDH in the 20–250 mg/L concentration range. They found that the RhB adsorption capacity rose initially and subsequently plateaued (50 mg/L) at a 200 mg/L initial concentration. Then, the removal efficiency decreased when the initial concentration was increased to more than this value, thereby affirming the above-mentioned essential principle. Although MO behaved differently, the adsorption capacity reached an equilibrium when the initial concentration of MO was more than 600 mg/L [71]. Rathee et al. [29] reported that NiTiAl-LDH had a high efficiency for tetracycline at initial concentrations of <60 mg/L. When the initial concentration of tetracycline was raised to 700 mg/L, the removal rate dropped to 53%. They clarified that once the active sites were full, an increase in the initial concentration of tetracycline would decrease production.

4.2.4. Effect of contact time

The contact time of the adsorbate–adsorbent system is an important parameter for the adsorption process's favorability. Upping the adsorption contact time generally leads to an increase in the elimination of contaminants from the liquid phase until equilibrium is reached. A summary of the equilibrium times for pollutants can be seen in Table S2. Fig. 10d demonstrates the influence of contact time on the uptake of Ni^{2+}, Pb^{2+}, and Cu^{2+} by palygorskite-modified MgAl-LDH (Pal/LDH). While the adsorption of these metal ions was rapid the first time, equilibrium was attained in 4 min [120]. Nazir et al. [141] synthesized the composites ZIF/67 and ZIF/67@CoAl-LDH to remove MO (anionic dye) and MB (cationic dye). They found that the removal efficiency for the dye MO was 70% and 72% after 90 min of contact time, and for the dye MB it was 80% and 67% after 100 min of contact time, respectively. Rosset et al. [142] examined the influence of altering the contact time on removing diclofenac by using different adsorbents, MgAl-CLDH, NiAl-CLDH, and ZnAl-CLDH. High removal efficiencies of 79.7% and 80.5% were reached after 90 min of contact time with ZnAl-CLDH and NiAl-CLDH, respectively. For the MgAl-CLDH adsorbent, however, it was necessary to wait 240 min to achieve 75.9% of diclofenac removal.

4.2.5. Effect of temperature

Temperature is a further vital parameter for the adsorption process. Increasing the temperature of the adsorption process typically increases the adsorption capacity of the LDH composites. This is a result of the increased contaminant mobility in aqueous solutions, which increases the accessible adsorption sites and enhances the affinity of the contaminant for the adsorbent. This indicates that the process of adsorption is endothermic [130]. For the adsorption of the Cr(VI) ions on G/MgAl/CLDH, the negative value of ΔG demonstrates the spontaneous nature of adsorption, and an augmentation of the negative value of ΔG with increased temperature indicates that an elevated temperature contributes significantly to the adsorption process, leading to a high driving force for adsorption [100].

MB dye adsorption is reduced on LDH-carbon as the temperature increases. This is because of the sensitivity of the strength and length of the H-bonds, which is assessed by the negative value of a parameter ΔH [110].

4.2.6. Effect of coexisting and competitive anions

While many studies concentrate on removing single contaminants from aqueous systems, in actual wastewater and contaminated natural water matrices, many kinds of pollutants will be present. The existence of these soluble ions may have a competing effect on the adsorption site [32,143]. The influence of coexisting anions on Cr removal by BC@EDTA-LDH has been studied. The interference of competing anions on Cr(VI) adsorption follows the order $NO^{3-} < Cl^- < SO_4^{2-}$, indicating that nitrate has a relatively low impact on its removal. The negative charge carried by Cl^- and NO^{3-} is lower than that of $Cr_2O_7^{2-}$, so the stability of LDH is relatively high, indicating that it is not easily replaced by Cl^- and NO^{3-}; also, the negative charge carried by SO_4^{2-} is the same as that of $Cr_2O_7^{2-}$, so it has a great impact on Cr removal (Fig. 11e) [143]. Guo et al. [144] investigated the effects of coexistent anions (Cl^-, CO_3^{2-}, NO^{3-}, SO_4^{2-}, and HPO_4^{2-}) on AS removal by using CuMgFeLa-LDHs as an adsorbent.

George et al. evaluated the impact of NaCl salt on the absorption of MG and CV dyes on C-Zn/Al-CLDH and noticed a reduction in the removal efficiency of dyes. This behavior may be due to decreased electrostatic interactions among the cations existing in the molecules of the dye and the C-ZnAl-LDH functional groups, or due to increased dye molecule protonation [13]. Clark et al. [58] studied the influence of Na_2SO_4 and Na_2CO_3 on the sorption of RO_{16} and RB5 dyes by ZnAl-CO_3-LDH. Their findings indicate that SO_4^{2-} has less influence on dye adsorption than CO_3^{2-}.

Additionally, Chen et al. [145] examined MO dye adsorption by NiAl-Cl-LDH after adding an additional anion (PO_4^{2-}) to the working solution. The order of the competitive effect on MO dye adsorption was found to be $NO^{3-} < Cl^- < SO_4^{2-} < CO_3^{2-} < PO_4^{2-}$.

Similarly, antibiotic sorption efficiency is also affected by the existence of competing anions. Eniola et al. [130] studied the effect of coexisting $CuSO_4$, NaCl, and $NaHCO_3$ salts on the adsorption of oxytetracycline (OTC) antibiotics by $CuFe_2O_4$-Ni/Mg/Al-LDH. Based on the results, $CuSO_4$ salt promotes OTC adsorption onto the LDH composite due to the protonation of the adsorbent surface by the Cu^{2+} ions, providing more active sites for negatively charged OTC molecule adsorption by electrostatic attraction, whereas NaCl salt suppresses OTC adsorption onto the LDH composite.

4.3. Adsorption isotherm models

Isotherm models are essential to foresee the full adsorption behavior of practical applications and calculate the maximum amount of contaminants removed from polluted water at a constant temperature. Freundlich and Langmuir adsorption isotherms are most commonly utilized to model isotherm data. The Freundlich adsorption isotherm has an empirical relationship and considers multilayer adsorption

with heterogeneous energy distribution of active sites, accompanied by the interactions of adsorbed molecules [146,147]. The Freundlich model is given by Eq. (9).

$$q_e = K_f \cdot C_e^{1/n} \tag{9}$$

where q_e is an adsorbed amount under equilibrium condition (mg/g); K_f a constant of the Freundlich isotherm (mg/g) (L/mg)$^{1/n}$; C_e a concentration of the sorbate at equilibrium (mg/L), and n is the intensity of the Freundlich adsorption parameter; this indicates the existence of adsorption driving forces and the degree of surface heterogeneity. The parameter n is a dimensionless number ranging from 0 to 10. Where $n > 10$ characterizes an irreversible isotherm, $n > 1$ characterizes preferential adsorption, and $n < 1$ characterizes poor adsorption.

Otherwise, the Langmuir adsorption isotherm is associated with the formation of a monolayer of solute molecules on an adsorbent surface with uniform binding sites. It hypothesizes an adsorption of a homogenous nature, with an equal energy of adsorption for all the active adsorption sites. The Langmuir model is represented by Eq. (10):

$$q_e = \frac{K_L \cdot q_{\max} \cdot C_e}{1 + K_L \cdot C_e} \tag{10}$$

where q_e is an equilibrium sorbate uptake value (mg/g); K_L a constant of the Langmuir isotherm (L/mg); $q_{\max}$ a maximum uptake of sorbate (mg/g); and C_e a concentration of the sorbate at equilibrium (mg/L).

The Langmuir parameters can be used to estimate the favorability and unfavorability of the sorption process. To do so, use Eq. (11) to calculate the dimensionless equilibrium constant R_L.

$$R_L = \frac{1}{1 + K_L C_0} \tag{11}$$

If $R_L > 1$, the process is unfavorable, $0 < R_L <$ L 1 is favorable, $R_L = 1$ is linear, and $R_L = 0$ represents the process's irreversible characteristics [12].

The Temkin adsorption isotherm (TM), a less widely used model, explores the impact of indirect adsorbate–adsorbate interactions on the adsorption system, presuming that the adsorption heat of all molecules in the layer reduces linearly as the surface coverage increases [83]; this is expressed in Eq. (12) [39]:

$$q_e = B \cdot \left(A_T \cdot C_e\right) \tag{12}$$

where B is a constant related to the heat of adsorption, and A_T is the constant of the Temkin isotherm.

The Dubinin–Radushkevich model determines if the sorption process is chemical or physical. It is based on the fact that the size of the sorbate is comparable to the size of the micropores (theory of micropore volume filling), and the adsorption potential (ε) can be used to represent the adsorption equilibrium relationship, independently of temperature. It is given in Eq. (13).

$$q_e = q_s \exp\left(-K_d \varepsilon^2\right) \tag{13}$$

where q_s represents theoretical saturation sorbate adsorption loading; K_d is a constant of Dubinin–Radushkevich; and ε is a potential of Polanyi [68,148,149]. Non-linear regression was employed by [6] to fit an equilibrium adsorption data to all of the previously discussed isotherm models. The best relationship in descending order is reported to ve as follows: Langmuir > Temkin > Freundlich > Dubin in–Radushkevich models, for both the Eriochrome Black T (EBT) and MO dyes. In most studies, the Freundlich model outperforms the Langmuir model in terms of the adsorption data fit [100,103,150]. The maximum adsorption capacities of the LDH-based composites for numerous toxic contaminants are summarized in Table S2.

4.4. Adsorption kinetic models

Adsorption kinetic models are important for fitting the equilibrium data of adsorption because they aid in illustrating rate-limiting steps, as well as the mechanism of interactions between the adsorbent and the adsorbate. Adsorption kinetics is used to measure the diffusion of the solute in the pores and assess the adsorption rate in relation to time, at a constant concentration. Its primary significance is in describing the rate of solute uptake and the time required by the adsorption process to reach equilibrium [12,19]. To predict the order and rate of the adsorption process, two kinetics models are used: The pseudo-first-order model (PFO) mentioned in Eq. (14) and the pseudo-second-order model (PSO) presented in Eq. (15).

$$\ln\left(q_e - q_t\right) = \ln q_e - k_1 \cdot t \tag{14}$$

$$\frac{t}{q_t} = \frac{t}{q_e} + \frac{1}{q_e^2 \cdot k_2} \tag{15}$$

where q_t and q_e are the adsorption rate (mg/g) at time and equilibrium, respectively; k_1 is a constant of the PFO (min^{-1}) and k_2 is a constant of PSO (g/mg·min) [19,129,151]. The regression coefficients and slopes of the straight lines of $\ln(q_e - q_t)$ vs. the time plot (PFO) and t/q_t vs. the time plot (PSO) can be used to postulate the order and rate constant of the adsorption process, respectively. The PSO works well when chemisorption is the rate-controlling step [19,152]. The RBB dye adsorption was investigated by Gidado and Akanyeti on six adsorbents, including MgAl-LDH, ZnAl-LDH, ZnMgAl-LDH, and the calcined forms of each calcined form. It is stated that all three pristine LDHs fit the PFO kinetic model, whereas the three calcined forms fit the PSO kinetic model [153]. Other studies that fit the equilibrium data to kinetic models are summarized in Table S2.

4.5. Regeneration processes

The reuse and regeneration of the spent LDHs is a vital determinant for making a large-scale adsorption system more efficient and economical. An efficient regeneration process should restore the adsorbent to its original properties for effective reuse. Several techniques are available for LDH-based adsorbent regeneration, utilized to remove the described pollutants: (i) thermal treatment, in

which saturated LDHs are heated to high temperatures; (ii) advanced oxidation methods; (iii) desorption processes, with alcohols or salts; and (iv) eluting/mixing appropriate solvents to allow contaminants to be desorbed. Thermal treatment is the most prevalent method for regenerating adsorbents. In the gathered literature, it is important to note that only a few research articles that include LDH regeneration studies were found [8,19,129].

A typical regeneration treatment process for Fe_3O_4-Mg/Al-LDH was conducted by adding 0.01 mol/L $NaNO_3$ and Co^{2+} to Fe_3O_4-Mg/Al-LDH. The solid obtained was washed with HCl and high-purity Milli-Q water, until Co^{2+} could not be determined in the supernatant. The sorption/desorption processes were repeated for eight cycles. Even after eight cycles, the sample that was regenerated was able to remove only 80% of the Co^{2+} [114].

Desorption of adsorbed-Cr(VI) was performed by [100] in the solution of a mixture of Na_2CO_3 and NaOH, and subsequent calcination at 500°C, which regenerated G-MgAl-CLDH at a desorption time of 12 h. After six consecutive adsorption/regeneration cycles, the regenerated sample showed 87.6% removal of Cr(VI), which decreased by only 7.4% compared to the original G-Mg/Al-CLDH.

Guo et al. [144] used the sodium salt of PO_4^{2-} as a desorption solution in their desorption experiment of arsenate As(V) from CuMgFeLa-LDH. The desorption rate of As(V) increased as the concentration of PO_4^{2-} increased. The desorption rate reached 52.5% when the PO_4^{2-} concentration was 1,000 mg/L. After six regeneration cycles using ethanol and an HCl mixture as regenerating agents, the adsorption efficiency of Pb^{2+} on G-MgAl-LDH was practically constant [133]. Sodium acetate was also utilized to investigate Pb^{2+} desorption [154].

The desorption of anionic dye happens easily in an alkaline solution, as the electrostatic attraction between the surface of the adsorbent and the dye molecule is weakened. Ahmed et al. [68] were successfully able to remove 90% of the dye after five cycles of elution in warm water for 2 h. For the cationic dye MB removal, Aldawsari et al. [155] utilized a mixture solution of NaCl and M HCl, which yielded 70% removal of the dye after five regeneration cycles. A mixture of Co^{2+} and ozone was used as a catalyst and oxidant to degrade MO adsorbed on a rGO/Ni/MMO hybrid for 5 min, showing just a 15% reduction in the removal efficiency of MO on the rGO/Ni/MMO hybrid after five regeneration cycles [101].

A different approach was employed by investigators [23] to remove MO dye from ZnAl-CLDH@C nanosheets, using desorption with Na_2CO_3 and NaOH solutions. Then, a thermal treatment was performed. Even after five cycles of regeneration, the composite nanosheets' morphology was still unchanged, as evidenced by the SEM photographs, and yielded up to 96% of MO dye removal. Meili et al. [156] desorbed MB from a biochar-LDH composite using a methanol and sodium chloride mixture. Six regeneration cycles were implemented; the thermal treatment was performed after the third cycle of regeneration because it was noticed that the LDH had lost its lamellar morphology after the third regeneration cycle. In general, thermal treatment is applied when the adsorbent-dye interaction is strong and the solvents do not yield the expected results. In this process, a dye-saturated LDH-based adsorbent was heated for a few hours at about 500°C, and the adsorbent's surface was regenerated before being reused [27,69].

The effective desorption of diclofenac antibiotic from spent SiO_2@LDH hierarchical spheres (SiO_2@LDH-HSs) was described by Chen [157]. The regeneration process included utilizing an advanced oxidation method by using an oxone as the oxidant and Co^{2+} ions as the catalysts to decompose the adsorbed diclofenac. The removal efficiency of the regenerated sample was consistently higher than 90%, even after four regeneration cycles. Despite being less efficient, the LDH-based adsorbents have also been regenerated by processes of desorption with ethanol [29], NaOH [128,158], or a mixed salt solution [159]. The antibiotic removal rate of the regenerated adsorbents decreased progressively with each run, which was mostly owing to the incomplete desorption process [128,160]. Table S2 also contains information about the reagents that are commonly used for the regeneration of spent LDHs from aqueous solutions.

4.6. Toxicity of LDH-based composites and related matters

LDHs and their composite materials have promising potential due to their null or low toxicity in water treatment operations. LDHs are suitable as alternative antibiotic delivery mechanisms because they are more stable, biocompatible, and less toxic than the standard nano-antibiotic carriers. Kura et al. [161] studied levodopa antibiotic delivery with Zn/Al-LDH. The negatively charged antibiotic levodopa provided further stability between the two positively charged layers of LDH. An intercalated, controlled, and targeted antibiotic delivery has been developed to be non-toxic. LDHs have also been investigated for pharmaceutical formulations, such as for cancer therapy, due to their non-toxicity, and it does not have side effects on human health therapy when compared to the other nano-antibiotic carriers [21]. Moreover, LDHs have been extensively used in water treatment research over the last decade, with no reported health risks. LDHs have the ability to efficiently remove toxic heavy metals and harmful dyes from water, making the water suitable for drinking. Furthermore, due to the clayey nature of LDHs, they have a beneficial health effect on humans rather than a toxic one [21].

5. Conclusion

The process of developing adsorbents is a continuous one due to the importance of these materials in the wastewater-treatment process, especially for the removal of pollutants that are dangerous or toxic in nature. This study has reviewed previous studies discussing the utilization of LDHs to remove various pollutants by adsorption. It finds that LDHs have a high adsorption capacity for many organic and inorganic pollutants. In addition, the LDH adsorption capacity is significantly dependent on environmental conditions such as the pH value. Isotherm and kinetic adsorption processes have also been discussed, and it is found that the adsorption process mostly obeys the Langmuir isotherm and second-order kinetic models, indicating the adsorption of pollutant molecules via chemosorption onto the monolayer of the homogeneous LDH active sites. However, there

is a scientific gap represented by the use of LDHs for the removal of radioactive materials and gaseous pollutants. In terms of performance, LDHs exhibit the highest adsorption capacity for dye removal, reaching up to 9,127 mg/g for Congo red dye.

Acknowledgment

The authors are grateful to the University of Baghdad, Al-Mustaqbal University College, and University of Kerbala.

Funding

The authors declare that no funds, grants, or other support were received during the preparation of this manuscript.

Declaration of interests

The authors declare that they have no known competing financial interests or personal relationships that could have appeared to influence the work reported in this paper.

References

[1] M. Manyangadze, N.H.M. Chikuruwo, T.B. Narsaiah, C.S. Chakra, M. Radhakumari, G. Danha, Enhancing adsorption capacity of nano-adsorbents via surface modification: a review, S. Afr. J. Chem. Eng., 31 (2020) 25–32.
[2] Y. Lu, B. Jiang, L. Fang, F. Ling, J. Gao, F. Wu, X. Zhang, High performance NiFe layered double hydroxide for methyl orange dye and Cr(VI) adsorption, Chemosphere, 152 (2016) 415–422.
[3] F.A. Al-Nasrawi, S.L. Kareem, L.A. Saleh, Using the Leopold Matrix Procedure to assess the environmental impact of pollution from drinking water projects in Karbala City, Iraq, IOP Conf. Ser.: Mater. Sci. Eng., 671 (2020) 012078, doi: 10.1088/1757-899X/671/1/012078.
[4] K. El Hassani, B.H. Beakou, D. Kalnina, E. Oukani, A. Anouar, Effect of morphological properties of layered double hydroxides on adsorption of azo dye methyl orange: a comparative study, Appl. Clay Sci., 140 (2017) 124–131.
[5] N.D. Mu'azu, N. Jarrah, T.S. Kazeem, M. Zubair, M. Al-Harthi, Bentonite-layered double hydroxide composite for enhanced aqueous adsorption of Eriochrome Black T, Appl. Clay Sci., 161 (2018) 23–34.
[6] N.I. Blaisi, M. Zubair, S. Ali, T.S. Kazeem, Date palm ash-MgAl-layered double hydroxide composite: sustainable adsorbent for effective removal of methyl orange and Eriochrome Black T from aqueous phase, Environ. Sci. Pollut. Res., 25 (2018) 34319–34331.
[7] M. Sajid, Toxicity of nanoscale metal organic frameworks: a perspective, Environ. Sci. Pollut. Res., 23 (2016) 14805–14807.
[8] M. Zubair, M. Daud, G. McKay, F. Shehzad, M.A. Al-Harthi, Recent progress in layered double hydroxides (LDH)-containing hybrids as adsorbents for water remediation, Appl. Clay Sci., 143 (2017) 279–292.
[9] WHO, Guidelines for Drinking-Water Quality, World Health Organization, Lenntech USA LLC, 2016.
[10] M. Boshir Ahmed, J.L. Zhou, H. Hao Ngo, W. Guo, N.S. Thomaidis, J. Xu, Progress in the biological and chemical treatment technologies for emerging contaminant removal from wastewater: a critical review, J. Hazard. Mater., 323 (2017) 274–298.
[11] D.P. Mohapatra, D.M. Kirpalani, Advancement in treatment of wastewater: fate of emerging contaminants, Can. J. Chem. Eng., 97 (2019) 2621–2631.
[12] F.A.M. Alnasrawi, S.L. Kareem, L.A. Mohammed Saleh, Adsorption of methylene blue from aqueous solution using different types of activated carbon, J. Appl. Water Eng. Res. (2022), doi: 10.1080/23249676.2022.2120918.
[13] G. George, M.P. Saravanakumar, Facile synthesis of carbon-coated layered double hydroxide and its comparative characterisation with Zn-Al LDH: application on crystal violet and malachite green dye adsorption—isotherm, kinetics and Box–Behnken design, Environ. Sci. Pollut. Res., 25 (2018) 30236–30254.
[14] L. Santamaría, M. López-aizpún, M. García-padial, M.A. Vicente, S.A. Korili, A. Gil, Zn-Ti-Al layered double hydroxides synthesized from aluminum saline slag wastes as efficient drug adsorbents, Appl. Clay Sci., 187 (2020) 105486, doi: 10.1016/j.clay.2020.105486.
[15] M. Shamsayei, Y. Yamini, H. Asiabi, Fabrication of zwitterionic histidine/layered double hydroxide hybrid nanosheets for highly efficient and fast removal of anionic dyes, J. Colloid Interface Sci., 529 (2018) 255–264.
[16] A. Li, H. Deng, C. Ye, Y. Jiang, Fabrication and characterization of novel ZnAl-layered double hydroxide for the superadsorption of organic contaminants from wastewater, ACS Omega, 5 (2020) 15152–15161.
[17] S. Yang, L. Wang, X. Zhang, W. Yang, G. Song, Enhanced adsorption of Congo red dye by functionalized carbon nanotube/mixed metal oxides nanocomposites derived from layered double hydroxide precursor, Chem. Eng. J., 275 (2015) 315–321.
[18] Z. Tang, Z. Qiu, S. Lu, X. Shi, Functionalized layered double hydroxide applied to heavy metal ions absorption: a review, Nanotechnol. Rev., 9 (2020) 800–819.
[19] J. Mittal, Recent progress in the synthesis of layered double hydroxides and their application for the adsorptive removal of dyes: a review, J. Environ. Manage., 295 (2021) 113017, doi: 10.1016/j.jenvman.2021.113017.
[20] Z. Gu, J. James Atherton, Z.P. Xu, Hierarchical layered double hydroxide nanocomposites: structure, synthesis and applications, Chem. Commun., 51 (2015) 3024–3036.
[21] C. Del Hoyo, Layered double hydroxides and human health: an overview, Appl. Clay Sci., 36 (2007) 103–121.
[22] M.A. González, I. Pavlovic, C. Barriga, Cu(II), Pb(II) and Cd(II) sorption on different layered double hydroxides. A kinetic and thermodynamic study and competing factors, Chem. Eng. J., 269 (2015) 221–228.
[23] M. Li, G. Wu, Z. Liu, X. Xi, Y. Xia, J. Ning, D. Yang, A. Dong, Uniformly coating ZnAl layered double oxide nanosheets with ultra-thin carbon by ligand and phase transformation for enhanced adsorption of anionic pollutants, J. Hazard. Mater., 397 (2020) 122766, doi: 10.1016/j.jhazmat.2020.122766.
[24] W. Chen, J. Xing, Z. Lu, J. Wang, S. Yu, W. Yao, A.M. Asiri, K.A. Alamry, X. Wang, S. Wang, Citrate-modified Mg-Al layered double hydroxides for efficient removal of lead from water, Environ. Chem. Lett., 16 (2018) 561–567.
[25] M. Laipan, J. Zhu, Y. Xu, L. Sun, R. Zhu, Fabrication of layered double hydroxide/carbon nanomaterial for heavy metals removal, Appl. Clay Sci., 199 (2020) 105867, doi: 10.1016/j.clay.2020.105867.
[26] D. Chaara, I. Pavlovic, F. Bruna, M.A. Ulibarri, K. Draoui, C. Barriga, Removal of nitrophenol pesticides from aqueous solutions by layered double hydroxides and their calcined products, Appl. Clay Sci., 50 (2010) 292–298.
[27] S. Boubakri, M.A. Djebbi, Z. Bouaziz, P. Namour, N. Jaffrezic-Renault, A.B.H. Amara, M. Trabelsi-Ayadi, I. Ghorbel-Abid, R. Kalfat, Removal of two anionic reactive textile dyes by adsorption into MgAl-layered double hydroxide in aqueous solutions, Environ. Sci. Pollut. Res., 25 (2018) 23817–23832.
[28] R.M.M. dos Santos, R.G.L. Gonçalves, V.R.L. Constantino, C.V. Santilli, P.D. Borges, J. Tronto, F.G. Pinto, Adsorption of Acid Yellow 42 dye on calcined layered double hydroxide: effect of time, concentration, pH and temperature, Appl. Clay Sci., 140 (2017) 132–139.
[29] G. Rathee, N. Singh, R. Chandra, Simultaneous elimination of dyes and antibiotic with a hydrothermally generated NiAlTi layered double hydroxide adsorbent, ACS Omega, 5 (2020) 2368–2377.

[30] C. Yang, L. Wang, Y. Yu, P. Wu, F. Wang, S. Liu, X. Luo, Highly efficient removal of amoxicillin from water by Mg-Al layered double hydroxide/cellulose nanocomposite beads synthesized through *in-situ* co-precipitation method, Int. J. Biol. Macromol., 149 (2020) 93–100.
[31] E. Li, L. Liao, G. Lv, Z. Li, C. Yang, Y. Lu, The interactions between three typical PPCPs and LDH, Front. Chem., 6 (2018) 1–9.
[32] A.L. Johnston, E. Lester, O. Williams, R.L. Gomes, Understanding layered double hydroxide properties as sorbent materials for removing organic pollutants from environmental waters, J. Environ. Chem. Eng., 9 (2021) 13, doi: 10.1016/j.jece.2021.105197.
[33] L.X. Zhao, J.L. Liang, N. Li, H. Xiao, L.Z. Chen, R.S. Zhao, Kinetic, thermodynamic and isotherm investigations of Cu^{2+} and Zn^{2+} adsorption on Li-Al hydrotalcite-like compound, Sci. Total Environ., 716 (2020) 137120, doi: 10.1016/j.scitotenv.2020.137120.
[34] X. He, X. Qiu, C. Hu, Y. Liu, Treatment of heavy metal ions in wastewater using layered double hydroxides: a review, J. Dispersion Sci. Technol., 39 (2018) 792–801.
[35] J.J. Bravo-Suárez, E.A. Páez-Mozo, S.T. Oyama, Review of the synthesis of layered double hydroxides: a thermodynamic approach, Quim. Nova, 27 (2004) 601–604.
[36] S. Daniel, S. Thomas, 1 - Layered Double Hydroxides: Fundamentals to Applications, S. Thomas, S. Daniel, Eds., Layered Double Hydroxide Polymer Nanocomposites: Woodhead Publishing Series in Composites Science and Engineering, Elsevier, 2020, doi: 10.1016/b978-0-08-101903-0.00001-5.
[37] F.A. Alnasrawi, A.A. Mohammed, T.J. Al-Musawi, Synthesis, characterization and adsorptive performance of CuMgAl-layered double hydroxides/montmorillonite nanocomposite for the removal of Zn(II) ions, Environ. Nanotechnol. Monit. Manage., 19 (2023) 100771, doi: 10.1016/j.enmm.2022.100771.
[38] Y. Cao, G. Li, X. Li, Graphene/layered double hydroxide nanocomposite: properties, synthesis, and applications, Chem. Eng. J., 292 (2016) 207–223.
[39] F.A. Alnasrawi, A.A. Mohammed, Enhancement of Cd^{2+} removal on CuMgAl-layered double hydroxide/montmorillonite nanocomposite: kinetic, isotherm, and thermodynamic studies, Arabian J. Chem., 16 (2023) 104471, doi: 10.1016/j.arabjc.2022.104471.
[40] M.V. Bukhtiyarova, A review on effect of synthesis conditions on the formation of layered double hydroxides, J. Solid State Chem., 269 (2019) 494–506.
[41] J. Wang, T. Zhang, M. Li, Y. Yang, P. Lu, P. Ning, Q. Wang, Arsenic removal from water/wastewater using layered double hydroxide derived adsorbents, a critical review, RSC Adv., 8 (2018) 22694–22709.
[42] F.L. Theiss, G.A. Ayoko, R.L. Frost, Synthesis of layered double hydroxides containing Mg^{2+}, Zn^{2+}, Ca^{2+} and Al^{3+} layer cations by co-precipitation methods – a review, Appl. Surf. Sci., 383 (2016) 200–213.
[43] J.J. Bravo-suárez, E.A. Páez-mozo, S.T. Oyama, Review of the synthesis of laywreds double hydroxides: a thermodynamic aproach, Quim. Nova, 27 (2004) 601–614.
[44] F.B.D. Saiah, B.L. Su, N. Bettahar, Nickel-iron layered double hydroxide (LDH): textural properties upon hydrothermal treatments and application on dye sorption, J. Hazard. Mater., 165 (2009) 206–217.
[45] R. Shan, L. Yan, Y. Yang, K. Yang, S. Yu, H. Yu, Highly efficient removal of three red dyes by adsorption onto Mg-Al-layered double hydroxide, J. Ind. Eng. Chem., 21 (2014) 561–568.
[46] W.K. Ng'etich, B.S. Martincigh, A critical review on layered double hydroxides: their synthesis and application in sunscreen formulations, Appl. Clay Sci., 208 (2021) 106095, doi: 10.1016/j.clay.2021.106095.
[47] G.E. de Souza dos Santos, P.V. dos Santos Lins, L.M.T. de Magalhães Oliveira, E.O. da Silva, I. Anastopoulos, A. Erto, D.A. Giannakoudakis, A.R.F. de Almeida, J.L. da Silva Duarte, L. Meili, Layered double hydroxides/biochar composites as adsorbents for water remediation applications: recent trends and perspectives, J. Cleaner Prod., 284 (2020) 124755, doi: 10.1016/j.jclepro.2020.124755.
[48] M. Daud, A. Hai, F. Banat, M.B. Wazir, M. Habib, G. Bharath, M.A. Al-Harthi, A review on the recent advances, challenges and future aspect of layered double hydroxides (LDH)-containing hybrids as promising adsorbents for dyes removal, J. Mol. Liq., 288 (2019) 110989, doi: 10.1016/j.molliq.2019.110989.
[49] X. Ruan, Y. Chen, H. Chen, G. Qian, R.L. Frost, Sorption behavior of methyl orange from aqueous solution on organic matter and reduced graphene oxides modified Ni-Cr layered double hydroxides, Chem. Eng. J., 297 (2016) 295–303.
[50] H.P. Chao, Y.C. Wang, H.N. Tran, Removal of hexavalent chromium from groundwater by Mg/Al-layered double hydroxides using characteristics of *in-situ* synthesis, Environ. Pollut., 243 (2018) 620–629.
[51] N. Chubar, V. Gerda, O. Megantari, M. Mičušík, M. Omastova, K. Heister, P. Man, J. Fraissard, Applications versus properties of Mg-Al layered double hydroxides provided by their syntheses methods: alkoxide and alkoxide-free sol–gel syntheses and hydrothermal precipitation, Chem. Eng. J., 234 (2013) 284–299.
[52] H.N. Tran, C. Lin, S. Han, H. Chao, Efficient removal of copper and lead by Mg/Al layered double hydroxides intercalated with organic acid anions: adsorption kinetics, isotherms, and thermodynamics, Appl. Clay Sci., 154 (2018) 17–27.
[53] H.N. Tran, D.T. Nguyen, G.T. Le, F. Tomul, E.C. Lima, S.H. Woo, A.K. Sarmah, H.Q. Nguyen, P.T. Nguyen, D.D. Nguyen, T.V. Nguyen, S. Vigneswaran, D.V.N. Vo, H.P. Chao, Adsorption mechanism of hexavalent chromium onto layered double hydroxides-based adsorbents: a systematic in-depth review, J. Hazard. Mater., 373 (2019) 258–270.
[54] L. Châtelet, J.Y. Bottero, J. Yvon, A. Bouchelaghem, Competition between monovalent and divalent anions for calcined and uncalcined hydrotalcite: anion-exchange and adsorption sites, Colloids Surf., A, 111 (1996) 167–175.
[55] S. Lin, H. Nguyen, H. Chao, J. Lee, Layered double hydroxides intercalated with sulfur-containing organic solutes for efficient removal of cationic and oxyanionic metal ions, Appl. Clay Sci., 162 (2018) 443–453.
[56] X. He, X. Qiu, J. Chen, Preparation of Fe(II)-Al layered double hydroxides: application to the adsorption/reduction of chromium, Colloids Surf., A, 516 (2017) 362–374.
[57] L. Alidokht, S. Oustan, A. Khataee, Removal of chromate from aqueous solution by reduction with nanoscale Fe-Al layered double hydroxide, Res. Chem. Intermed., 44 (2018) 2319–2331.
[58] I. Clark, J. Smith, R.L. Gomes, E. Lester, Continuous synthesis of Zn_2Al-CO_3 layered double hydroxides for the adsorption of reactive dyes from water, J. Environ. Chem. Eng., 7 (2019) 103175, doi: 10.1016/j.jece.2019.103175.
[59] K. Takehira, Recent development of layered double hydroxide-derived catalysts − rehydration, reconstitution, and supporting, aiming at commercial application, Appl. Clay Sci., 136 (2017) 112–141.
[60] L.A. Ramírez-Llamas, R. Leyva-Ramos, A. Jacobo-Azuara, J.M. Martínez-Rosales, E. Isaacs-Paez, Adsorption of fluoride from aqueous solution on calcined and uncalcined, Adsorpt. Sci. Technol., 44 (2015) 393–410.
[61] J. Oh, S. Hwang, J. Choy, The effect of synthetic conditions on tailoring the size of hydrotalcite particles, Solid State Ionics. 151 (2002) 285–291.
[62] N.B. Allou, P. Saikia, A. Borah, R.L. Goswamee, Hybrid nanocomposites of layered double hydroxides: an update of their biological applications and future prospects, Colloid Polym Sci., 295 (2017) 725–747.
[63] G. Li, Z. Zhao, J. Liu, G. Jiang, Effective heavy metal removal from aqueous systems by thiol functionalized magnetic mesoporous silica, J. Hazard. Mater., 192 (2011) 277–283.
[64] D.G. Evans, R.C.T. Slade, Structural Aspects of Layered Double Hydroxides, 2005, pp. 1–87.
[65] G. Abellán, J.A. Carrasco, E. Coronado, 10 – Layered Double Hydroxide Nanocomposites Based on Carbon Nanoforms, S. Thomas, S. Daniel, Eds., Layered Double Hydroxide Polymer

Nanocomposites: Woodhead Publishing Series in Composites Science and Engineering, Woodhead Publishing, 2020, pp. 411–460, doi: 10.1016/b978-0-08-101903-0.00010-6.
[66] L. Guo, W. Wu, Y. Zhou, F. Zhang, R. Zeng, J. Zeng, Layered double hydroxide coatings on magnesium alloys: a review, Mater. Sci. Technol., 34 (2018) 1455–1466.
[67] S.M. Auerbach, K.A. Carrado, P.K. Dutta, Handbook of Layered Materials, Marcel Dekker Inc., New York, 2004.
[68] M.A. Ahmed, A.A. Brick, A.A. Mohamed, An efficient adsorption of indigo carmine dye from aqueous solution on mesoporous Mg/Fe layered double hydroxide nanoparticles prepared by controlled sol–gel route, Chemosphere, 174 (2017) 280–288.
[69] K. Abdellaoui, I. Pavlovic, M. Bouhent, A. Benhamou, C. Barriga, A comparative study of the amaranth azo dye adsorption/desorption from aqueous solutions by layered double hydroxides, Appl. Clay Sci., 143 (2017) 142–150.
[70] A. Grover, I. Mohiuddin, A.K. Malik, J.S. Aulakh, K.H. Kim, Zn-Al layered double hydroxides intercalated with surfactant: synthesis and applications for efficient removal of organic dyes, J. Cleaner Prod., 240 (2019) 118090, doi: 10.1016/j.jclepro.2019.118090.
[71] P. Zhang, S. Ouyang, P. Li, Y. Huang, R.L. Frost, Enhanced removal of ionic dyes by hierarchical organic three-dimensional layered double hydroxide prepared via soft-template synthesis with mechanism study, Chem. Eng. J., 360 (2019) 1137–1149.
[72] M. Adachi-Pagano, C. Forano, J.P. Besse, Synthesis of Al-rich hydrotalcite-like compounds by using the urea hydrolysis reaction – control of size and morphology, J. Mater. Chem., 13 (2003) 1988–1993.
[73] H. Pang, Y. Wu, X. Wang, B. Hu, X. Wang, Recent advances in composites of graphene and layered double hydroxides for water remediation: a review, Chem. – An Asian J., 14 (2019) 2542–2552.
[74] J. Liu, J. Song, H. Xiao, L. Zhang, Y. Qin, D. Liu, W. Hou, N. Du, Synthesis and thermal properties of ZnAl layered double hydroxide by urea hydrolysis, Powder Technol., 253 (2014) 41–45.
[75] C. Lei, X. Zhu, B. Zhu, C. Jiang, Y. Le, J. Yu, Superb adsorption capacity of hierarchical calcined Ni/Mg/Al layered double hydroxides for Congo red and Cr(VI) ions, J. Hazard. Mater., 321 (2016) 801–811.
[76] M. Bini, F. Monteforte, Layered double hydroxides (LDHs): versatile and powerful hosts for different applications, Anal. Pharm. Res., 7 (2018) 12–14.
[77] T. Lopez, P. Bosch, E. Ramos, R. Gomez, O. Novaro, D. Acosta, F. Figueras, Synthesis and characterization of sol–gel hydrotalcites. Structure and texture, Langmuir, 12 (1996) 189–192.
[78] S.M.C. Verryn, Æ.W.W. Focke, Surfactant-assisted fatty acid intercalation of layered double hydroxides, J. Mater. Sci. Technol., 43 (2008) 1033–1043.
[79] A. De Roy, C. Forano, J.P. Besse, Layered Double Hydroxides: Synthesis and Post Synthesis Modification, V. Rives, Ed., Layered Double Hydroxides: Present and Future, New York, 2001, pp. 1–39.
[80] Y. Cao, D. Zheng, F. Zhang, J. Pan, C. Lin, Layered double hydroxide (LDH) for multi-functionalized corrosion protection of metals: a review, J. Mater. Sci. Technol., 102 (2022) 232–263.
[81] G. Starukh, O. Rozovik, O. Oranska, Organo/Zn-Al LDH nanocomposites for cationic dye removal from aqueous media, Nanoscale Res. Lett., 11 (2016) 228, doi: 10.1186/s11671-016-1402-0.
[82] N. Almoisheer, F.A. Alseroury, R. Kumar, M. Aslam, M.A. Barakat, Adsorption and anion-exchange insight of indigo carmine onto CuAl-LDH/SWCNTs nanocomposite: kinetic, thermodynamic and isotherm analysis, RSC Adv., 9 (2019) 560–568.
[83] X. Zhang, L. Yan, J. Li, H. Yu, Adsorption of heavy metals by L-cysteine intercalated layered double hydroxide: kinetic, isothermal and mechanistic studies, J. Colloid Interface Sci., 562 (2020) 149–158.
[84] S. Lei, S. Wang, B. Gao, Y. Zhan, Q. Zhao, S. Jin, G. Song, X. Lyu, Y. Zhang, Y. Tang, Ultrathin dodecyl-sulfate-intercalated Mg-Al layered double hydroxide nanosheets with high adsorption capability for dye pollution, J. Colloid Interface Sci., 577 (2020) 181–190.
[85] M.T. Amin, A.A. Alazba, M. Shafiq, LDH of NiZnFe and its composites with carbon nanotubes and data-palm biochar with efficient adsorption capacity for RB5 dye from aqueous solutions: isotherm, kinetic, and thermodynamics studies, Curr. Appl. Phys., 40 (2022) 90–100.
[86] F. Lyu, H. Yu, T. Hou, L. Yan, X. Zhang, B. Du, Efficient and fast removal of Pb^{2+} and Cd^{2+} from an aqueous solution using a chitosan/Mg-Al-layered double hydroxide nanocomposite, J. Colloid Interface Sci., 539 (2019) 184–193.
[87] J.-W. Zhang, A.D. Nur'aini, Y.-C. Wang, N.D. Hai, D. Van Minh, H.-P. Chao, Multiple pollutants removal by carbon sphere and layered double hydroxide composites: adsorption behavior and mechanisms, J. Environ. Chem. Eng., 10 (2022) 108014, doi: 10.1016/j.jece.2022.108014.
[88] D. Bin Jiang, C. Jing, Y. Yuan, L. Feng, X. Liu, F. Dong, B. Dong, Y.X. Zhang, 2D-2D growth of NiFe LDH nanoflakes on montmorillonite for cationic and anionic dye adsorption performance, J. Colloid Interface Sci., 540 (2019) 398–409.
[89] Z.-Q. Zhang, H.-Y. Zeng, X.-J. Liu, S. Xu, C.-R. Chen, J.-D. Du, Modification of MgAl hydrotalcite by ammonium sulfate for enhancement of lead adsorption, J. Taiwan Inst. Chem. Eng., 60 (2016) 361–368.
[90] Y. Li, H.Y. Bi, X.Q. Shi, Simultaneous adsorption of heavy metal and organic pollutant onto citrate-modified layered double hydroxides with dodecylbenzenesulfonate, J. Environ. Eng. Sci., 32 (2015) 666–675.
[91] L. Ma, Q. Wang, S.M. Islam, Y. Liu, S. Ma, M.G. Kanatzidis, Highly selective and efficient removal of heavy metals by layered double hydroxide intercalated with the MoS_4^{2-} ion, J. Am. Chem. Soc., 138 (2016) 2858–2866.
[92] M.A. González, I. Pavlovic, R. Rojas-Delgado, C. Barriga, Removal of Cu^{2+}, Pb^{2+} and Cd^{2+} by layered double hydroxide-humate hybrid. Sorbate and sorbent comparative studies, Chem. Eng. J., 254 (2014) 605–611.
[93] X. Liang, W. Hou, Y. Xu, G. Sun, L. Wang, Y. Sun, X. Qin, Sorption of lead ion by layered double hydroxide intercalated with diethylenetriaminepentaacetic acid, Colloids Surf., A, 366 (2010) 50–57.
[94] G. Liu, Z. Zhu, N. Zhao, Y. Fang, Y. Gao, Y. Zhu, L. Zhang, Mn-Fe layered double hydroxide intercalated with ethylenediaminetetraacetate anion: synthesis and removal of As(III) from aqueous solution around pH 2–11, Int. J. Environ. Res. Public Health., 17 (2020) 9341, doi: 10.3390/ijerph17249341.
[95] Y. Shen, X. Zhao, X. Zhang, S. Li, D. Liu, L. Fan, Removal of Pb^{2+} from the aqueous solution by tartrate intercalated layered double hydroxides, Korean J. Chem. Eng., 33 (2016) 159–169.
[96] L. Chen, H. Xu, J. Xie, X. Liu, Y. Yuan, P. Liu, Z. Qu, N. Yan, $[SnS_4]^{4-}$ clusters modified MgAl-LDH composites for mercury ions removal from acid wastewater, Environ. Pollut., 247 (2019) 146–154.
[97] M.R. Pérez, I. Pavlovic, C. Barriga, J. Cornejo, M.C. Hermosín, M.A. Ulibarri, Uptake of Cu^{2+}, Cd^{2+} and Pb^{2+} on Zn-Al layered double hydroxide intercalated with EDTA, Appl. Clay Sci., 32 (2006) 245–251.
[98] N. Rouahna, D. Barkat, A. Ouakouak, E. Srasra, Synthesis and characterization of Mg-Al layered double hydroxide intercalated with D_2EHPA: application for copper ions removal from aqueous solution, J. Environ. Chem. Eng., 6 (2018) 1226–1232.
[99] S. Olivera, C. Hu, G.S. Nagananda, N. Reddy, K. Venkatesh, H.B. Muralidhara, Multipurpose composite for heavy metal sorption, antimicrobial, and antioxidant applications, Int. J. Environ. Sci. Technol., 16 (2019) 2017–2030.

[100] X. Yuan, Y. Wang, J. Wang, C. Zhou, Q. Tang, X. Rao, Calcined graphene/MgAl-layered double hydroxides for enhanced Cr(VI) removal, Chem. Eng. J., 221 (2013) 204–213.
[101] Z. Yang, S. Ji, W. Gao, C. Zhang, L. Ren, W. Weei, Z. Zhang, J. Pan, T. Liu, Magnetic nanomaterial derived from graphene oxide/layered double hydroxide hybrid for efficient removal of methyl orange from aqueous solution, J. Colloid Interface Sci., 408 (2013) 25–32.
[102] X.L. Wu, L. Wang, C.L. Chen, A.W. Xu, X.K. Wang, Water-dispersible magnetite-graphene-LDH composites for efficient arsenate removal, J. Mater. Chem., 21 (2011) 17353–17359.
[103] J. Gong, T. Liu, X. Wang, X. Hu, L. Zhang, Efficient removal of heavy metal ions from aqueous systems with the assembly of anisotropic layered double hydroxide nanocrystals@ carbon nanosphere, Environ. Sci. Technol., 45 (2011) 6181–6187.
[104] X. Zhang, J. Wang, R. Li, Q. Dai, R. Gao, Q. Liu, M. Zhang, Preparation of Fe_3O_4@C@layered double hydroxide composite for magnetic separation of uranium, Ind. Eng. Chem. Res., 52 (2013) 10152–10159.
[105] M. Zhang, B. Gao, Y. Yao, M. Inyang, Phosphate removal ability of biochar/MgAl-LDH ultra-fine composites prepared by liquid-phase deposition, Chemosphere, 92 (2013) 1042–1047.
[106] L. Tan, Y. Wang, Q. Liu, J. Wang, X. Jing, L. Liu, J. Liu, D. Song, Enhanced adsorption of uranium(VI) using a three-dimensional layered double hydroxide/graphene hybrid material, Chem. Eng. J., 259 (2015) 752–760.
[107] N. Wang, J. Sun, H. Fan, S. Ai, Anion-intercalated layered double hydroxides modi fi ed test strips for detection of heavy metal ions, Talanta, 148 (2016) 301–307.
[108] S. Ma, Q. Chen, H. Li, P. Wang, S.M. Islam, Q. Gu, X. Yang, M.G. Kanatzidis, Highly selective and efficient heavy metal capture with polysulfide intercalated layered double hydroxides, J. Mater. Chem. A, 2 (2014) 10280–10289.
[109] G. Huang, D. Wang, S. Ma, J. Chen, L. Jiang, P. Wang, A new, low-cost adsorbent: preparation, characterization, and adsorption behavior of Pb(II) and Cu(II), J. Colloid Interface Sci., 445 (2015) 294–302.
[110] M. Zhang, Q. Yao, C. Lu, Z. Li, W. Wang, Layered double hydroxide-carbon dot composite: high-performance adsorbent for removal of anionic organic dye, ACS Appl. Mater. Interfaces, 6 (2014) 20225–20233.
[111] M. Daud, M.S. Kamal, F. Shehzad, M.A. Al-harthi, Graphene/layered double hydroxides nanocomposites: a review of recent progress in synthesis and applications, Carbon N.Y., 104 (2016) 241–252.
[112] R. ran Shan, L. guo Yan, K. Yang, Y. feng Hao, B. Du, Adsorption of Cd(II) by Mg-Al-CO_3- and magnetic Fe_3O_4/Mg-Al-CO_3-layered double hydroxides: kinetic, isothermal, thermodynamic and mechanistic studies, J. Hazard. Mater., 299 (2015) 42–49.
[113] D. Chen, Y. Li, J. Zhang, J. Zhou, Y. Guo, H. Liu, Magnetic Fe_3O_4/ZnCr-layered double hydroxide composite with enhanced adsorption and photocatalytic activity, Chem. Eng. J., 185–186 (2012) 120–126.
[114] J. Shou, C. Jiang, F. Wang, M. Qiu, Q. Xu, Fabrication of Fe_3O_4/MgAl-layered double hydroxide magnetic composites for the effective decontamination of Co(II) from synthetic wastewater, J. Mol. Liq., 207 (2015) 216–223.
[115] H. Zhang, F. Huang, D. Liu, P. Shi, Highly efficient removal of Cr(VI) from wastewater via adsorption with novel magnetic Fe_3O_4@C@MgAl-layered double-hydroxide, Chin. Chem. Lett., 26 (2015) 1137–1143.
[116] D.N. Ahmed, L.A. Naji, A.A.H. Faisal, N. Al-Ansari, M. Naushad, Waste foundry sand/MgFe-layered double hydroxides composite material for efficient removal of Congo red dye from aqueous solution, Sci. Rep., 10 (2020) 1–12.
[117] I. Harizi, D. Chebli, A. Bouguettoucha, A new Mg-Al-Cu-Fe-LDH composite to enhance the adsorption of Acid Red 66 dye: characterization, kinetics and isotherm analysis, Arabian J. Sci. Eng., 44 (2019) 5245–5261.
[118] H. Zhang, F. Huang, D.L. Liu, P. Shi, Highly efficient removal of Cr(VI) from wastewater via adsorption with novel magnetic Fe_3O_4@C@MgAl-layered double-hydroxide, Chin. Chem. Lett., 26 (2015) 1137–1143.
[119] A. Abbas, A.M. Al-Amer, T. Laoui, M. Almarri, M. Nasser, M. Khraisheh, M.A. Atieh, Heavy metal removal from aqueous solution by advanced carbon nanotubes: critical review of adsorption applications, Sep. Purif. Technol., 157 (2015) 141–161.
[120] F. Yang, S. Sun, X. Chen, Y. Chang, F. Zha, Z. Lei, Mg-Al layered double hydroxides modified clay adsorbents for efficient removal of Pb^{2+}, Cu^{2+} and Ni^{2+} from water, Appl. Clay Sci., 123 (2016) 134–140.
[121] W. Tian, X. Kong, M. Jiang, X. Lei, X. Duan, Hierarchical layered double hydroxide epitaxially grown on vermiculite for Cr(VI) removal, Mater. Lett., 175 (2016) 110–113.
[122] D. Chen, Y. Li, J. Zhang, W. Li, J. Zhou, L. Shao, G. Qian, Efficient removal of dyes by a novel magnetic Fe_3O_4/ZnCr-layered double hydroxide adsorbent from heavy metal wastewater, J. Hazard. Mater., 243 (2012) 152–160.
[123] R. Dos Santos, R. Gonçalves, L. Constantino, L. Da Costa, L. Da Silva, J. Tronto, G. Pinto, Removal of Acid Green 68: 1 from aqueous solutions by calcined and uncalcined layered double hydroxides, Appl. Clay Sci., 80–81 (2013) 189–195.
[124] R. Shan, L. Yan, K. Yang, S. Yu, Y. Hao, Magnetic Fe_3O_4/MgAl-LDH composite for effective removal of three red dyes from aqueous solution, Chem. Eng. J., 252 (2014) 38–46.
[125] L. El Gaini, M. Lakraimi, E. Sebbar, A. Meghea, M. Bakasse, Removal of indigo carmine dye from water to Mg-Al-CO_3-calcined layered double hydroxides, J. Hazard. Mater., 161 (2009) 627–632.
[126] N. Drici Setti, N. Jouini, Z. Derriche, Sorption study of an anionic dye – benzopurpurine 4B – on calcined and uncalcined Mg-Al layered double hydroxides, J. Phys. Chem. Solids, 71 (2010) 556–559.
[127] R. Extremera, I. Pavlovic, M.R. Pérez, C. Barriga, Removal of Acid orange 10 by calcined Mg/Al layered double hydroxides from water and recovery of the adsorbed dye, Chem. Eng. J., 213 (2012) 392–400.
[128] X. Tan, S. Liu, Y. Liu, Y. Gu, G. Zeng, X. Cai, One-pot synthesis of carbon supported calcined-Mg/Al layered double hydroxides for antibiotic removal by slow pyrolysis of biomass waste, Sci. Rep., 6 (2016) 1–12, doi: 10.1038/srep39691.
[129] K. Nava-Andrade, G.G. Carbajal-Arízaga, S. Obregón, V. Rodríguez-González, Layered double hydroxides and related hybrid materials for removal of pharmaceutical pollutants from water, J. Environ. Manage., 288 (2021) 112399, doi: 10.1016/j.jenvman.2021.112399.
[130] J.O. Eniola, R. Kumar, O.A. Mohamed, A.A. Al-Rashdi, M.A. Barakat, Synthesis and characterization of $CuFe_2O_4$/NiMgAl-LDH composite for the efficient removal of oxytetracycline antibiotic, J. Saudi Chem. Soc., 24 (2019) 139–150.
[131] S.A. Abdel Moaty, R.K. Mahmoud, N.A. Mohamed, Y. Gaber, A. Farghali, M.S.M.A. Wahed, H.A. Younes, Synthesis and characterization of LDH-type anionic nanomaterials for effective removal of doxycycline from aqueous media, Water Environ. J., 43 (2016) 1–34, doi: 10.1111/wej.12526.
[132] M. Noori, T.J. Al-musawi, E. Ghahramani, H. Kazemian, M. Zarrabi, Adsorption performance of magnesium/aluminum layered double hydroxide nanoparticles for metronidazole from aqueous solution, Arabian J. Chem., 10 (2017) 611–623.
[133] Z. Yang, F. Wang, C. Zhang, G. Zeng, X. Tan, Z. Yu, Y. Zhong, H. Wang, F. Cui, Utilization of LDH-based materials as potential adsorbents and photocatalysts for the decontamination of dyes wastewater: a review, RSC Adv., 6 (2016) 79415–79436.
[134] F. Yang, S. Sun, X. Chen, Y. Chang, F. Zha, Z. Lei, Mg-Al layered double hydroxides modified clay adsorbents for efficient removal of Pb^{2+}, Cu^{2+} and Ni^{2+} from water, Appl. Clay Sci., 123 (2016) 134–140.
[135] K.H. Goh, T.T. Lim, Z. Dong, Application of layered double hydroxides for removal of oxyanions: a review, Water Res., 42 (2008) 1343–1368.

[136] S. Mallakpour, M. Naghdi, Design and identification of poly(vinyl chloride)/layered double hydroxide@MnO_2 nanocomposite films and evaluation of the methyl orange uptake: linear and non-linear isotherm and kinetic adsorption models, New J. Chem., 44 (2020) 6510–6523.
[137] J. Li, N. Zhang, D.H.L. Ng, Synthesis of a 3D hierarchical structure of γ-AlO(OH)/Mg-Al-LDH/C and its performance in organic dyes and antibiotics adsorption, J. Mater. Chem. A, 3 (2015) 21106–21115.
[138] L. Bo, Q. Li, Y. Wang, L. Gao, X. Hu, J. Yang, One-pot hydrothermal synthesis of thrust spherical Mg-Al layered double hydroxides/MnO_2 and adsorption for Pb(II) from aqueous solutions, J. Environ. Chem. Eng., 3 (2015) 1468–1475.
[139] X. Pan, M. Zhang, H. Liu, S. Ouyang, N. Ding, P. Zhang, Adsorption behavior and mechanism of Acid orange 7 and methylene blue on self-assembled three-dimensional MgAl layered double hydroxide: experimental and DFT investigation, Appl. Surf. Sci., 522 (2020) 146370, doi: 10.1016/j.apsusc.2020.146370.
[140] M. Chen, P. Wu, Z. Huang, J. Liu, Y. Li, N. Zhu, Environmental application of MgMn-layered double oxide for simultaneous efficient removal of tetracycline and Cd pollution: performance and mechanism, J. Environ. Manage., 246 (2019) 164–173.
[141] M.A. Nazir, N.A. Khan, C. Cheng, S.S.A. Shah, T. Najam, M. Arshad, A. Sharif, S. Akhtar, A. ur Rehman, Surface induced growth of ZIF-67 at Co-layered double hydroxide: removal of methylene blue and methyl orange from water, Appl. Clay Sci., 190 (2020) 105564, doi: 10.1016/j.clay.2020.105564.
[142] M. Rosset, L. Weidlich, G. Edith, N. Hidalgo, Adsorbents derived from hydrotalcites for the removal of diclofenac in wastewater, Appl. Clay Sci., 175 (2019) 150–158.
[143] D. Huang, C. Liu, C. Zhang, R. Deng, R. Wang, Bioresource Technology Cr(VI) removal from aqueous solution using biochar modified with Mg/Al-layered double hydroxide intercalated with ethylenediaminetetraacetic acid, Bioresour. Technol., 276 (2019) 127–132.
[144] Y. Guo, Z. Zhu, Y. Qiu, J. Zhao, Adsorption of arsenate on Cu/Mg/Fe/La layered double hydroxide from aqueous solutions, J. Hazard. Mater., 239–240 (2012) 279–288.
[145] Y. Chen, C. Jing, X. Zhang, D. Jiang, X. Liu, B. Dong, L. Feng, S. Li, Y. Zhang, Acid-salt treated CoAl layered double hydroxide nanosheets with enhanced adsorption capacity of methyl orange dye, J. Colloid Interface Sci., 548 (2019) 100–109.
[146] K. Vijayaraghavan, Y.S. Yun, Bacterial biosorbents and biosorption, Biotechnol. Adv., 26 (2008) 266–291.
[147] X. Zhang, L. Yan, J. Li, H. Yu, Adsorption of heavy metals by L-cysteine intercalated layered double hydroxide: kinetic, isothermal and mechanistic studies, J. Colloid Interface Sci., 562 (2020) 149–158.
[148] J. Mittal, Recent progress in the synthesis of layered double hydroxides and their application for the adsorptive removal of dyes: a review, J. Environ. Manage., 295 (2021) 113017, doi: 10.1016/j.jenvman.2021.113017.
[149] S.L. Kareem, A.A. Mohammed, Removal of tetracycline from wastewater using circulating fluidized bed, Iraqi J. Chem. Pet. Eng., 21 (2020) 29–37.
[150] B. Zhang, Z. Dong, D. Sun, T. Wu, Y. Li, Enhanced adsorption capacity of dyes by surfactant-modified layered double hydroxides from aqueous solution, J. Ind. Eng. Chem., 49 (2017) 208–218.
[151] A.A. Mohammed, Biosorption of lead, cadmium, and zinc onto sunflower shell: equilibrium, kinetic, and thermodynamic studies, Iraqi J. Chem. Pet. Eng., 16 (2015) 91–105.
[152] A.A. Mohammed, S.L. Kareem, Adsorption of tetracycline fom wastewater by using Pistachio shell coated with ZnO nanoparticles: equilibrium, kinetic and isotherm studies, Alexandria Eng. J., 58 (2019) 917–928.
[153] S.M. Gidado, I. Akanyeti, Comparison of Remazol Brilliant Blue reactive adsorption on pristine and calcined ZnAl, MgAl, ZnMgAl layered double hydroxides, Water Air Soil Pollut., 231 (2020) 18, doi: 10.1007/s11270-020-04522-0.
[154] S. Yanming, L. Dongbin, L. Shifeng, F. Lihui, C. Shuai, Removal of lead from aqueous solution on glutamate intercalated layered double hydroxide, Arabian J. Chem., 10 (2017) S2295–S2301.
[155] A.M. Aldawsari, I. Alsohaimi, H.M.A. Hassan, Z.E.A. Abdalla, I. Hassan, M.R. Berber, Tailoring an efficient nanocomposite of activated carbon-layered double hydroxide for elimination of water-soluble dyes, J. Alloys Compd., 857 (2021) 157551, doi: 10.1016/j.jallcom.2020.157551.
[156] L. Meili, P.V. Lins, C.L.P.S. Zanta, J.I. Soletti, L.M.O. Ribeiro, C.B. Dornelas, T.L. Silva, M.G.A. Vieira, MgAl-LDH/biochar composites for methylene blue removal by adsorption, Appl. Clay Sci., 168 (2019) 11–20.
[157] C. Chen, P. Wang, T. Lim, L. Liu, S. Liu, R. Xu, A facile synthesis of monodispersed hierarchical layered double hydroxide on silica spheres for efficient removal of pharmaceuticals from water, J. Mater. Chem. A, 1 (2013) 3877–3880.
[158] P.V. dos Santos Lins, D.C. Henrique, A.H. Ide, C.L. de Paiva e Silva Zanta, L. Meili, Evaluation of caffeine adsorption by MgAl-LDH/biochar composite, Environ. Sci. Pollut. Res., 26 (2019) 31804–31811.
[159] K. Panplado, M.S. Subsadsana, S. Srijaranai, S. Sansuk, Rapid removal and efficient recovery of tetracycline antibiotics in aqueous solution using layered double hydroxide components in an *in-situ*-adsorption process, Crystals, 9 (2019) 342, doi: 10.3390/cryst9070342.
[160] R. Ghemit, M. Boutahala, A. Kahoul, Removal of diclofenac from water with calcined ZnAlFe-CO_3 layered double hydroxides: effect of contact time, concentration, pH and temperature, Desal. Water Treat., 83 (2017) 75–85.
[161] A.U. Kura, N.M. Ain, M.Z. Hussein, S. Fakurazi, S.H. Hussein-Al-Ali, Toxicity and metabolism of layered double hydroxide intercalated with levodopa in a Parkinson's disease model, Int. J. Mol. Sci., 15 (2014) 5916–5927.

Supporting information

Table S1
Details of methods and conditions for the synthesis of various layered double hydroxides and their composites

Adsorbent (LDH/ composite)	Adsorbate	Method of synthesis	Cation precursors			Experimental steps/conditions followed	pH	Calcination		References
			Cation	Molar ratio	Anion precursors or/and other compounds			Temp	Time	
Heavy metal as adsorbate										
LDH-H (humate)	Cu^{2+}, Pb^{2+}, Cd^{2+}	C.P.	Magnesium chloride hexahydrates, aluminum chloride hexahydrates, NaCl	–	NaOH, humate	Synthesis was in N_2 atmosphere. The synthesis of (LDH-H) was carried out in 2 steps: the preparation of a chloride, dispersed in a sodium humate solution	8	–	–	[S1]
Citrate-Mg/ Al-LDH	Pb^{2+}	H.Y.	Sodium citrate, magnesium nitrate hexahydrate, aluminum nitrate nonahydrate	–	HNO_3, NaOH, citrate	Stirred for 0.5-h, heated at 80°C for 12-h, the citric-LDH absorbent was acquired by centrifugation, washed, dried at 70°C in vacuum for 12-h	9–10	–	–	[S2]
Mg/Al-LDH	Cu^{2+}, Ni^{2+}, Co^{2+}, Zn^{2+}, Fe^{2+}	C.P.	Magnesium nitrate hexahydrate, aluminum nitrate	3:1	NaOH	Stirring was continued for 24-h room temperature, filtered, washed and precipitate was dried at 80°C	10	–	–	[S3]
Hierarchical calcined (NMA-LDHs)	Cr(VI)	H.Y.	Nickel sulfate, magnesium sulfate, aluminum nitrate	1:1:1:6	Urea [$CO(NH_2)_2$]	Heating in the autoclave at 180°C for 6-h, cooled at room temp. centrifugal, dried at 80°C for 12-h. The NMA-LDHs heated at 600°C for 2-h	–	600°C	2-h	[S4]
Mg/Fe-LDH	Cu^{2+}, Co^{2+}, Pb^{2+}	C.P.	Copper sulfate pentahydrate, cobalt sulfate heptahydrate, cadmium sulfate	2:1, 3:1	HNO_3, NaOH	Aging for 24 h for at 80°C. filtering, washed with hot-distilled water, thermal treatment of the obtained carbonated forms of Mg/Fe-LDH	10 ± 0.5	400°C	1-h	[S5]
M-CLDH	Cr(VI)	C.P.	Mg/Fe-LDH	2:1	NaOH, magnesite (M)	Aged for 24 h at room temperature (22°C), centrifuged, washed with re-distilled water, and dried at 60°C overnight	10	450°C	3-h	[S6]
H-CLDH	Cr(VI)	C.P.	Mg/Fe-LDH	2:1	Halloysite (H), NaOH	Aged for 24 h at room temperature (22°C), centrifuged, washed with redistilled water, and dried at 60°C overnight	10	450°C	3-h	[S6]

(Continued)

Table S1 *Continued*

Adsorbent (LDH/ composite)	Adsorbate	Method of synthesis	Cation precursors		Anion precursors or/and other compounds	Experimental steps/conditions followed	pH	Calcination		References
			Cation	Molar ratio				Temp	Time	
H-CLDHM	Cr(VI)	C.P.	Mg/Fe-LDH	2:1	Halloysite, magnesite, NaOH	Aged for 24 h at room temperature (22°C), centrifuged, washed with redistilled water, and dried at 60°C overnight	10	450°C	3-h	[S6]
$[SnS_4]^{4-}$-Mg/Al-LDH	Hg^{2+}	C.P.	Magnesium nitrate, aluminum nitrate, sodium sulfide, tin chloride pentahydrate	2:1	NaOH, $[SnS_4]^{4-}$	Stirring for 10-h using N_2 protection, centrifuged, rinsed, ultrasonic treatment of MgAl-LDHs for 2-h. 0.5 g Na_4SnS_4 was added and kept stirring for 12-h, mixture were filtered, washed with ethanol, and dried at 80°C for 12-h	10	–	–	[S7]
Fe^{2+}-Al-LDH-2, Fe^{2+}-Al-LDH-3	Cr(VI)	H.Y.	Iron(II) chloride tetrahydrate, aluminum chloride hexahydrate	2:1, 3:1	NaOH	Precipitated was centrifuged, washed, and subsequently dried at 40°C for 12 h	7	–	–	[S8]
BC@EDTA-LDH	Cr(VI)	C.P., precoated, pyrolysis	Magnesium chloride hexahydrate, aluminum chloride hexahydrate	3:1	NaOH, EDTA-2Na	Mixture was stabilized under 60°C for 12 h, filtered, washed, dried. A tube furnace was used to obtain carbonized biochar heated to 480°C, cooled	10	–	–	[S9]
Citrate-Mg/Al LDH, malate-Mg/Al LDH, tartrate-Mg/Al LDH	Cu^{2+}, Cd^{2+}	C.P.	Magnesium nitrate hexahydrate, aluminum nitrate nonahydrate	3:1	NaOH, citrate, malate, tartrate	Mg-Al solution to citrate, malate, tartrate solutions, respectively at 30°C with stirring, kept standing at 30°C for1 h then filtering, drying under reduced pressure (133 Pa) for 40-h	10.5	–	–	[S10]
SDBS-citrate-LDH	Cd^{2+}, Cu^{2+}	C.P.	Magnesium nitrate hexahydrate, aluminum nitrate nonahydrate	2:1	NaOH, citrate sodium dodecylbenzenesulfonate	Composite prepared by added Mg-Al LDH to 0.1 M SDBS solution, shaken at 200 r/min for 24 h at 293 K, sodium citrate (more than 50% TAEC of LDH) was added, centrifuged, decanted, washed thrice with dried at 338 K	10	–	–	[S11]

Mg/Al-MoS_4-LDH	Mixed Co^{2+}, Ni^{2+}, Cu^{2+}, Zn^{2+}, Ag^{+}, Pb^{2+}, Cd^{2+}, Hg^{2+}	–	Mg/Al-NO_3-LDH,	–	NaOH, $(NH_4)_2MoS_4$	0.2 g $(NH_4)_2MoS_4$ and 0.2 g NO_3-LDH were dispersed in 10 mL degassed deionized water, stirring at ambient temperature for 24-h, filtered, washed and finally air-dried	–	–	–	[S12]
Au/MF-LDO	As(V), Cr(VI)	One-step thermal method	Magnesium acetate tetrahydrate, iron chloride hexahydrate, sodium arsenate dibasic heptahydrate	–	($NaBH_4$), 4-nitrophenol, sodium chloride	Stirring for 4-h, heated at 200°C in an for 8 h. cooled to room temperature, washed, drying overnight at 80°C. The MF-LDO obtained by heat treatment of MF-LDH at 400°C for 1-h	–	–	–	[S13]
Mg/Al-CO_3-CLDHs	Zn^{2+}, Cu^{2+}	C.P.	Magnesium nitrate hexahydrates, aluminum nitrate nonahydrate	3:1	NaOH, Na_2CO_3	Final precipitate was separated by vacuum filtration, and the filter cake was heated at 80°C for 24-h to crystallize, the samples were freeze-dried	10 ± 0.5	450°C	2-h	[S14]
Cys-LDH	Pb^{2+}, Cd^{2+}, Cu^{2+}, Ni^{2+}	C.P.	Magnesium nitrate hexahydrates, aluminum nitrate nonahydrate	–	NaOH, Na_2CO_3, L-cysteine (Cys)	Reaction carried out under N_2, LDH intercalated with cysteine, agitation, centrifugation, washed, dried	12	–	–	[S15]
PEX-LDH	Pb^{2+}, Cd^{2+}, Cu^{2+}, Ni^{2+}	C.P.	Magnesium nitrate hexahydrates, aluminum nitrate nonahydrate	–	NaOH, Na_2CO_3, xanthate (PEX)	Reaction carried out under N_2, LDH intercalated with xanthate, agitation, centrifugation, washed, dried	12	–	–	[S15]
SDS-LDH	Pb^{2+}, Cd^{2+}, Cu^{2+}, Ni^{2+}	C.P.	Magnesium nitrate hexahydrates, aluminum nitrate nonahydrate	–	NaOH, Na_2CO_3, sulfate sodium dodecyl (SDS)	Reaction carried out under N_2, LDH intercalated with sulfate sodium dodecyl, agitation, centrifugation, washed, dried	12	–	–	[S15]
$(NH_4)_2SO_4$-LDH	Pb^{2+}	H.Y.	Magnesium nitrate hexahydrates, aluminum nitrate nonahydrate, urea	Mg/Al = 3:1, U:NO_3 = 4:1	NaOH, HCl, $(NH_4)_2SO_4$	Stirring, aged, filtered, washed, dried, cooled to room temp. reflux condenser and Teflon stirrer, and adjusted to pH 4.5 continuously stirring at 85°C cooled to room temperature, centrifuged	4.5	–	–	[S16]
Fe/Mn/Mg-LDH	Cd^{2+}	C.P.	Iron chloride hexahydrate, manganese chloride tetrahydrate, magnesium chloride hexahydrate	1:1:2	NaOH (or KOH)	Reaction carried out under N_2, vigorous, stirring stirred for 1-h and aged for 24-h, centrifuged, filtered, washed, freezing dried for 96-h	10 ± 0.1	–	–	[S17]

(Continued)

Table S1 *Continued*

Adsorbent (LDH/ composite)	Adsorbate	Method of synthesis	Cation precursors			Experimental steps/conditions followed	pH	Calcination		References
			Cation	Molar ratio	Anion precursors or/and other compounds			Temp	Time	
Zn/Al-ED-TA-LDH	Cu^{2+}, Ni^{2+}, Co^{2+}	C.P.	Zn/Al-CO_3-LDH	Zn/EDTA = 4, Al/EDTA = 2	NaOH, Na_2CO_3, Na_2H_2EDTA	Reaction carried out under N_2 at 75°C, stirred for 30 min, aged at 60°C for 24-h	8	–	–	[S18]
Mesoporous Cu/Mg/Fe-LDH	As(V)	C.P.	Copper nitrate hydrate, magnesium nitrate hexahydrate, iron chloride hexahydrate	–	NaOH, Na_2CO_3	Synthetic process carried out at 25°C, aged at 80°C for 20-h, filtered, washed with deionized water to remove excessive salts	10.5	–	–	[S19]
Li/Al-HT-lc-LDH	Cu^{2+}, Zn^{2+}	H.Y.	Lithium chloride, aluminum chloride anhydrous	4:1	Urea, hydrotalcite-like compounds (HTlcs)	Poured into Teflon-lined autoclave, hydrothermally treated at 120°C for 24-h, centrifuged, washed, and dried at 60°C	–	–	–	[S20]
Mg/Al-DT-PA-LDH	Pb^{2+}	C.P.	Magnesium chloride hexahydrate, aluminum chloride hexahydrate	2:1	$NH_3{\cdot}H_2O$, DTPA	Stirred, aged, filtered, washed, the filter cakes were heated at 80°C for 24-h to improve their crystallinity, dried, sieved to collect the particles of <90 m in diameter	10	–	–	[S21]
Mg/Al/G-LDH	Pb^{2+}	C.P.	Magnesium nitrate hexahydrates, aluminum nitrate nonahydrate	3:1, 2:1	NaOH, glutamate solution	Mg-Al solution was added to the glutamate, LDH recovered by filtering, washing, drying at 80°C for 12-h. (N_2) was bubbled into the solution	10.5	–	–	[S22]
Ni/Al-LDH@PAB	Cr(VI)	H.Y.	Nickel nitrate hexahydrate, aluminum nitrate nonahydrate	–	NaOH, H_3PO_4 activated biomass-based carbons (PAB)	Reaction carried out in N_2 atmosphere	10	–	–	[S23]
Ni/Mg/Al@PAB	Cr(VI)	H.Y.	Nickel nitrate hexahydrate, magnesium nitrate hexahydrates, aluminum nitrate nonahydrate	–	NaOH, H_3PO_4 activated biomass-based carbons (PAB)	Reaction carried out in N_2 atmosphere	10	–	–	[S23]

Mag-LDO/C	Cd^{2+}, Pb^{2+}, Cu^{2+}	Solvothermal	Mg/Al-LDH, ferric chloride hexahydrate	–	NaOH, humic acid	Stirred for 30 min, heated at 200°C for 8-h, washed, drying at 60°C, the humic acid mining with Mag-LDH to obtain Mag-LDH/HA	–	500°C	2-h	[S24]
Mg/Al-CO_3-LDH	Cr(VI)	*In-situ*, C.P.	Magnesium nitrate hexahydrates, aluminum nitrate nonahydrate	3:1	NaOH, Na_2CO_3	Vigorously stirred for 1-h, hydrothermal treatment at 150°C, filtration, washed repeatedly until the pH near 7.0, dried	12	–	–	[S25]
MoS_4-LDH	Ag^{+}, Pb^{2+}, Zn^{2+}, Fe^{3+}, Cu^{2+}, Ni^{2+}	H.Y.	Ni/Fe/Ti-CO_3 LDH	–	MoS_4, NaOH	Stirred for 36-h at 20°C to exchange NO_3 anion from NiFe-Ti-NO_3-LDH by $(MoS_4)^{2-}$ anion. The obtained was filtered, washed, air-dried to get MoS_4-LDH	–	–	–	[S26]
Magnetic Fe_3O_4-Mg/Al-CO_3-LDH	Cd^{2+}	Low saturation C.P.	Magnesium nitrate hexahydrate, aluminum nitrate nonahydrate, ferric chloride hexahydrate	2:1	NaOH, $NaCO_3$, NaAc, HNO_3, ethylenediamine	Mg/Al-CO_3-LDH was synthesized via a C.P., Fe_3O_4 was synthesized via a H.Y. method, the composite was treated according to the procedure of Mg/Al-CO_3-LDH to yield Fe_3O_4-Mg/Al-CO_3-LDH	9–10	–	–	[S27,S95]
Magnetic $CoFe_2O_4$/MgAl-LDH	Cr(VI)	C.P.	Aluminum nitrate nonahydrate, magnesium nitrate hexahydrate, iron sulfate heptahydrate	–	Na_2CO_3, NaOH, HCl, $CoCl_2{\cdot}H_2O$	After complete addition $CoFe_2O_4$, MgAl-LDH solutions, aged for 8-h, washing, dried at 60°C for 12-h	10 ± 0.5	–	–	[S28]
Zn/Al-DTPA-LDH	Cu^{2+}, Cd^{2+}, Pb^{2+}	IE, C.P.	Zn/Al-NO_3-LDH	–	Diethylenetriaminepentaacetate (DTPA)	Solution was purged with N_2 to avoid CO_2, the end products, were separated by centrifugation, washed and dried at 60°C	5.5	–	–	[S29]
Zn/Al-DMSA-LDH	Cu^{2+}, Cd^{2+}, Pb^{2+}	IE, C.P.	Zn/Al-NO_3-LDH	–	Meso-2,3-dimercaptosuccinate (DMSA)	Solution was purged with N_2 to avoid CO_2, the end products, were separated by centrifugation, washed and dried at 60°C	5.5	–	–	[S29]
Cu/Mg/Fe/La-LDH	As(III)	C.P.	Copper nitrate hydrate, magnesium nitrate hexahydrate, iron chloride hexahydrate, lanthanum nitrate hexahydrate	(Cu + Mg)/(Fe + La) = 3	NaOH, Na_2CO_3	Resulting slurry was aged for 20 h at 80°C, centrifuged, washed, dried at 150°C	10.5	–	–	[S30]

(Continued)

Table S1 *Continued*

Adsorbent (LDH/ composite)	Adsorbate	Method of synthesis	Cation precursors			Experimental steps/conditions followed	pH	Calcination		References
			Cation	Molar ratio	Anion precursors or/and other compounds			Temp	Time	
EDTA@ MF-LDHs	As(III), As(V)	Low saturation C.P.	Iron chloride hexahydrate, manganese chloride tetrahydrate	–	NaOH, Na_2CO_3, EDTA-2Na	Reaction carried out under N_2, after dropping the mixture was stirred for 10 min, aged for 2-h at 60°C, washed, filter, dried at 40°C	12 ± 0.1	–	–	[S31]
CO_3@MF-LDHs	As(III), As(V)	C.P.	Iron chloride hexahydrate, manganese chloride tetrahydrate	–	NaOH, Na_2CO_3	Reaction carried out under N_2, after dropping the mixture was stirred for 10 min, aged for 2-h at 60°C, washed, filter, dried at 40°C	12 ± 0.1	–	–	[S31]
CMCD·Zn/ Al-LDH	Cu^{2+}, Ni^{2+}	C.P.	Zinc nitrate hexahydrate, aluminum nitrate nonahydrate	2:1	NaOH, carboxymethyl-modified cyclodextrin (CMCD)	After dropping, the mixture were kept at 30°C, LDH were obtained by filtering, drying under 133 Pa at 40°C for 40-h. N_2 gas was bubbled into the solution	10	–	–	[S32]
CS-LDH	Cd^{2+}, Pb^{2+}	Emulsion cross-linking	Mg/Al-LDH	–	NaOH, chitosan (CS)	Ultrasonic dispersion, mixed and stirred for 1-h, the formaldehyde solution was dripped into the reaction vessel, agitated at 60°C for 1-h, washed, dried	9	–	–	[S33]
G-Mg/Al-CLDH	Cr(VI)	H.Y.	Magnesium nitrate hexahydrate, aluminum nitrate nonahydrate	–	Urea, fabricate graphene (G)	Mixed solution was thermally treated in an oven at 120°C for 24-h, cooling to room temperature, filtration, dried	–	500°C	5-h	[S34]
MoS_2-Mg/ Al-LDHs	Cr(VI)	–	Magnesium chloride hexahydrate, aluminum chloride hexahydrate	–	NaOH, molybdenum disulfide (MoS_2)	Mixture of LDHs, Na_2MoO_4, CH_3CSNH_2 stirred, heated at 200°C for 24-h, washing, dried	–	–	–	[S35]
CNF-Ni/Al-DH	Cu^{2+}, Cr(VI)	H.Y.	Nickel nitrate hexahydrate, aluminum nitrate nonahydrate	–	$CO(NH_2)_2$, NH_4F, carbonaceous nanofiber (CNF)	CNF was synthesized by a template-directed hydrothermal carbonization, final suspension was held at 110°C for 8-h, rinsed d dried overnight at 80°C	–	–	–	[S36]

PPy-Mg/Al-LDHs	Cr(VI)	H.Y. *in-situ* oxidative polymerization	Magnesium nitrate hexahydrate, aluminum nitrate nonahydrate	3:1	NaOH, Na_2CO_3, polypyrrole (PPy)	Reaction was performed in an ice bath, irradiated with microwave to get highly crystalline, aged for 12-h, centrifugation, washing, the final product was dried at 90°C ± 2°C	–	–	–	[S37]
Zn/Al-LDH@OA, Zn/Al-LDO@C nanosheets	Cr(VI)	C.P.	ZnAl-LDH nanosheets	2:1	OA, NaOH, Na_2CO_3	ZnAl-modified by OA, precipitate was redispersed in chloroform to obtain ZnAl-LDH@OA then calcined LDH LDH@OA under N_2	–	450°C	2-h	[S38]
Zn/Fe-LDH-PVA, sponge	As(V)	H.Y.	Zinc nitrate hexahydrate, iron nitrate nonahydrate	–	Urea, polyvinyl alcohol sponge	Heated at 110°C for 12 h. Finally, washed dried at 60°C	–	–	–	[S39]
Dyes as adsorbate										
Bentonite-Co/Al-LDH	EBT	–	Cobalt nitrate hexahydrate, aluminum nitrate nonahydrate	–	Bentonite, NaOH	Stirring speed was 600 rpm at 60°C for 15 min before adding NaOH but after addition become 1,000 rpm at 90°C, centrifuged, washed, dried at 90°C	10 ± 0.5	–	–	[S40]
Zn/Al/Cl-LDHs	AG 1	C.P.	Zinc chloride ($ZnCl_2$), aluminum chloride ($AlCl_3$)	2:1	NaOH	Reaction carried out under at N_2, slurry stirred for 72-h, filtered, washed, dried at 25°C	9	–	–	[S41]
NO_3-LDH, His-LDH	CR, IC, SY	Nucleation and aging	Magnesium nitrate hexahydrate, aluminum nitrate nonahydrate	–	Histidine (His), NaOH	Gelatinous precipitate was aged at 80°C for 24-h, centrifuge, washed, dried at 70°C	9.5–10.5	–	–	[S42]
C-Zn/Al-LDH	MG, CV	C.P.	Zinc nitrate hexahydrate, aluminum nitrate nonahydrate	–	NaOH, Na_2CO_3, glucose powder	Magnetic stirrer for 24-h, glucose encapsulated LDHs were dried using bio-chem hot-air oven at 50°C for 24-h, dried at 350°C for 15 min	11–12	–	–	[S43]
Mg/Al-LDH, Fe_3O_4-Mg/Al-LDH	RR, CR, AR 1	C.P.	Magnesium nitrate hexahydrate, aluminum nitrate nonahydrate	2:1	HNO_3, NaOH, Na_2CO_3	Precipitate was aged for 18-h, washed, centrifuged, dried at 80°C in the oven, all products were ground	9–10	–	–	[S44]
Ni/Fe-CO_3-LDH	EBT	C.P.	Nickel chloride hexahydrate, ferric chloride hexahydrate	3:1	NaOH, Na_2CO_3	Stirred mechanically for 1-h, aged at 85°C to 180°C, different hydrothermal treatment, aged 3-h to 15 d, filtered, washed, dried in an oven at 60°C	11	–	–	[S45]

(Continued)

Table S1 *Continued*

Adsorbent (LDH/ composite)	Adsorbate	Method of synthesis	Cation precursors			Experimental steps/conditions followed	pH	Calcination		References
			Cation	Molar ratio	Anion precursors or/and other compounds			Temp	Time	
DBS-Ni/Cr-LDH	MO	C.P.	Nickel nitrate hexahydrate, chromium nitrate solution	2:1	NaOH, Na_2CO_3 (DBS)	Synthesis carried out at 60°C, aging for 16-h, filtration, washed, dried	–	–	–	[S46]
rGO-Ni/ Cr-LDH	MO	C.P.	Nickel nitrate hexahydrate, chromium nitrate solution	2:1	Crystalline flake graphite, NaOH, Na_2CO_3	GO was synthesized by a modified Hummer's method, follow by thermal exfoliation to obtain (rGO). Synthesis carried out at 60°C, aging for 16-h, filtration, washed, dried	–	–	–	[S46]
Laurate-Ni/ Cr-LDH	MO	C.P.	Nickel nitrate hexahydrate, chromium nitrate solution	2:1	Sodium laurate, NaOH, Na_2CO_3	Synthesis carried out at 60°C, aging for 16-h, filtration, washed, dried	–	–	–	[S46]
MgAl-NO_3-LDH	RR-120, RBB-150	C.P.	Magnesium nitrate hexahydrate, aluminum nitrate nonahydrate	2:1	NaOH	Suspension was aged for 24-h under (stirring and N_2 gas flow), centrifugation, dried, kept at 22°C for 24-h	9	–	–	[S47]
Mg/Al-LDH	AY	C.P.	Magnesium nitrate hexahydrate, aluminum nitrate nonahydrate	–	NaOH, Na_2CO_3	Reaction carried out under N_2, washed by centrifugation/ resuspension, hydrothermally treated at 65°C for 24-h, dried in the presence of silica gel	10	550°C	4-h	[S48]
Mg/Al-CO_3-LDH, Mg/ Al-NO_3-LDH, Cal. Mg/ Al-LDH	AMR	C.P.	Magnesium nitrate hexahydrate, aluminum nitrate nonahydrate	2:1	NaOH, Na_2CO_3	Reaction carried out under N_2, mixture hydrothermally treated at 80°C, washed, dried at 60°C	10.0 ± 0.3	550°C	3-h	[S49]
Mesoporous Mg/Fe-LDH	Indigo carmine (IC)	Sol–gel	Magnesium nitrate hexahydrates (99%), iron nitrate nonahydrate	–	NaOH, CTAB (99%)	Precipitate stirring for 2-h, the sol was aging for 2-d, filtration gel particles formed, washed with water then by ethanol dried at 100°C for 24-h	–	–	–	[S50]
DS-Zn/Al-LDHs	CR, MO, BG	H.Y.	Zinc chloride, aluminum chloride	–	NaOH, urea, SDS	Zn/Al LDHs microspheres were dispersed in a SDS solution, adjusted pH. Finally, LDHs were formed and dried in air	9 ± 0.5	–	–	[S51]

O_3D-LDH, Mg/Al-LDH	MO, RhB	Soft-template, H.Y.	Magnesium nitrate hexahydrate, aluminum nitrate nonahydrate	2:1	Urea, SDS	SDS was immediately added into the salt solution, vigorously, sonicated for 30 min, heated at 150°C for 6-h centrifugation, washed, dried at 70°C for 6-h	–	–	–	[S52]
Ni/Mg/Al-CLDHs	Congo red	H.Y.	Nickel sulfate hexahydrate, magnesium sulfate heptahydrate, aluminum nitrate nonahydrate	1:1:1:6	Urea [$CO(NH_2)_2$]	Heating in the autoclave at 180°C for 6-h, cooled at room temp. centrifugal, dried at 80°C for 12-h. The NMA-LDHs heated at 600°C for 2-h	–	600°C	2-h	[S4]
Zn/Al-LDH/DS	MB	C.P., ion-exchange	Zinc nitrate hexahydrate, aluminum nitrate nonahydrate	1:2	NaOH, Na_2CO_3, sodium dodecyl sulfate (SDS)	LDH heated up to 85°C, stirring, filtration and washed. Zn/Al-LDH was modified with sodium dodecyl sulfate by reconstruction method	10	450°C	2-h	[S53]
Ni/Al-LDH@PAB	MO	H.Y.	Nickel nitrate hexahydrate, aluminum nitrate nonahydrate	–	NaOH, H_3PO_4 activated biomass-based carbons (PAB)	Reaction carried out in N_2 atmosphere	10	–	–	[S23]
Zn/Al-LDO@C nanosheets	MO	C.P.	Zn/Al-LDH nanosheets	2:1	OA, NaOH, Na_2CO_3	ZnAl-modified by OA, precipitate was redispersed in chloroform to obtain ZnAl-LDH@OA then calcined LDH LDH@OA under N_2	–	450°C	2-h	[S38]
Zn/Fe-LDH-PVA, sponge	MO	H.Y.	Zinc nitrate hexahydrate, iron nitrate nonahydrate	–	Urea, polyvinyl alcohol sponge	Heated at 110°C for 12-h. Finally, washed dried at 60°C	–	–	–	[S39]
3D-Co/Fe-LDHs	MO, RhB, NB	H.Y.	Cobalt nitrate hexahydrate, iron nitrate nonahydrate	2:1	Urea, NH_4F	Stirred for 2 h, heated 120°C for 12-h	–	–	–	[S54]
SCD-Mg/Al-NO_3-LDH	MB	C.P., IE	Mg/Al-NO_3-LDH	–	Sulfated sodium salt (SCD)	Reaction carried out under N_2 at 100°C for 24-h, centrifuged, washed	–	–	–	[S55]
Zn/Al-CLDH, Mg/Al-CLDH	RBBR	C.P.	Magnesium nitrate hexahydrate, magnesium nitrate hexahydrate, aluminium nitrate nonahydrate	3:1	NaOH, $NaCO_3$	Solutions were purged by N_2 and stirred, aged at 60°C, centrifuged, washed, dried at 80°C for 24-h, ground and sieved	10 ± 0.5	500°C	4-h	[S56]

(Continued)

Table S1 *Continued*

Adsorbent (LDH/ composite)	Adsorbate	Method of synthesis	Cation precursors			Experimental steps/conditions followed	pH	Calcination		References
			Cation	Molar ratio	Anion precursors or/and other compounds			Temp	Time	
Zn/Mg/ Al-CLDH	RBBR	C.P.	Magnesium nitrate hexahydrate, magnesium nitrate hexahydrate, aluminium nitrate nonahydrate	3:1	NaOH, $NaCO_3$	Solutions were purged by N_2 and stirred, aged at 60°C for 2-h, centrifuged, washed, dried at 80°C for 24-h, ground and sieved	10 ± 0.5	500°C	4-h	[S56]
Zn/Ni/Fe-LDH-DPb	RB5	C.P.	Nickel nitrate hexahydrate, zinc nitrate hexahydrate, iron nitrate nonahydrate	0.5:1:1	(DPb)	Agitated, washed, the resultant slurry was over-dried for a couple of hours at 100°C	10	–	–	[S57]
Zn/Ni/Fe-LDH-CNT	RB5	C.P.	Zinc nitrate hexahydrate, nickel nitrate hexahydrate, iron nitrate nonahydrate	0.5:1:1	Single-wall carbon nanotubes (CNT), ammonia	Washed several times until a neutral pH was attained, over-dried at 100°C	10	–	–	[S57]
Mg/Al-LDH-DIA	Tar, Er	–	Magnesium nitrate hexahydrate, aluminium nitrate nonahydrate	–	Diatomite solution (DIA)	The obtained gelatinous precipitate was aged at 80°C for 24-h centrifuged, dried at 70°C for 6-h in the oven	9.5–10.5	–	–	[S58]
Starch-Ni/ Fe-LDH	MO	C.P.	Nickel nitrate hexahydrate, iron nitrate nonahydrate	3:1	Starch, NaOH	Sonicated for 5 min, stirred vigorously for 15 min at 90°C, refluxed at 90°C for 24-h, centrifuged, washed, dried at 40°C	10 ± 0.5	–	–	[S59]
Cu/Al-LDH/ SWCNT	IC	H.Y.	Copper sulfate $CuSO_4$, aluminum nitrate $Al(NO_3)_3$	–	Single-walled carbon nanotubes (SWCNT), urea,	Stirred for 30 min, with urea stirred for 1-h, hydrothermal for 1-h, filtered, washed, dried at 105°C for 24-h	–	–	–	[S60]
ZIF-67@Co/ Al-LDH	MB, MO	–	Co/Al-LDH	–	NaOH, ZIF-67	Ultra-sonicated for 50-min, centrifuged, washed, dried at 50°C	–	–	–	[S61]
C/NiFe-LDH	MO, CR	H.Y.	Nickel nitrate hexahydrate, iron nitrate nonahydrate	–	$CO(NH_2)_2$, PAN, NH_4F	Mixture was decanted to autoclave. Carbon fiber was then added, heated at 110°C for 12 h	–	–	–	[S62]
Mg/Al-LDH-AC	MB	–	Magnesium nitrate hexahydrate, aluminum nitrate nonahydrate	–	Urea NaOH, HCl, H_2SO_4, AC of date palm pits	Mixture was sonicated for 1-h, heated at 120°C for 1-d, filtered, washed, oven dried	–	–	–	[S63]

Mg/Al-CLDH, Co/Al-CLDH, Ni/Fe-CLDH	EBT	C.P.	Aluminium nitrate nonahydrate, iron nitrate nonahydrate, magnesium nitrate hexahydrate, cobalt nitrate hexahydrate, nickel nitrate hexahydrate	3:1	NaOH	Stirred vigorously for 2-h at 45°C, heated to 90°C, refluxing at 90°C for 24-h, centrifuged, washed with water and ethanol, dried at 60°C in vacuum oven overnight	10 ± 0.5	350°C	3-h	[S64]
PPy NF-Zn/Fe-LDH	Safranin dye	C.P.	Zinc nitrate hexahydrate, iron nitrate nonahydrate	2:1	NaOH, pyrrole, potassium persulfate, hydrochloric acid, chloroform	Composite was prepared by the incorporation Zn-Fe LDH in the polymerization system during the interfacial-polymerization of pyrrole	–	–	–	[S65]
Organo-LDHs	AR-GR, DO-11, BY-2	–	Aluminum chloride hexahydrate, magnesium chloride hexahydrate, ammonia water	–	SHS, SNS, SDS	Prepared by addition SHS, SNS, and SDS solutions to Mg/Al-LDH sol., stirred for 24-h at 25°C, centrifuged, washed dried at 60°C in a vacuum oven	–	–	–	[S66]
Mg/Al/Cu/Fe-LDH	AR66	C.P.	Magnesium chloride hexahydrate, copper chloride dehydrate, aluminum chloride hexahydrate, iron(III) chloride	$M^{2+}/M^{3+} = 3$	NaOH, $NaCO_3$	Reaction carried out at inert gas atmosphere (argon) and $T = 65$°C, stirred for 2-h, centrifuged, washed, dried at 70°C	10.5 ± 0.1	550°C	1-h	[S67]
rGO/Ni/MMO	MO	H.Y.	Aluminum chloride hexahydrate, nickel(II) chloride hexahydrate, potassium monopersulfate triple salt	–	Urea, H_2SO_4, $NaNO_3$, graphite	GO was synthesized according to a modified hummers method, rGO/Ni/MMO hybrid was obtained by the calcination of GO/LDH hybrid	–	600°C	5-h	[S68]
LDH-carbon dot	MB, MO	C.P.	Magnesium nitrate hexahydrate, aluminum nitrate nonahydrate	–	NaOH, Na_2CO_3, carbon dot	Carbon dots and LDH-carbon dot composites were synthesized by a microwave and colloidal deposition method, respectively	–	–	–	[S69]
WFS/MgFe-LDH	CR	C.P.	Magnesium nitrate hexahydrate, iron(III) chloride hexahydrate	4:1, 3:1, 2:1, 1:1	NaOH, Na_2CO_3, WFS	Stirring for 1-h, filtrated, dried at 80°C for 24-h	7	–	–	[S70]
3D-LDH, 3D-CLDH	CR, MB, MO	Double drop C.P.	Magnesium nitrate hexahydrate, aluminum nitrate nonahydrate	4:1	NaOH, Na_2CO_3	Double-drop process was conducted for 0.5 h. aged at 65°C for 15-h, filtered, washed dried at 80°C for 6-h	9.2 ± 0.2	500°C	5-h	[S71]

(Continued)

Table S1 *Continued*

Adsorbent (LDH/ composite)	Adsorbate	Method of synthesis	Cation precursors			Experimental steps/conditions followed	pH	Calcination		References
			Cation	Molar ratio	Anion precursors or/and other compounds			Temp	Time	
Ni/Fe/Ti-LDHs	MB, MO, CR, OG	H.Y.	Nickel(II) nitrate hexahydrate, iron(III) nitrate nonahydrate, titanium tetrachloride	–	Urea	Stirred, hydrothermally aged at 160°C for 2-d, washed, dried at 80°C	–	–	–	[S72]
Cu/Mg/Al-LDH	MO, BTB, CR, MB, RhB	C.P.	Copper(II) nitrate trihydrate, magnesium nitrate hexahydrate, aluminum nitrate nonahydrate	(Cu + Mg)/ Al = 3:1, Cu/ Mg = 0:3, 1:2, 1:1, 2:1	NaOH, Na_2CO_3	Stirred for 1-h, aged in the mother liquor at 80°C for 24-h, filtered, washed, dried at 80°C in the oven for 15-h	7	–	–	[S73]
Cu/Al-LDH	MO	C.P.	Copper nitrate trihydrate, aluminum nitrate nonahydrate	3:1, 5:2, 2:1	NaOH, Na_2CO_3	Vigorously stirred for 6-h, left overnight at room temperature with no stirring, centrifuged	10	500°C	4-h	[S74]
[CuCo]/Al-LDH	MO	C.P.	Copper nitrate trihydrate, aluminum nitrate nonahydrate, cobalt nitrate hexahydrate	3:1, 5:2, 2:1	NaOH, Na_2CO_3, $Cr(NO_3)_3{\cdot}9H_2O$	Vigorously stirred for 6-h, left overnight at room temperature with no stirring, centrifuged	10	500°C	4-h	[S74]
Magnetic SF-B-Co/Ni/ Al-LDH	MO, EBT	–	Cobalt nitrate hexahydrate, nickel nitrate hexahydrate, aluminum nitrate nonahydrate	2:1:1	NaOH, HNO_3, hydrazine, strontium ferrite, bentonite (50:50)	Magnetic stirring, refluxed at 90°C for 24-h, centrifuged, the magnetic composite dried at 90°C for 24 h in an oven	10	350°C	3-h	[S75]
Co-Fe-LDH@ UiO-66-NH_2	MR, MB	C.P.	Co-Fe-LDH	–	NaOH, N,N-DMF, $ZrCl_4$, MOF (UiO-66-NH_2)	Mixture heated to 100°C for 8-h, washed by distilled water and methanol/DMF, dried at 80°C for overnight	8	–	–	[S76]
Ni/Fe-LDH-$SiW_{12}O_{40}$	MB	C.P., IE	Nickel nitrate, iron(III) nitrate	–	Na_2CO_3, $K[\alpha\text{-}SiW_{12}O_{40}]_4^-$	Mixture under N_2 condition, and 40°C, where Ni/Fe-NO_3 LDH prepared by C.P., and $SiW_{12}O_{40}$ replaced by NO_3 by IE	10–11	–	–	[S77]
Fe_3O_4/SiO_2/ FeS-CoS-Mg/ Al-LDH	DB, BG	–	Magnesium nitrate hexahydrate, aluminum nitrate nonahydrate	–	NaOH, Fe_3O_4/SiO_2/ FeS-CoS	Mixture was exposed to ultrasonic irradiation at 65°C for 90-min, filtered, rinsed dried at 60°C overnight	10	–	–	[S78]
Mg/Fe-CO_3-CLDH	MB, MG, MO	C.P.	Magnesium nitrate hexahydrate, ferric chloride hexahydrate	3:1	Na_2CO_3, NaOH	Heated to 80°C for 24-h, filtered, washed solids obtained were dried at 80°C for 24-h	10	500°C	3-h, 3-h	[S79]

Ni/Fe-CO_3-CLDH	MB, MG, MO	C.P.	Nickel nitrate hexahydrate, ferric chloride hexahydrate	3:1	Na_2CO_3, NaOH	Heated to 80°C for 24-h, filtered, washed solids obtained were dried at 80°C for 24-h	10	400°C		[S79]
PVDF@Co/Al-LDH	MO	–	Cobalt sulfate heptahydrate, aluminum chloride nonahydrate	2:1	Poly(vinylidene fluoride) (PVDF), urea	Heated, kept at 105°C for 12-h, cooled to 25°C, washed, dried at 60°C for 2-h	–	–	–	[S80]
ECs as adsorbate										
Mg/Al-CO_3-LDHs	DNP, DNOC	C.P., sol–gel	$Mg_6Al_2(OH)_2CO_3^{2-}H_2O$, aluminum solutions ($Al^{3+}H_2O_6$)	2:1, 3:1, 4:1	NaOH, Na_2CO_3	Reactions were carried out under N_2 hydrothermally treated at 80°C, washed, dried at 60°C	–	500°C	3-h	[S81]
Zn/Ti/Al-LDH	Diclofenac sodium	C.P.	Zinc nitrate hexahydrates, aluminium nitrate hexahydrate, titanium(III) chloride	Zn^{2+}:(Al, Ti)$^{3+}$ 3:1	NaOH	Stirred at 60°C aged for 24-h, centrifuged, washed, 80°C for 16-h, manually grounded with a mortar	10	400°C	4-h	[S82]
NiAlTi-LDH	Tetracycline	H.Y.	Nickel(II) nitrate hexahydrate, aluminum nitrate nonahydrate, titanium tetrachloride	–	Urea	Stirred, hydrothermally aged at 160°C for 2-d, washed, dried at 80°C	–	–	–	[S83]
Mg/Al-LDH/(CB)	Amoxicillin	C.P.	Magnesium nitrate hexahydrate (99%), aluminium nitrate nonahydrate (98%)	–	Urea, cellulose beads (CB)	CB was added in the mixture, refluxed at 100°C and stirring for 12 h. Finally, Mg/AL-LDH@CB were washed with water	–	–	–	[S84]
ZnAlLa-CLDH, CM-CLDH catalyst	Ibuprofen	C.P.	Zinc nitrate hexahydrate, lanthanum nitrate hexahydrate, aluminum nitrate nonahydrate	–	NaOH, Na_2CO_3, amaranth	Stirred 1-h, drying for 24 h, aging, filtered, washed, dried at 80°C, then ZnAlLa-LDH was calcined at different temp. then resulted LDH mixed with amaranth, and calcined again	10 ± 0.1	400°C, 500°C, 600°C	–	[S85]
Cl-LDH	Tetracycline, diclofenac sodium, chloramphenicol	C.P.	Magnesium chloride hexahydrate, aluminium chloride hexahydrate	–	NaOH, NaCl	Reaction carried out at an inert atmosphere of N_2, stirred, aged for 12-h at 70°C, centrifuged, washed then LDHs obtained after drying at 110°C for 24-h	10	–	–	[S86]
MgAl/-CLDH	Oxytetracycline	C.P.	Magnesium nitrate hexahydrates, aluminum nitrate	3:1	NaOH, $CuSO_4$, $NiSO_4$, $CoCl_2$, $ZnSO_4$	Stirring was continued for 24-h room temperature	10	–	–	[S3]
Mg/Al-LDH	Tetracycline	C.P.	Magnesium chloride hexahydrate, aluminium chloride hexahydrate	3:1	NaCl, NaOH	Hydrothermal treatment at 120°C for 48 h was done into the Teflon coated stainless steel autoclave	12	–	–	[S87]

(Continued)

Table S1 *Continued*

Adsorbent (LDH/ composite)	Adsorbate	Method of synthesis	Cation precursors			Experimental steps/conditions followed	pH	Calcination		References
			Cation	Molar ratio	Anion precursors or/and other compounds			Temp	Time	
Mg/Fe-LDH	Amoxicillin	C.P.	Magnesium chloride, iron chloride	1.5:1	NaOH	Agitation at room temp. for 4-h, the precipitate was washed, centrifuged for 5 min and dried at 65°C for 24 h. final MgFe/LDH was crushed to dp < 0.212 mm	13	–	–	[S88]
Zn_2/Al-CO_3-LDH	Sulfamethoxazole	C.P.	Aluminum chloride hexahydrate, zinc chloride	–	NaOH, Na_2CO_3	Agitation for 72-h, precipitate filtered, washed, dried at room temp. (25°C)	10	500°C	5-h	[S89]
Mg/Al-CO_3^{2-} CLDH	Tetracycline	H.Y.	Magnesium nitrate, aluminum nitrate	2:1, 3:1, 4:1	NaOH, Na_2CO_3	Heated in Teflon-lined autoclave at 120°C for 24-h, filtration, washed, drying at 80°C for 8-h	–	450°C	4-h	[S90]
Zn/Al-CO_3-LDH	Salicylic acid	C.P.	Zinc nitrate hexahydrate, aluminum nitrate nonahydrate	1:1, 3:1, 5:1	NaOH, Na_2CO_3	Gel formed was stirred for 4-h, heated at 75°C for 16-h, filtered, washed, dried at 100°C for 24 h	8.5 ± 0.2	300°C, 400°C, 500°C	6-h	[S91]
M^{2+}/Al-LDH (M = Mg, Ni, and Zn)	Sodium diclofenac	C.P.	Magnesium, nickel, and zinc nitrate hexahydrates, aluminium nitrate hexahydrate	2:1	NaOH, Na_2CO_3	Reaction carried out at temperature of 50°C, the result in was collected, agitation for crystallization at 50°C for 1-h, filtered, washed dried in at 80°C	8–9 ± 0.1	400°C	12-h	[S92]
M^{2+}/Al-LDH (Co, Ni, and Zn)	Diclofenac, salicylic acid	C.P.	Cobalt, nickel, and zinc nitrate hexahydrates, aluminium nitrate hexahydrate	3:1	NaOH, Na_2CO_3, HNO_3	Mixture was stirred at 60°C for 1-h, aged for 24-h, centrifuged, washed, dried for 16 h at 80°C, grounded with a mortar	10	400°C	4-h	[S93]
Mg/Al-LDH	Diclofenac, salicylic acid	C.P.	Magnesium nitrate hexahydrates, aluminium nitrate hexahydrate	3:1	NaOH, Na_2CO_3, HNO_3	Mixture was stirred at 60°C for 1-h, aged for 24-h, centrifuged, washed, dried for 16 h at 80°C, grounded with a mortar	–	550°C	4-h	[S93]
Mg/Al/Sn-LDHs	Norfloxacin	C.P.	Magnesium nitrate hexahydrates, aluminium nitrate hexahydrate, tin chloride pentahydrate	4:1, 3:1, 2:1, Mg^{2+}/ Al^{3+}/Sn^{4+}, 3:0.9:0.1, 3:0.8:0.2, 3:0.6:0.4	NaOH, Na_2CO_3, HNO_3	Mg/Al and Mg/Al/Sn-LDHs with different interlayer anions (CO_3^{2-}, Cl^-) prepared, reaction under N_2 atmosphere. All suspensions were aged centrifuged, washed, then the CO_3-LDHs dried and Cl-LDHs were freeze dried	10 ± 0.2	–	–	[S94]

Zn/Ti/Al-LDH	Salicylic acid	C.P.	Zinc nitrate hexahydrates, aluminium nitrate hexahydrate, titanium chloride	Zn^{2+}:(Al, Ti)$^{3+}$ 3:1	NaOH	Stirred at 60°C aged for 24-h, centrifuged, washed, 80°C for 16-h, manually grounded with a mortar	10	400°C	4-h	[S82]
Mg/Mn-CLDH	Tetracycline	C.P.	Magnesium chloride, hexahydrate, manganese dichloride tetrahydrate	2:1	NaOH, Na_2CO_3	Stirred for 2-h, washed being freeze drought for 24-h, Mg/Mn-LDH was calcined under N_2 atmospheres	–	350°C	3-h	[S95]
Zn/Al-CLDH	Diclofenac sodium	C.P.	Magnesium chloride hexahydrate, aluminum chloride hexahydrate	2:1	NaOH, Na_2CO_3	N_2 was bubbled throughout reaction, suspensions were stirred for 6-h, aged at 65°C for 16-d, centrifuging, washed, dried	10 ± 0.3	500°C	4-h	[S96]
Mg/Al-LDH	Metronidazole	–	Magnesium nitrate hexahydrates, aluminium nitrate nonahydrate	–	Urea, NaOH or H_2SO_4	Heated at 150°C for 24-h, washed, final product was dried at 120°C for 24-h	–	–	–	[S97]
Zn/Al-CLDH	Acetylsalicylic acid	C.P.	Zinc and aluminum nitrate salts	2:1	–	Preparation was conducted at a temperature of 50°C	9 ± 0.1	400°C	12-h	[S98]
LDH-PmPDs	Diclofenac sodium	–	Mg/Al-LDH	–	$Na_2S_2O_8$, m-phenylenediamine, NaOH	DH-PmPDs was prepared by a chemical oxidation method, solution stirred for 30 min prior to the polymerization	–	–	–	[S99]
CLDH/γ-AlO(OH)/N-T	Minocycline	–	Aluminium nitrate nonahydrate, magnesium sulfate heptahydrate	–	γ-AlO(OH) nanowires, amorphous carbon, kapok	Suspension treated under a hydrothermal condition at 160°C for 10-h, washed, dried in air at 80°C	–	500°C	1-h	[S100]
MC-LDH	Diclofenac sodium	–	Ca/Al-LDH, iron chloride tetrahydrate	–	Urea, NaOH, cellulose, epichlorohydrin (EPH), pyridine	Mixture of cellulose, LDH, iron was irradiated sonically at 60°C for 1-h, filtered, washed, dried at 70°C for 5-h then EPH was added to the suspension and stirred	–	–	–	[S101]
Mg/Al-LDH-biochar	Diclofenac sodium	C.P.	Magnesium chloride hexahydrate, aluminium chloride hexahydrate	–	Biochar	Mixture is stirring for 2-h, washed, dried in an oven for 18-h at 60°C and, finally, crushed and sieved	10	–	–	[S102]
Mg/Al-LDH-biochar	Caffeine	–	Magnesium chloride hexahydrate, aluminium chloride hexahydrate	2:1	NaOH, biochar	After 4-h, the material was centrifuged, washed, dried in an oven for 15-h at 60°C, crushed	10	–	–	[S103]

(Continued)

Table S1 *Continued*

Adsorbent (LDH/ composite)	Adsorbate	Method of synthesis	Cation precursors			Experimental steps/conditions followed	pH	Calcination		References
			Cation	Molar ratio	Anion precursors or/and other compounds			Temp	Time	
Zn/Fe-LDH	Diclofenac sodium	C.P.	Zinc nitrate hexahydrate, iron nitrate nonahydrate	4:1	NaOH, HCl	Precipitate was filtered, washed till the pH of the filtrate reaches 7, then Zn/Fe-LDH dried at 50°C for 2-h	9	–	–	[S104]
Co/Fe/La-LDHs	Tetracycline	C.P.	Cobaltous nitrate hexahydrate, lanthanum nitrate hexahydrate, iron nitrate nonahydrate	20:8:2	NaOH, Na_2CO_3, HCl	Suspension was aged at 60°C for 12-h, washed, Finally, the CoFeLa-LDH_2 was dried at 60°C for 24-h	10	–	–	[S105]
Zn/Al-LDH	Levofloxacin	C.P.	Zinc chloride ($ZnCl_2$), aluminum chloride ($AlCl_3$)	3:1	NaOH	Suspension was centrifuged to separate the precipitate, washed, dried at 50°C for 24 h until it was completely dry	10	–	–	[S106]
Mg/Al-LDH	Amoxicillin	C.P.	Magnesium chloride hexahydrate, aluminium chloride hexahydrate	2:1	NaOH, HCl	Aged for 18-h, stirred, centrifugation, washed, dried at 60°C	9	–	–	[S107]
Ca/Al-MoS_4-LDH	Ciprofloxacin, ofloxacin	C.P.	Calcium nitrate tetrahydrate, aluminum nitrate nonahydrate	–	$(NH_4)_6Mo_7O_{24}{\cdot}4H_2O$, NaOH, H_2S	Reaction carried out under N_2 atmosphere, aged for 12-h, ultrasonicated, centrifugation, washed, kept in Teflon autoclave 12 h at 150°C, dried at 60°C	10.5	–	–	[S108]
$CuFe_2O_4$-Ni/Mg/Al-LDH	Oxytetracycline	H.Y.	Nickel chloride hexahydrate, magnesium dichloride dehydrate, aluminum nitrate nonahydrate	–	NaOH, $CuFe_2O_4$, urea	Vigorous stirring for 2-h, heated at 170°C for 12 h, filtered, washed, dried at 105°C	–	–	–	[S109]
Mg/Al-MWCNT-LDH	Doxycycline	C.P.	Magnesium nitrate hexahydrate, aluminum nitrate nonahydrate	2:1	NaOH, HCl, MWCNT	Suspended solutions were kept to age. After that, they were filtered, washed, dried at 80°C overnight	10	–	–	[S110]

Table S2
Details of parameters for the adsorption of various toxic contaminants over LDHs and their hybrids/composites

Adsorbent	Adsorbate	BET (m^2/g)	Adsorption condition			Isotherms	Adsorption capacity (mg/g)	Kinetic pseudo-second-order		Regeneration		Adsorption mechanism	References
			Dosage (g)	pH	Time (min)			k_2 (mg/g·min)	q_e (mg/g)	Reagent	Cycle		
Heavy metal as adsorbate													
Ni/Mg/Al-CLDHs	Cr(VI)	179	0.01	7	350	L, F	103.4	0.4×10^{-3}	92.6	–	–	–	[S4]
$[SnS_4]^{4-}$-Mg/Al-LDH	Hg^{2+}	74.713	–	1	60	L, F	360.6	–	–	Na_2S solution	–	Ion-exchange, Surface complexation	[S7]
Mag-LDO/C	Cd^{2+}, Pb^{2+}, Cu^{2+}	132.4	0.03	6 ± 0.05, 6 ± 0.05, 6 ± 0.05	90, 120, 400	L	386.1, 359.7, 192.7	3×10^{-3}, 3×10^{-3}, 1×10^{-3}	145.3, 263.9, 147.5	HCl, deionized water	5	–	[S24]
Fe^{2+}-Al-LDH	Cr(VI)	46.85	–	7	–	–	800	–	–	–	–	Ion-exchange, surface sorption, redox reaction	[S8]
BC@EDTA-LDH	Cr(VI)	48.894	0.01	3	–	L, F	7.88	0.3×10^{-3}	38	–	–	electrostatic interaction	[S9]
SDBS-citrate-LDH	Cd^{2+}, Cu^{2+}	–	0.05, 0.05	5.5, 5.5	240, 240	L, F	41, 97.09	–	–	–	–	–	[S11]
Au/MF-LDO	As(V), Cr(VI)	205.82	0.02	–	20, 20	L, F	178.6, 148.7	2.744×10^{-3}, 2.483×10^{-3}	6.835, 8.333	Aqueous solution of As(V) and Cr(VI), water	5	–	[S13]
Mg/Al-CO_3-CLDHs	Cu^{2+}, Zn^{2+}	260.7	0.05	2.1	–	L, F	422.08, 508.21	0.339×10^{-3}, 0.064×10^{-3}	148.59, 263.16	Thermal regeneration	5	Surface sorption	[S14]
$(NH_4)_2SO_4$-LDH	Pb^{2+}	104.5	0.01	4.5	300	L, F	102.2	3.2×10^{-3}	268.9	–	–	Electrostatic binding reaction, Chemical binding	[S16]
Fe/Mn/Mg-LDH	Cd^{2+}	–	0.050	5.5	240	D-R, L, F	59.99	5.53×10^{-3}	31.47	–	–	–	[S17]
Mesoporous Cu/Mg/Fe-LDH	As(V)	70	0.02	6	–	L, F	15.6	2×10^{-3}	7.46	–	–	Ion-exchange, ligand exchange process with the layer OH group	[S19]

(Continued)

Table S2 *Continued*

Adsorbent	Adsorbate	BET (m^2/g)	Adsorption condition			Isotherms	Adsorption capacity (mg/g)	Kinetic pseudo-second-order		Regeneration		Adsorption mechanism	References
			Dosage (g)	pH	Time (min)			k_2 (mg/g·min)	q_e (mg/g)	Reagent	Cycle		
Li/Al-HT-lc-LDH	Cu^{2+}, Zn^{2+}	–	1.0, 1.0	5, 5	1,200, 500	L, F	41.1, 49.9	2.3×10^{-3}, 1.6×10^{-3}	30, 37.3	–	–	Surface complexation Isomorphic substitution	[S20]
Mg/Al-DT-PA-LDH	Pb^{2+}	–	0.5	6	–	L, F	170	3.6×10^{-4}	156.56	–	–	surface-induced precipitation	[S21]
Mg/Al/G-LDH	Pb^{2+}	–	–	5	–	L, F	68.49	5.4172×10^{-3}	20.95	–	–	–	[S22]
EDTA@ MF-LDHs	As^{3+}	–	0.5	7 ± 0.2	1,400	L, F	68.49	1×10^{-3}	71.940	–	–	Ion-exchange, Surface oxidation	[S31]
Ni/Al-LDH@ PAB	Cr(VI)	1,158	0.01	2	–	L, F	271.5	–	–	NaOH	–	Electrostatic attraction, isomorphic substitution, pore filling effect on porous adsorbents, Reduction.	[S23]
Mg/Al-CO_3-LDH	Cr(VI)	–	0.1	5	–	R-P, L, F	339	PSO	–	–	–	Anion-exchange, reduction	[S25]
Magnetic Fe_3O_4-Mg/Al-CO_3-LDH	Cd^{2+}	–	–	–	–	L, F	54.7	1.77×10^{-3}	22.6	–	–	Surface sorption, outer-sphere surface complexes, anion-exchange.	[S27]
Magnetic $CoFe_2O_4$/MgAl-LDH	Cr(VI)	120.75	0.15	–	–	L, F	72.4	2.4×10^{-3}	54.41	Na_2CO_3	6	Surface complexation and ion-exchange interaction	[S28]
Cu/Mg/Fe/La-LDH	As(III)	134	0.02	6	–	L, F, D-R	43.5	6.64×10^{-3}	22.2	Sodium salt of HPO_4^{2-}	–	Ion-exchange and layer ligand exchange	[S30]

CS-LDH	Cd^{2+}, Pb^{2+}	80.6	0.05	–	–	L, F	140.8, 333.3	0.0397, 0.6729	39.89, 119.9	–	–	precipitation, surface complexation, isomorphic substitution	[S33]
G-Mg/Al-CLDH	Cr(VI)	34.97	0.05	2	–	L, F	172.55	4.59×10^{-3}	172.41	Na_2CO_3, NaOH	6	surface adsorption, synergistic contribution	[S34]
MoS_2-Mg/Al-LDHs	Cr(VI)	–	–	5	1,440	L, F	76.3	–	–	–	–	electrostatic attraction and outer-sphere surface complexation	[S35]
CNF-Ni/Al-DH	Cu^{2+}, Cr(VI)	43.7	0.2	–	120	L, F	219.6, 341.2	–	–	Na_2CO_3	5	surface complexation, electrostatic interaction	[S36]
PPy-Mg/Al-LDHs	Cr(VI)	93	–	7	100	D-R, L, TM, F	76.21	3×10^{-3}	26.79	CH_3COOH, NaOH, HCl, water solution	–	Ion-exchange, electrostatic attractions, hydrogen bonding	[S37]
Zn/Al-LDO@C nanosheets	Cr(VI)	177.8	0.05	–	720	L, F	411.5	2.42×10^{-3}	199.2	NaOH, Na_2CO_3	5	electrostatic attraction and/or surface coordination	Li et al. [S38]
Dyes as adsorbate													
Bentonite-Co/Al-LDH	EBT	44.2	0.005	2	120	L, F	675.75	1.38×10^{-3}	588.23	–	–	Electrostatic, surface adsorption and chemical interaction	[S40]
Zn/Al/Cl-LDHs	AG 1	–	0.1	8	1,880	F, El, D-R	485.4	2×10^{-3}	199.13	–	–	–	[S41]
His-LDH	CR, IC, SY	169	0.01	–	–	L, F	1,112, 625, 400	2.5×10^{-3}, 2.3×10^{-3}, 4.4×10^{-3}	52.91, 52.91, 51.81	Ethanol, $NaNO_3$	12	Electrostatic interactions, PI-PI and H-bonding interaction	[S42]
C-Zn/Al-LDH	CV, MG	38.267	–	–	–	L, F, TM	129.87, 126.58	0.8×10^{-3}, 0.5×10^{-3}	106.38, 99	NaOH solution, NaOH solution	5, 5	Electrostatic attraction, H-bonding, n-π and π–π interactions	[S43]

(Continued)

Table S2 *Continued*

Adsorbent	Adsorbate	BET (m^2/g)	Adsorption condition			Isotherms	Adsorption capacity (mg/g)	Kinetic pseudo-second-order		Regeneration		Adsorption mechanism	References
			Dosage (g)	pH	Time (min)			k_2 (mg/g·min)	q_e (mg/g)	Reagent	Cycle		
Mg/Al-LDH	RR, CR, AR 1	104	1	10	60, 60, 60	F, L	19.94, 20.33, 19.92	3.728, 0.0151, 0.3	19.94, 20.33, 19.92	–	–	electrostatic attraction, ion-exchange	[S44]
MgAl-NO_3-LDH	RR-120, RBB-150	159	–	–	–	L, F, L, F	800, 910	1.25×10^{-3}, 1.60×10^{-3}	355.6, 391	Thermal regeneration	5, 5	–	[S47]
Mg/Al-LDH	AY	105	0.01	7	420	L, F	1,266	1.05×10^{-3}	1,399	Thermal treatment	5	–	[S48]
Mg/Al-CO_3-LDH, Mg/Al-NO_3-LDH, Cal. Mg/Al-LDH	AMR, AMR, AMR	10, 78, 160	–	6, 4, 6	180, 180, 180	L, L, L	0.8, 0.2, 1.6	0.184×10^{-3}, 0.22×10^{-3}, 0.0334×10^{-3}	0.184, 0.680, 0.704	Water, ethanol Na_2CO_3, Na_2HPO_4 water, ethanol	3	–	[S49]
Mesoporous Mg/Fe-LDH	Indigo carmine (IC)	85.6	–	9.5	–	L, F, L, F	62.8	0.022	62.8	–	5	–	Ahmed et al. [S50]
DS-Zn/Al-LDHs	CR, MO, BG	–	0.5	–	–	L, F	49.3, 114.9, 87	1.64×10^{-3}, 1.95×10^{-3}, 1.96×10^{-3}	84.03, 83.33, 56.8	NaOH, $NaHCO_3$	5	–	[S51]
O_3D-LDH, Mg/Al-LDH	MO	49.2	–	–	480	–	377.89	0.063	171.75	–	–	Hydrogen bonding, anion-exchange	[S52]
O_3D-LDH, Mg/Al-LDH	RhB	49.2	–	–	480	–	48.29	0.52	54.71	–	–	Hydrogen bonding, electrostatic attractions	[S52]
Ni/Mg/Al-CLDHs	CR	179	0.05	7	350	L, F	1,250	0.2×10^{-3}	476	–	–	–	[S4]
Ni/Al-LDH@PAB	MO	1,158	0.01	4.5	–	L, F	412.8	–	–	Methanol	–	Surface complexation, electrostatic attraction, H-bonding pore filling effect on porous adsorbents	[S23]

Zn/Al-LDO@C nanosheets	MO	177.8	0.05	–	720	L, F	1,538.9	3.73×10^{-3}	704.2	NaOH, Na_2CO_3	5	π –π stacking interaction, electrostatic attraction and/or hydrogen bonding	[S38]
SCD-Mg/Al-NO_3-LDH	MB	37.85	0.1	7	–	L, F	85.26	276,167	86.50	–	–	–	[S55]
Zn/Mg/Al-CLDH	RBBR	156.2	0.5	7	–	F, R-P	263	1.7×10^{-4}	324.7	–	–	Ligand exchange	[S56]
Zn/Ni/Fe-LDH-CNT	RB5	74	–	–	–	R-P, L, D-R, F, TM	–	PSO		–	–	–	[S57]
Zn/Ni/Fe-LDH-DPb	RB5	97	–	–	–	R-P, L, D-R, F, TM	–	PSO		–	–	–	[S57]
Mg/Al-LDH-DIA	Tar, Er	555.6, 625.2	0.01, 0.01	–	–	L, F, R-P	601.5, 649.2	0.014, 0.012	20.92, 21.05	NaOH, NaOH	10	–	[S58]
Starch-Ni/Fe-LDH	MO	–	0.01	–	360	L, F, R-P	387.59	0.026	391.50	NaOH	4	–	[S59]
Cu/Al-LDH/SWCNT	IC	–	0.01	–	360	L, F	294.117	1.057×10^{-3}	277.77	–	–	Anion-exchange, electrostatic interaction, π–π stacking, H-bonding	[S60]
ZIF-67@Co/Al-LDH	MB, MO	374.3	0.05	–	100, 90	L, F, L, F	57.24, 180.5	–	–	Ethanol	44	Electrostatic interaction, H-bonding, π–π stacking	[S61]
C/NiFe-LDH	MO, CR	232	0.02	–	–	L, F	323.6, 448.4	0.018, 0.017	172, 183	NaOH	5	Electrostatic attraction	[S62]
Mg/Al-LDH-AC	MB	745	0.01	9	180	L, F	816	1.03×10^{-3}	816.1	HCl, NaCl	5	Electrostatic interaction, π–π stacking, H-bonding	[S63]
PPy NF-Zn/Fe-LDH	Safranin dye	23.27	0.05	–	120	L, F, TM	63.4	0.0127	14.68	–	–	–	[S65]
Mg/Al/Cu/Fe-LDH	AR66	69.67	0.02	6.8	–	L, F	931.24	7.161×10^{-2}	516.32	–	–	–	[S67]

(Continued)

Table S2 *Continued*

Adsorbent	Adsorbate	BET (m^2/g)	Adsorption condition			Isotherms	Adsorption capacity (mg/g)	Kinetic pseudo-second-order		Regeneration		Adsorption mechanism	References
			Dosage (g)	pH	Time (min)			k_2 (mg/g·min)	q_e (mg/g)	Reagent	Cycle		
rGO/Ni/MMO	MO	–	–	–	960	R-P, L, F	210.8	0.015	87.7	Oxone and Co^{2+} ion	5	–	[S68]
WFS/MgFe-LDH	CR	13,305	0.55	3	60	L, F	9,127.08	1×10^{-3}	182.35	NaOH	6	–	[S70]
Magnetic SF-B-Co/Ni/Al-LDH	EBT, MO	206.23	0.01, 0.01	–	360, 360	L, F, TM	329.61, 219.56	10.79, 5.19	357.14, 285.71	NaOH, NaOH	3	–	[S75]
Co_4Al_1-Cl^--LDH	MO	20	0.08	7	–	L	801.08	0.126×10^{-3}	796.07	–	–	Anion-exchange, expansion-extrusion	[S111]
Co-Fe-LDH@UiO-66-NH_2	MR, MB	950	0.25	8	10	L	588.2, 555.6	–	–	–	–	hydrogen bonding, π–π interaction, π-aromatic systems	[S76]
PVDF@Co/Al-LDH	MO	12.14	0.004	–	420	L, F	621.17	0.17	273.76	–	–	Electrostatic interaction	[S80]
Fe_3O_4-Zn/Cr-LDH	MO	114	0.8	–	1,440	L	528	–	–	–	–	–	[S112]
Antibiotic as adsorbate													
Mg/Al-LDH/(CB)	Amoxicillin	74.46	0.03	–	1,440	L, F	138.3	4.19×10^{-3}	5.38	–	–	Electrostatic interaction	[S84]
CM-CLDH catalyst	Ibuprofen	–	–	–	120	L, F	100	2.853×10^{-4}	114	–	–	–	[S85]
Mg/Fe-LDH	Amoxicillin	136.4	–	–	180	–	9.11	0.07	8.49	–	–	–	[S88]
Zn_2/Al-CO_3-LDH	Sulfamethoxazole	–	–	–	–	L	4,314	0.002	500	Na_2CO_3	6	–	[S89]
Zn/Al-CLDH	Diclofenac sodium	77	–	–	–	L, F	737.02	4×10^3	96.2	Ethanol	4	–	[S96]
Zn/Al-CLDH	Acetylsalicylic acid	120	–	10	45	R-P, L, F	167.9	PSO		Thermal regeneration	6	–	[S98]

LDH-PmPDs	Diclofenac sodium	–	–	–	–	L, F	588	0.4×10^{-4}	404	–	–	Electrostatic interaction, H-bonding, π–π interaction	[S99]
Mg/Al-LDH-biochar	Diclofenac sodium	168.02	0.1	–	–	R-P, L, F	168.05	–	39.46	–	–	–	[S102]
Mg/Al-LDH-biochar	Caffeine	46.43	–	12	20	R-P, L, F	26.219	0.38×10^{-6}	3.01	NaCl, pure MeOH	6	–	[S103]
Zn/Fe-LDH	Diclofenac sodium	71.6	–	–	30	D-R, L, F	74.50	0.1×10^{-6}	14.44	–	–	hydrogen bonds, metal complexation	[S104]
Zn/Al-LDH	Levofloxacin	40.65	0.125	9	–	L, F, T, D-R	11.87	–	–	–	–	Hydrogen bonding, electrostatic interaction	[S106]
Mg/Al-LDH	Amoxicillin	–	0.02	–	120 min	R-P, L, F	32.42	–	16.001	Thermal regeneration	3	–	[S107]
Ca/Al-MoS_4-LDH	Ciprofloxacin, ofloxacin	60.95	–	6, 6	–	L, F, L, F	707.20, 476.74	0.6×10^{-3}, 0.1×10^{-3}	372.51, 333.5	KCl solution	3	Hydrogen bonding, anionic exchange, electrostatic interaction	[S108]
$CuFe_2O_4$-Ni/Mg/Al-LDH	Oxytetracycline	–	–	4	–	L, L	192	0.16×10^{-3}	80.28	NaOH solution, acetone, ethanol	3	Hydrogen bonding, anionic exchange, electrostatic interaction	[S109]
Mg/Al-MWCNT-LDH	Doxycycline	92		4	60		100	5.8×10^{-4}	106.4	NaOH	7	intermolecular interactions, chemical interaction between, hydrogen bonding	[S110]

Details of parameters for the adsorption of various toxic contaminants over LDHs and their hybrids/composites;
D-R: Dubinin–Radushkevich isotherm model; El: Elovich model; F: Freundlich isotherm model; L: Langmuir isotherm model; R-P: Redlich–Peterson model; TM: Temkin isotherm model.

References

[S1] M.A. González, I. Pavlovic, R. Rojas-Delgado, C. Barriga, Removal of Cu^{2+}, Pb^{2+} and Cd^{2+} by layered double hydroxide-humate hybrid. Sorbate and sorbent comparative studies, Chem. Eng. J., 254 (2014) 605–611.

[S2] W. Chen, J. Xing, Z. Lu, J. Wang, S. Yu, W. Yao, A.M. Asiri, K.A. Alamry, X. Wang, S. Wang, Citrate-modified Mg-Al layered double hydroxides for efficient removal of lead from water, Environ. Chem. Lett., 16 (2018) 561–567.

[S3] M.E.M. Hassouna, R.R. Amin, A.A. Ahmed-Anwar, R.K. Mahmoud, Efficient removal of oxytetracycline and some heavy metals from aqueous solutions by Mg-Al layered double hydroxide nanomaterial, Egypt. J. Chem., 62 (2019) 177–195.

[S4] C. Lei, X. Zhu, B. Zhu, C. Jiang, Y. Le, J. Yu, Superb adsorption capacity of hierarchical calcined Ni/Mg/Al layered double hydroxides for Congo red and Cr(VI) ions, J. Hazard. Mater., 321 (2016) 801–811.

[S5] L.N. Puzyrnaya, G.N. Pshinko, V.Y.A. Zub, O. V Zuy, Removal of Cu(II), Co(II) and Cd(II) from water solutions by layered-double hydroxides with different [Mg(II)]/[Fe(III)] molar ratios, Bull. Mater. Sci., (2020), doi: 10.1007/s12034-019-1969-z.

[S6] J. Matusik, K. Rybka, Removal of chromates and sulphates by Mg/Fe LDH and heterostructured LDH/halloysite materials: Efficiency, selectivity, and stability of adsorbents in single- and multi-element systems, Materials (Basel), 12 (2019), doi: 10.3390/ma12091373.

[S7] L. Chen, H. Xu, J. Xie, X. Liu, Y. Yuan, P. Liu, Z. Qu, N. Yan, $[SnS_4]^{4-}$ clusters modified MgAl-LDH composites for mercury ions removal from acid wastewater, Environ. Pollut., 247 (2019) 146–154.

[S8] X. He, X. Qiu, J. Chen, Preparation of Fe(II)-Al layered double hydroxides: application to the adsorption/reduction of chromium, Colloids Surf., A, 516 (2017) 362–374.

[S9] D. Huang, C. Liu, C. Zhang, R. Deng, R. Wang, Bioresource Technology Cr(VI) removal from aqueous solution using biochar modified with Mg/Al-layered double hydroxide intercalated with ethylenediaminetetraacetic acid, Bioresour. Technol., 276 (2019) 127–132.

[S10] T. Kameda, H. Takeuchi, T. Yoshioka, Kinetics of uptake of Cu^{2+} and Cd^{2+} by Mg-Al layered double hydroxides intercalated with citrate, malate, and tartrate, Colloids Surf., A, 355 (2010) 172–177.

[S11] Y. Li, H.Y. Bi, X.Q. Shi, Simultaneous adsorption of heavy metal and organic pollutant onto citrate-modified layered double hydroxides with dodecylbenzenesulfonate, J. Environ. Eng. Sci., 32 (2015) 666–675.

[S12] L. Ma, Q. Wang, S.M. Islam, Y. Liu, S. Ma, M.G. Kanatzidis, Highly selective and efficient removal of heavy metals by layered double hydroxide intercalated with the MoS_4^{2-} ion, J. Am. Chem. Soc., 138 (2016) 2858–2866.

[S13] M. Mubarak, H. Jeon, S. Islam, C. Yoon, One-pot synthesis of layered double hydroxide hollow nanospheres with ultrafast removal ef fi ciency for heavy metal ions and organic contaminants, Chemosphere, 201 (2018) 676–686.

[S14] Y. Xiao, M. Sun, L. Zhang, X. Gao, J. Su, H. Zhu, The co-adsorption of Cu^{2+} and Zn^{2+} with adsorption sites surface-lattice reforming on calcined layered double hydroxides, RSC Adv., 5 (2015) 28369–28378.

[S15] S. Lin, H. Nguyen, H. Chao, J. Lee, Layered double hydroxides intercalated with sulfur-containing organic solutes for efficient removal of cationic and oxyanionic metal ions, Appl. Clay Sci., 162 (2018) 443–453.

[S16] Z.-Q. Zhang, H.-Y. Zeng, X.-J. Liu, S. Xu, C.-R. Chen, J.-D. Du, Modification of MgAl hydrotalcite by ammonium sulfate for enhancement of lead adsorption, J. Taiwan Inst. Chem. Eng., 60 (2016) 361–368.

[S17] H. Zhou, Z. Jiang, S. Wei, Adsorption of Cd(II) from aqueous solutions by a novel layered double hydroxide FeMnMg-LDH, Water Air Soil Pollut., 229 (2018), doi: 10.1007/s11270-017-3597-9.

[S18] V.V. Goncharuk, L.N. Puzyrnaya, G.N. Pshinko, A.A. Kosorukov, V.Y. Demchenko, Removal of Cu(II), Ni(II), and Co(II) from aqueous solutions using layered double hydroxide intercalated with EDTA, J. Water Chem. Technol., 33 (2011) 288–292.

[S19] Y. Guo, Z. Zhu, Y. Qiu, J. Zhao, Synthesis of mesoporous Cu/Mg/Fe layered double hydroxide and its adsorption performance for arsenate in aqueous solutions, J. Environ. Sci. (China), 25 (2013) 944–953.

[S20] L.X. Zhao, J.L. Liang, N. Li, H. Xiao, L.Z. Chen, R.S. Zhao, Kinetic, thermodynamic and isotherm investigations of Cu^{2+} and Zn^{2+} adsorption on Li-Al hydrotalcite-like compound, Sci. Total Environ., 716 (2020) 137120, doi: 10.1016/j.scitotenv.2020.137120.

[S21] X. Liang, W. Hou, Y. Xu, G. Sun, L. Wang, Y. Sun, X. Qin, Sorption of lead ion by layered double hydroxide intercalated with diethylenetriaminepentaacetic acid, Colloids Surf., A, 366 (2010) 50–57.

[S22] S. Yanming, L. Dongbin, L. Shifeng, F. Lihui, C. Shuai, Removal of lead from aqueous solution on glutamate intercalated layered double hydroxide, Arabian J. Chem., 10 (2017) S2295–S2301.

[S23] S. Chen, Y. Huang, X. Han, Z. Wu, C. Lai, J. Wang, Q. Deng, Z. Zeng, S. Deng, Simultaneous and efficient removal of Cr(VI) and methyl orange on LDHs decorated porous carbons, Chem. Eng. J., 352 (2018) 306–315.

[S24] T. Hou, L. Yan, J. Li, Y. Yang, L. Shan, X. Meng, X. Li, Y. Zhao, Adsorption performance and mechanistic study of heavy metals by facile synthesized magnetic layered double oxide/carbon composite from spent adsorbent, Chem. Eng. J., 384 (2020) 123331, doi: 10.1016/j.cej.2019.123331.

[S25] H.P. Chao, Y.C. Wang, H.N. Tran, Removal of hexavalent chromium from groundwater by Mg/Al-layered double hydroxides using characteristics of *in-situ* synthesis, Environ. Pollut., 243 (2018) 620–629.

[S26] G. Rathee, S. Kohli, A. Awasthi, N. Singh, R. Chandra, MoS_4^{2-}intercalated NiFeTi LDH as an efficient and selective adsorbent for elimination of heavy metals, RSC Adv., 10 (2020) 19371–19381.

[S27] R. ran Shan, L. guo Yan, K. Yang, Y. feng Hao, B. Du, Adsorption of Cd(II) by Mg-Al-CO_3- and magnetic Fe_3O_4/Mg-Al-CO_3-layered double hydroxides: kinetic, isothermal, thermodynamic and mechanistic studies, J. Hazard. Mater., 299 (2015) 42–49.

[S28] L. Deng, Z. Shi, X. Peng, Adsorption of Cr(VI) onto a magnetic $CoFe_2O_4$/MgAl-LDH composite and mechanism study, RSC Adv., 5 (2015) 49791–49801.

[S29] I. Pavlovic, M.R. Pérez, C. Barriga, M.A. Ulibarri, Adsorption of Cu^{2+}, Cd^{2+} and Pb^{2+} ions by layered double hydroxides intercalated with the chelating agents diethylenetriaminepentaacetate and meso-2,3-dimercaptosuccinate, Appl. Clay Sci., 43 (2009) 125–129.

[S30] Y. Guo, Z. Zhu, Y. Qiu, J. Zhao, Adsorption of arsenate on Cu/Mg/Fe/La layered double hydroxide from aqueous solutions, J. Hazard. Mater., 239–240 (2012) 279–288.

[S31] G. Liu, Z. Zhu, N. Zhao, Y. Fang, Y. Gao, Y. Zhu, L. Zhang, Mn-Fe layered double hydroxide intercalated with ethylenediaminetetraacetate anion: synthesis and removal of As(III) from aqueous solution around pH 2–11, Int. J. Environ. Res. Public Health., 17 (2020) 9341, doi: 10.3390/ijerph17249341.

[S32] T. Kameda, M. Takaizumi, S. Kumagai, Y. Saito, T. Yoshioka, Uptake of Ni^{2+} and Cu^{2+} by Zn-Al layered double hydroxide intercalated with carboxymethyl-modified cyclodextrin: equilibrium and kinetic studies, Mater. Chem. Phys., 233 (2019) 288–295.

[S33] F. Lyu, H. Yu, T. Hou, L. Yan, X. Zhang, B. Du, Efficient and fast removal of Pb^{2+} and Cd^{2+} from an aqueous solution using a chitosan/Mg-Al-layered double hydroxide nanocomposite, J. Colloid Interface Sci., 539 (2019) 184–193.

[S34] X. Yuan, Y. Wang, J. Wang, C. Zhou, Q. Tang, X. Rao, Calcined graphene/MgAl-layered double hydroxides for enhanced Cr(VI) removal, Chem. Eng. J., 221 (2013) 204–213.

[S35] J. Wang, P. Wang, H. Wang, J. Dong, W. Chen, X. Wang, S. Wang, T. Hayat, A. Alsaedi, X. Wang, Preparation of molybdenum disulfide coated Mg/Al layered double hydroxide composites for efficient removal of chromium(VI), ACS Sustainable Chem. Eng., 5 (2017) 7165–7174.
[S36] S. Yu, Y. Liu, Y. Ai, X. Wang, R. Zhang, Z. Chen, Z. Chen, G. Zhao, X. Wang, Rational design of carbonaceous nanofiber/Ni-Al layered double hydroxide nanocomposites for high-efficiency removal of heavy metals from aqueous solutions, Environ. Pollut., 242 (2018) 1–11.
[S37] S. Sahu, P. Kar, N. Bishoyi, L. Mallik, R.K. Patel, Synthesis of polypyrrole-modified layered double hydroxides for efficient removal of Cr(VI), J. Chem. Eng. Data, 64 (2019) 4357–4368.
[S38] M. Li, G. Wu, Z. Liu, X. Xi, Y. Xia, J. Ning, D. Yang, A. Dong, Uniformly coating ZnAl layered double oxide nanosheets with ultra-thin carbon by ligand and phase transformation for enhanced adsorption of anionic pollutants, J. Hazard. Mater., 397 (2020) 122766, doi: 10.1016/j.jhazmat.2020.122766.
[S39] X. Dai, S. Zhang, G.I.N. Waterhouse, H. Fan, S. Ai, Recyclable polyvinyl alcohol sponge containing flower-like layered double hydroxide microspheres for efficient removal of As(V) anions and anionic dyes from water, J. Hazard. Mater., 367 (2019) 286–292.
[S40] N.D. Mu'azu, N. Jarrah, T.S. Kazeem, M. Zubair, M. Al-Harthi, Bentonite-layered double hydroxide composite for enhanced aqueous adsorption of Eriochrome Black T, Appl. Clay Sci., 161 (2018) 23–34.
[S41] E.H. Elkhattabi, M. Lakraimi, M. Berraho, A. Legrouri, R. Hammal, L. El Gaini, Acid Green 1 removal from wastewater by layered double hydroxides, Appl. Water Sci., 8 (2018) 1–11.
[S42] M. Shamsayei, Y. Yamini, H. Asiabi, Fabrication of zwitterionic histidine/layered double hydroxide hybrid nanosheets for highly efficient and fast removal of anionic dyes, J. Colloid Interface Sci., 529 (2018) 255–264.
[S43] G. George, M.P. Saravanakumar, Facile synthesis of carbon-coated layered double hydroxide and its comparative characterisation with Zn-Al LDH: application on crystal violet and malachite green dye adsorption—isotherm, kinetics and Box–Behnken design, Environ. Sci. Pollut. Res., 25 (2018) 30236–30254.
[S44] R. Shan, L. Yan, Y. Yang, K. Yang, S. Yu, H. Yu, Highly efficient removal of three red dyes by adsorption onto Mg-Al-layered double hydroxide, J. Ind. Eng. Chem., 21 (2014) 561–568.
[S45] F.B.D. Saiah, B.L. Su, N. Bettahar, Nickel-iron layered double hydroxide (LDH): textural properties upon hydrothermal treatments and application on dye sorption, J. Hazard. Mater., 165 (2009) 206–217.
[S46] X. Ruan, Y. Chen, H. Chen, G. Qian, R.L. Frost, Sorption behavior of methyl orange from aqueous solution on organic matter and reduced graphene oxides modified Ni-Cr layered double hydroxides, Chem. Eng. J., 297 (2016) 295–303.
[S47] S. Boubakri, M.A. Djebbi, Z. Bouaziz, P. Namour, N. Jaffrezic-Renault, A.B.H. Amara, M. Trabelsi-Ayadi, I. Ghorbel-Abid, R. Kalfat, Removal of two anionic reactive textile dyes by adsorption into MgAl-layered double hydroxide in aqueous solutions, Environ. Sci. Pollut. Res., 25 (2018) 23817–23832.
[S48] R.M.M. dos Santos, R.G.L. Gonçalves, V.R.L. Constantino, C.V. Santilli, P.D. Borges, J. Tronto, F.G. Pinto, Adsorption of Acid Yellow 42 dye on calcined layered double hydroxide: effect of time, concentration, pH and temperature, Appl. Clay Sci., 140 (2017) 132–139.
[S49] K. Abdellaoui, I. Pavlovic, M. Bouhent, A. Benhamou, C. Barriga, A comparative study of the amaranth azo dye adsorption/desorption from aqueous solutions by layered double hydroxides, Appl. Clay Sci., 143 (2017) 142–150.
[S50] M.A. Ahmed, A.A. Brick, A.A. Mohamed, An efficient adsorption of indigo carmine dye from aqueous solution on mesoporous Mg/Fe layered double hydroxide nanoparticles prepared by controlled sol–gel route, Chemosphere, 174 (2017) 280–288.
[S51] A. Grover, I. Mohiuddin, A.K. Malik, J.S. Aulakh, K.H. Kim, Zn-Al layered double hydroxides intercalated with surfactant: synthesis and applications for efficient removal of organic dyes, J. Cleaner Prod., 240 (2019) 118090, doi: 10.1016/j.jclepro.2019.118090.
[S52] P. Zhang, S. Ouyang, P. Li, Y. Huang, R.L. Frost, Enhanced removal of ionic dyes by hierarchical organic three-dimensional layered double hydroxide prepared via soft-template synthesis with mechanism study, Chem. Eng. J., 360 (2019) 1137–1149.
[S53] G. Starukh, O. Rozovik, O. Oranska, Organo/Zn-Al LDH nanocomposites for cationic dye removal from aqueous media, Nanoscale Res. Lett., 11 (2016) 228, doi: 10.1186/s11671-016-1402-0.
[S54] S. Bao, Y. Shi, Y. Zhang, L. He, W. Yu, Study on the efficient removal of azo dyes by heterogeneous photo-Fenton process with 3D flower-like layered double hydroxide, Water Sci. Technol., 81 (2020) 2368–2380.
[S55] W. Hu, X. Wu, F. Jiao, W. Yang, Y. Zhou, Preparation and characterization of magnetic Fe_3O_4@sulfonated β-cyclodextrin intercalated layered double hydroxides for methylene blue removal, Desal. Water Treat., 3994 (2016), doi: 10.1080/19443994.2016.1155173.
[S56] S.M. Gidado, İ. Akanyeti, Comparison of Remazol Brilliant Blue reactive adsorption on pristine and calcined ZnAl, MgAl, ZnMgAl layered double hydroxides, Water Air Soil Pollut., 231 (2020) 18, doi: 10.1007/s11270-020-04522-0.
[S57] M.T. Amin, A.A. Alazba, M. Shafiq, LDH of NiZnFe and its composites with carbon nanotubes and data-palm biochar with efficient adsorption capacity for RB5 dye from aqueous solutions: isotherm, kinetic, and thermodynamics studies, Curr. Appl. Phys., 40 (2022) 90–100.
[S58] M. Shamsayei, Y. Yamini, H. Asiabi, A novel diatomite supported layered double hydroxide as reusable adsorbent for efficient removal of acidic dyes, Int. J. Environ. Anal. Chem., 102 (2020) 1849–1865.
[S59] M. Zubair, N. Jarrah, A. Khalid, M. Saood, Starch-NiFe-layered double hydroxide composites: Efficient removal of methyl orange from aqueous phase, J. Mol. Liq., 249 (2018) 254–264.
[S60] N. Almoisheer, F.A. Alseroury, R. Kumar, M. Aslam, M.A. Barakat, Adsorption and anion-exchange insight of indigo carmine onto CuAl-LDH/SWCNTs nanocomposite: kinetic, thermodynamic and isotherm analysis, RSC Adv., 9 (2019) 560–568.
[S61] M.A. Nazir, N.A. Khan, C. Cheng, S.S.A. Shah, T. Najam, M. Arshad, A. Sharif, S. Akhtar, A. ur Rehman, Surface induced growth of ZIF-67 at Co-layered double hydroxide: removal of methylene blue and methyl orange from water, Appl. Clay Sci., 190 (2020) 105564, doi: 10.1016/j.clay.2020.105564.
[S62] H. Hu, S. Wageh, A.A. Al-Ghamdi, S. Yang, Z. Tian, B. Cheng, W. Ho, NiFe-LDH nanosheet/carbon fiber nanocomposite with enhanced anionic dye adsorption performance, Appl. Surf. Sci., 511 (2020) 145570, doi: 10.1016/j.apsusc.2020.145570.
[S63] A.M. Aldawsari, I. Alsohaimi, H.M.A. Hassan, Z.E.A. Abdalla, I. Hassan, M.R. Berber, Tailoring an efficient nanocomposite of activated carbon-layered double hydroxide for elimination of water-soluble dyes, J. Alloys Compd., 857 (2021) 157551, doi: 10.1016/j.jallcom.2020.157551.
[S64] M. Zubair, N. Jarrah, M.S. Manzar, M. Al-Harthi, M. Daud, N.D. Mu'azu, S.A. Haladu, Adsorption of Eriochrome Black T from aqueous phase on MgAl-, CoAl- and NiFe- calcined layered double hydroxides: kinetic, equilibrium and thermodynamic studies, J. Mol. Liq., 230 (2017) 344–352.
[S65] F. Mohamed, M.R. Abukhadra, M. Shaban, Removal of safranin dye from water using polypyrrole nanofiber/Zn-Fe layered double hydroxide nanocomposite (PPy NF/Zn-Fe LDH) of enhanced adsorption and photocatalytic properties, Sci. Total Environ., 640–641 (2018) 352–363.
[S66] B. Zhang, Z. Dong, D. Sun, T. Wu, Y. Li, Enhanced adsorption capacity of dyes by surfactant-modified layered double hydroxides from aqueous solution, J. Ind. Eng. Chem., 49 (2017) 208–218.
[S67] I. Harizi, D. Chebli, A. Bouguettoucha, A new Mg-Al-Cu-Fe-LDH composite to enhance the adsorption of Acid Red 66

dye: characterization, kinetics and isotherm analysis, Arabian J. Sci. Eng., 44 (2019) 5245–5261.
[S68] Z. Yang, S. Ji, W. Gao, C. Zhang, L. Ren, W. Weei, Z. Zhang, J. Pan, T. Liu, Magnetic nanomaterial derived from graphene oxide/layered double hydroxide hybrid for efficient removal of methyl orange from aqueous solution, J. Colloid Interface Sci., 408 (2013) 25–32.
[S69] M. Zhang, Q. Yao, C. Lu, Z. Li, W. Wang, Layered double hydroxide-carbon dot composite: high-performance adsorbent for removal of anionic organic dye, ACS Appl. Mater. Interfaces, 6 (2014) 20225–20233.
[S70] D.N. Ahmed, L.A. Naji, A.A.H. Faisal, N. Al-Ansari, M. Naushad, Waste foundry sand/MgFe-layered double hydroxides composite material for efficient removal of Congo red dye from aqueous solution, Sci. Rep., 10 (2020) 1–12.
[S71] L. Zhang, D. Guo, X. Tantai, B. Jiang, Y. Sun, N. Yang, Synthesis of three-dimensional hierarchical flower-like Mg-Al layered double hydroxides with excellent adsorption performance for organic anionic dyes, Trans. Tianjin Univ., (2020), doi: 10.1007/s12209-020-00249-5.
[S72] G. Rathee, A. Awasthi, D. Sood, R. Tomar, V. Tomar, R. Chandra, A new biocompatible ternary layered double hydroxide adsorbent for ultrafast removal of anionic organic dyes, Sci. Rep., 9 (2019) 1–14.
[S73] D. Bharali, R.C. Deka, Preferential adsorption of various anionic and cationic dyes from aqueous solution over ternary CuMgAl-layered double hydroxide, Colloids Surf., A, 525 (2017) 64–76.
[S74] A.S. Berner, P. Araya, J. Govan, H. Palza, Cu/Al and Cu/Cr based layered double hydroxide nanoparticles as adsorption materials for water treatment, J. Ind. Eng. Chem., 59 (2018) 134–180.
[S75] K.H.A. Elkhider, I. Ihsanullah, M. Zubair, M.S. Manzar, N.D. Mu'azu, M.A. Al-Harthi, Synthesis, characterization and dye adsorption performance of strontium ferrite decorated bentonite-CoNiAl magnetic composite, Arabian J. Sci. Eng., 45 (2020) 7397–7408.
[S76] M. Khajeh, A.R. Oveisi, A. Barkhordar, Z. Sorinezami, Co-Fe-layered double hydroxide decorated amino-functionalized zirconium terephthalate metal-organic framework for removal of organic dyes from water samples, Spectrochim. Acta, Part A, 234 (2020) 118270, doi: 10.1016/j.saa.2020.118270.
[S77] A. Lesbani, T. Taher, N.R. Palapa, R. Mohadi, A. Yuliana, Methyl orange dye removal using Ni/Fe-NO_3 and Ni/Fe-[α-$SiW_{12}O_{40}$] layered double hydroxides, IOP Conf. Ser.: Mater. Sci. Eng., 902 (2020) 012042, doi: 10.1088/1757-899X/902/1/012042.
[S78] E.S. Behbahani, K. Dashtian, M. Ghaedi, Fe/Co-chalcogenide-stabilized Fe_3O_4 nanoparticles supported MgAl-layered double hydroxide as a new magnetically separable sorbent for the simultaneous spectrophotometric determination of anionic dyes, Microchem. J., 152 (2020) 104431, doi: 10.1016/j.microc.2019.104431.
[S79] R. Elmoubarki, F.Z. Mahjoubi, A. Elhalil, H. Tounsadi, M. Abdennouri, M. Sadiq, S. Qourzal, A. Zouhri, N. Barka, Ni/Fe and Mg/Fe layered double hydroxides and their calcined derivatives: preparation, characterization and application on textile dyes, J. Mater. Res. Technol., 6 (2017) 271–283.
[S80] Q. Mei, W. Lv, M. Du, Q. Zheng, Layered double hydroxide composite fibers using for dye removal, RSC Adv., 7 (2017) 46576–46588.
[S81] D. Chaara, I. Pavlovic, F. Bruna, M.A. Ulibarri, K. Draoui, C. Barriga, Removal of nitrophenol pesticides from aqueous solutions by layered double hydroxides and their calcined products, Appl. Clay Sci., 50 (2010) 292–298.
[S82] L. Santamaría, M.A. Vicente, S.A. Korili, A. Gil, Saline slag waste as an aluminum source for the synthesis of Zn-Al-Fe-Ti layered double-hydroxides as catalysts for the photodegradation of emerging contaminants, J. Alloys Compd., 843 (2020) 156007, doi: 10.1016/j.jallcom.2020.156007.
[S83] G. Rathee, N. Singh, R. Chandra, Simultaneous elimination of dyes and antibiotic with a hydrothermally generated NiAlTi layered double hydroxide adsorbent, ACS Omega, 5 (2020) 2368–2377.
[S84] C. Yang, L. Wang, Y. Yu, P. Wu, F. Wang, S. Liu, X. Luo, Highly efficient removal of amoxicillin from water by Mg-Al layered double hydroxide/cellulose nanocomposite beads synthesized through *in-situ* co-precipitation method, Int. J. Biol. Macromol., 149 (2020) 93–100.
[S85] X. Shen, Z. Zhu, H. Zhang, G. Di, T. Chen, Y. Qiu, D. Yin, Carbonaceous composite materials from calcination of azo dye-adsorbed layered double hydroxide with enhanced photocatalytic efficiency for removal of Ibuprofen in water, Environ. Sci. Eur., 32 (2020), doi: 10.1186/s12302-020-00351-4.
[S86] E. Li, L. Liao, G. Lv, Z. Li, C. Yang, Y. Lu, The interactions between three typical PPCPs and LDH, Front. Chem., 6 (2018) 1–9.
[S87] K. Panplado, M.S. Subsadsana, S. Srijaranai, S. Sansuk, Rapid removal and efficient recovery of tetracycline antibiotics in aqueous solution using layered double hydroxide components in an *in-situ*-adsorption process, Crystals, 9 (2019) 342, doi: 10.3390/cryst9070342.
[S88] D.P. De Lima, M. Ferreira, A. Ferreira, Antibiotic Removal From Water Using MgFe/Layered Double Hydroxide as Adsorbent, EBA 13 - Brazilian Meeting on Adsorption, Fortaleza, Ceará, Brazil, 2020, p. 5.
[S89] E.H. Mourid, M. Lakraimi, L. Benaziz, E.H. Elkhattabi, A. Legrouri, Wastewater treatment test by removal of the sulfamethoxazole antibiotic by a calcined layered double hydroxide, Appl. Clay Sci., 168 (2019) 87–95.
[S90] Z. Xu, J. Fan, S. Zheng, F. Ma, D. Yin, On the adsorption of tetracycline by calcined magnesium-aluminum hydrotalcites, J. Environ. Qual., 38 (2009) 1302–1310.
[S91] A. Elhalil, M. Farnane, A. Machrouhi, F.Z. Mahjoubi, Effect of molar ratio and calcination temperature on the adsorption performance of Zn/Al layered double hydroxide nanoparticles in the removal of pharmaceutical pollutants, J. Sci. Adv. Mater. Dev., 3 (2018) 188–195.
[S92] M. Rosset, L. Weidlich, G. Edith, N. Hidalgo, Adsorbents derived from hydrotalcites for the removal of diclofenac in wastewater, Appl. Clay Sci., 175 (2019) 150–158.
[S93] L. Santamaría, F. Devred, E.M. Gaigneaux, M.A. Vicente, S.A. Korili, A. Gil, Effect of the surface properties of Me^{2+}/Al layered double hydroxides synthesized from aluminum saline slag wastes on the adsorption removal of drugs, Microporous Mesoporous Mater., 309 (2020) 110560, doi: 10.1016/j.micromeso.2020.110560.
[S94] M. Sui, Y. Zhou, L. Sheng, B. Duan, Adsorption of norfloxacin in aqueous solution by Mg-Al layered double hydroxides with variable metal composition and interlayer anions, Chem. Eng. J., 210 (2012) 451–460.
[S95] M. Chen, P. Wu, Z. Huang, J. Liu, Y. Li, N. Zhu, Environmental application of MgMn-layered double oxide for simultaneous efficient removal of tetracycline and Cd pollution: performance and mechanism, J. Environ. Manage., 246 (2019) 164–173.
[S96] N. Boukhalfa, M. Boutahala, Synthesis and characterization of ZnAl-layered double hydroxide and organo-K10 montmorillonite for the removal of diclofenac from aqueous solution, Adsorpt. Sci. Technol., 35 (2016) 17, doi: 10.1177/0263617416666548.
[S97] M. Noori, T.J. Al-musawi, E. Ghahramani, H. Kazemian, M. Zarrabi, Adsorption performance of magnesium/aluminum layered double hydroxide nanoparticles for metronidazole from aqueous solution, Arabian J. Chem., 10 (2017) 611–623.
[S98] M. Rosset, L.W. Sfreddo, O.W. Perez-Lopez, L.A. Féris, Effect of concentration in the equilibrium and kinetics of adsorption of acetylsalicylic acid on ZnAl layered double hydroxide, J. Environ. Chem. Eng., 8 (2020), doi: 10.1016/j.jece.2020.103991.
[S99] T. Xiong, X. Yuan, H. Wang, Z. Wu, L. Jiang, L. Leng, Highly efficient removal of diclofenac sodium from medical wastewater by Mg/Al layered double hydroxide-poly (m-phenylenediamine) composite, Chem. Eng. J., 366 (2019) 83–91.
[S100] C. Chen, P. Wang, T. Lim, L. Liu, S. Liu, R. Xu, A facile synthesis of monodispersed hierarchical layered double hydroxide on

silica spheres for efficient removal of pharmaceuticals from water, J. Mater. Chem. A, 1 (2013) 3877–3880.
[S101] M. Hossein Beyki, M. Mohammadirad, F. Shemirani, A.A. Saboury, Magnetic cellulose ionomer/layered double hydroxide: an efficient anion-exchange platform with enhanced diclofenac adsorption property, Carbohydr. Polym., 157 (2017) 438–446.
[S102] G.E. de Souza dos Santos, A.H. Ide, J.L.S. Duarte, G. McKay, A.O.S. Silva, L. Meili, Adsorption of anti-inflammatory drug diclofenac by MgAl/layered double hydroxide supported on *Syagrus coronata* biochar, Powder Technol., 364 (2020) 229–240.
[S103] P.V. dos Santos Lins, D.C. Henrique, A.H. Ide, C.L. de Paiva e Silva Zanta, L. Meili, Evaluation of caffeine adsorption by MgAl-LDH/biochar composite, Environ. Sci. Pollut. Res., 26 (2019) 31804–31811.
[S104] H.A. Younes, R. Khaled, H.M. Mahmoud, H.F. Nassar, M.M. Abdelrahman, F.I. Abo El-Ela, M. Taha, Computational and experimental studies on the efficient removal of diclofenac from water using ZnFe-layered double hydroxide as an environmentally benign absorbent, J. Taiwan Inst. Chem. Eng., 102 (2019) 297–311.
[S105] X. Li, T. Hou, L. Yan, L. Shan, X. Meng, Y. Zhao, Efficient degradation of tetracycline by CoFeLa-layered double oxides catalyzed peroxymonosulfate: synergistic effect of radical and nonradical pathways, J. Hazard. Mater., 398 (2020) 1–41.
[S106] S.M. Mahgoub, M.R. Shehata, F.L. Abo El-Ela, A. Farghali, A. Zaher, R.K. Mahmoud, Sustainable waste management and recycling of Zn-Al layered double hydroxide after adsorption of levofloxacin as a safe anti-inflammatory nanomaterial, RSC Adv., 10 (2020) 27633–27651.
[S107] A. Elhaci, F. Labed, A. Khenifi, Z. Bouberka, K. Benabbou, MgAl-layered double hydroxide for amoxicillin removal from aqueous media, J. Environ. Anal. Chem., 101 (2020) 2876–2898.
[S108] K. Gupta, J.B. Huo, J.C.E. Yang, M.L. Fu, B. Yuan, Z. Chen, $(MoS_4)^{2-}$ intercalated $CAMoS_4$·LDH material for the efficient and facile sequestration of antibiotics from aqueous solution, Chem. Eng. J., 355 (2019) 637–649.
[S109] J.O. Eniola, R. Kumar, O.A. Mohamed, A.A. Al-Rashdi, M.A. Barakat, Synthesis and characterization of $CuFe_2O_4$/NiMgAl-LDH composite for the efficient removal of oxytetracycline antibiotic, J. Saudi Chem. Soc., 24 (2019) 139–150.
[S110] S.A. Abdel Moaty, R.K. Mahmoud, N.A. Mohamed, Y. Gaber, A. Farghali, M.S.M.A. Wahed, H.A. Younes, Synthesis and characterization of LDH-type anionic nanomaterials for effective removal of doxycycline from aqueous media, Water Environ. J., 43 (2016) 1–34, doi: 10.1111/wej.12526.
[S111] Y. Chen, C. Jing, X. Zhang, D. Jiang, X. Liu, B. Dong, L. Feng, S. Li, Y. Zhang, Acid-salt treated CoAl layered double hydroxide nanosheets with enhanced adsorption capacity of methyl orange dye, J. Colloid Interface Sci., 548 (2019) 100–109.
[S112] D. Chen, Y. Li, J. Zhang, J. Zhou, Y. Guo, H. Liu, Magnetic Fe_3O_4/ZnCr-layered double hydroxide composite with enhanced adsorption and photocatalytic activity, Chem. Eng. J., 185–186 (2012) 120–126.